4-30-2021

Improving the cost-effectiveness of water wave measurements and understanding of its impact on natural and restored marsh communities

Nigel Temple
757nigel@gmail.com

Improving the cost-effectiveness of water wave measurements and understanding of its impact on natural and restored marsh communities

By

Nigel Temple

Approved by:

Eric Sparks (Major Professor)
Just Cebrian
Anna C. Linhoss
Adam Skarke
Kevin M. Hunt (Graduate Coordinator)
L.Wes Burger (Dean, College of Forest Resources)

A Dissertation
Submitted to the Faculty of
Mississippi State University
in Partial Fulfillment of the Requirements
for the Degree of Doctor of Philosophy
in Forest Resources
in the Department of Wildlife, Fisheries and Aquaculture

Mississippi State, Mississippi

April 2021

Name: Nigel Temple

Date of Degree: April 30, 2021

Institution: Mississippi State University

Major Field: Forest Resources

Select Appropriate Title: Eric Sparks

Title of Study: Improving the cost-effectiveness of water wave measurements and understanding of its impact on natural and restored marsh communities

Pages in Study: 149

Candidate for Degree of Doctor of Philosophy

Coastal restoration has become a necessary and ubiquitous practice to enhance and conserve the many ecosystem services lost by marsh degradation. Wave climate is one of the most critical factors to consider for restoration projects. However, knowledge of the ways that waves affect marsh plants and the ecosystem services they provide is limited. The purpose of my dissertation was to improve the effectiveness of coastal marsh restoration by addressing the limitations and gaps associated with plant and ecosystem responses to waves through empirical research with three primary goals: 1) develop and test a low-cost wave gauge, 2) use it to compare above- and below-ground plant growth responses along a wave climate gradient, and 3) evaluate the effects of waves on nutrient removal in constructed marshes. I used three field and laboratory experiments to accomplish these goals. The low-cost wave gauge was developed using an Arduino microcontroller and various accessories. After development, the gauge was evaluated against a commercial gauge in a series of laboratory and field tests. Comparisons revealed over 90% agreement between the gauges and confirmed the applicability of the low-cost gauge. A total of thirty gauges were then constructed and deployed at sites within Mobile Bay, Alabama and surrounding tributaries. In addition to wave energy, plant data was also

collected at each site, including above- and below-ground biomass, shoot density, height, and diameter. These data suggested that waves affect plant growth responses in ways not explained by the current plant response paradigm. For example, while greater diameter shoots best attenuate waves, shoot diameter declined with greater wave exposure in this study. This response was common among the study species. Other plant responses were species-specific. Finally, a field experiment was constructed to examine the main and interactive effects of sediment type, initial planting density, platform slope, and platform position at sites exposed to and protected from waves. Results from this experiment suggested that waves may potentially mitigate the effective removal potential of constructed marshes. Taken together, this dissertation advances research on plant responses to waves and provides new tools for land managers working on coastal restoration and conservation projects.

DEDICATION

This dissertation is dedicated to my grandparents, Dallas and Doris Cowell and L.D. and Joanne Temple, who taught me the value of hard work, determination and selflessness, and to my wife, Jamie Phillips-Temple, for her constant love and support.

ACKNOWLEDGEMENTS

First, I would like to thank my committee for their constant support, guidance, and advice. I am sincerely grateful to my major professor, Dr. Eric Sparks, for allowing me the space, personnel and financial support to push the limits of field ecological research, and the opportunity to grow both academically and professionally. I would also like to thank him for quick email replies and phone calls, and ALL the mucho macho burritos. I am grateful to Dr. Just Cebrian for his eternally optimistic attitude in the field, research support and willingness to share relevant literature, and to Dr. Anna Linhoss and Dr. Adam Skarke for their willingness to share coding and for demystifying geotechnical and coastal engineering concepts. I am grateful to Dr. Bret Webb for answering all of my questions, use of his wave tank, MATLAB guidance, and for several afternoon lunches and frosties at Mellow Mushroom. I am also grateful to the Management Application Team and the Weeks Bay National Estuarine Research Reserve for their guidance and support of this research.

I would like to thank the Wildlife, Fisheries and Aquaculture staff for their administrative support and faculty for teaching and learning opportunities in their classes. I would like to thank all of the undergraduate student workers, interns and lab technicians in the Coastal Conservation and Restoration Program that provided valuable assistance to my research. I would also like to thank my cohort of original Sparks Lab members: Sara Martin for support and encouragement in her own way and Daniel Firth for always getting in the thick of it. In addition, I am thankful to

my Master's advisor Julia Cherry for her constant support and for introducing me to all of these wonderful Gulf Coast folks.

Finally, and most importantly, I would like to thank my family and friends. Thank you to our little village of friends in Fairhope for the good times and adventure away from work. Thank you to Adam Constantin for the laughs, quick reads and edits on emails and manuscript drafts, and for lending an ear and advice on research obstacles and general questions. Thank you to my cousins, Davey and Skeet Daniels, for their example. Thank you to my birth parents, Gene and Ellee, and my "adopted" parents, Jim and Alicia Phillips and Sherri Temple, for their constant support, encouragement, and love. Thank you to my sister, Erin, for her unwavering faith in my abilities. Lastly, thank you to my wife, Jamie, for putting up with me all these years. I could not have done this without you.

TABLE OF CONTENTS

DEDICATION ii

ACKNOWLEDGEMENTS iii

LIST OF TABLES viii

LIST OF FIGURES x

CHAPTER

I. INTRODUCTION 1

1.1 Impetus for Dissertation 1
1.2 Dissertation Goal and Objectives 4
1.3 Organization of Dissertation 4
1.4 Literature Cited 6

II. LOW-COST PRESSURE GAUGES FOR MEASURING WATER WAVES 9

2.1 Abstract 9
2.2 Introduction 10
2.3 Methods 11
2.3.1 DIY Wave Gauge Description 11
2.3.1.1 Sensing Water Levels 11
2.3.1.2 Logging Water Levels 12
2.3.1.3 DIY Wave Gauge Housing and Deployment 13
2.3.2 Laboratory and Field Testing 14
2.3.2.1 Wave Channel and Wave Test Description 14
2.3.2.2 Field Performance Test 15
2.3.2.3 Gap-filling DIY Pressure Data 17
2.3.2.4 Statistical Analyses 17
2.4 Results 18
2.5 Discussion 19
2.5.1 Agreement 19
2.5.2 Applications 21
2.5.2.1 Data Processing for Wave Climate Inferences 22
2.6 Conclusions 23
2.7 Literature Cited 29

III. PLANT RESPONSES ALONG A WAVE CLIMATE GRADIENT 31

3.1 Abstract 31
3.2 Introduction 32
3.3 Methods 37
3.3.1 Study Site Description 37
3.3.2 Wave Data Collection and Processing 39
3.3.3 Plant Response Variables 40
3.3.3.1 Subplot Establishment and Data Collection 40
3.3.3.2 Aboveground Plant Data 41
3.3.3.3 Belowground Biomass 42
3.3.4 Environmental Characteristics 43
3.3.4.1 Soil Bulk Density 43
3.3.4.2 Marsh Platform Elevation and Slope 44
3.3.5 Statistical Analyses 44
3.4 Results 45
3.4.1 Wave climate 45
3.4.2 Site environmental characteristics 47
3.4.3 Plant responses 48
3.4.3.1 Diversity across study sites 48
3.4.3.2 Aboveground shoot responses 49
3.4.3.3 Belowground root responses 51
3.5 Discussion 52
3.6 Conclusions 60
3.7 Literature Cited 70

IV. NITROGEN REMOVAL IN CONSTRUCTED MARSHES AT SITES PROTECTED FROM AND EXPOSED TO WAVES 77

4.1 Abstract 77
4.2 Introduction 78
4.3 Methods 83
4.3.1 Study Site Description 83
4.3.2 Experimental Design and Site Construction 84
4.3.3 Experimental Run-off Simulations 87
4.3.4 Porewater Sampling and Processing 88
4.3.5 Percent Cover Change 88
4.3.6 Statistical Analyses 88
4.4 Results 89
4.4.1 Main Treatment Effects 89
4.4.2 Effects of Sediment Type and Initial Planting Density at the Protected Site 90
4.4.3 Plant Cover at the Exposed and Protected Sites 91
4.5 Discussion 92
4.6 Conclusions 97
4.7 Literature Cited 109

V. SYNTHESIS....115

5.1 Overview....115
5.2 Development of the Low-cost Wave Gauge....116
5.3 Plant Responses Along a Wave Climate Gradient....117
5.4 Wave and Other Environmental Effects on the Nutrient Removal Capacity of Constructed Marshes....118
5.5 Summary of Gained Insights and Recommendations for Future Research....119
5.6 Literature Cited....122

APPENDIX

A. CHAPTER II APPENDIX....124

A.1 Mississippi State University Coastal Conservation and Restoration Program (CCR) Waves Website....125
A.2 Video Tutorial....125
A.3 Additional Building Instructions....125
A.3.1 Downloading Arduino© Integrated Development Environment (IDE) and Libraries Required for DIY Gauge Code....125
A.3.2 Initial Testing of Sensors and Atmospheric Pressure Adjustments in the Field....126
A.3.3 Setting the Real Time Clock (RTC)....126
A.3.4 Uploading the Gauge Code....127
A.3.5 Biofouling....127
A.4 DIY Gauge Data Loss....128
A.5 Data Processing for Statistical Analyses....128
A.6 Using MATLAB Scripts....129
A.7 Literature Cited....138

B. CHAPTER III APPENDIX....139

B.1 Wind Rose Data....140
B.2 Gauge Record Data Comparisons to 10-year Wind-wave Models....141
B.3 Literature Cited....145

C. CHAPTER IV APPENDIX....146

LIST OF TABLES

Table 2.1 Commercial and DIY pressure gauge features and costs including sensor characteristics. 25

Table 2.2 Laboratory wave channel test description and results. 25

Table 3.1 Gauge deployment schedule within waterbodies and corresponding US National Holidays. 62

Table 3.2 Record-length bay and river site wave statistics. 62

Table 3.3 Mean (± SE) record wave statistics, windowed wave statistics and environmental characteristics of data collected at each of the study waterbodies. 63

Table 3.4 Regression models relating plant response variables to log-transformed fiftieth percentile wave height for both *J. roemerianus* and *S. alterniflora.* 64

Table 3.5 Correlation matrices for plant response variables, log-transformed fiftieth percentile wave heights, and environmental characteristics. 65

Table 4.1 Results from ANOVA models examining the main effects of experimental treatments at protected and exposed sites for A and B well NOx concentrations. 99

Table 4.2 Reduced ANOVA model results constructed from protected site data collected from a and b wells and following spring and post summer simulations. 100

Table 4.3 Cover contrasts from reduced ANOVA models constructed from protected site data collected from A and B wells and following spring and post summer simulations. 101

Table 4.4 Pairwise comparisons of sediment type and initial planting density treatments effects on porewater NO_x concentrations collected from A wells following simulation 2. 102

Table A.1 A complete list of all materials needed to construct the DIY wave gauge including estimated costs (USD before taxes and based on 2019 prices) and web links for purchasing. 131

Table C.1 Kruskal-Wallis model results constructed from protected and exposed site observed cover data. 147

LIST OF FIGURES

Figure 2.1 DIY wave gauge housing and deployment methods. 26

Figure 2.2 Overlaid DIY and RBR pressure signals through time. 27

Figure 2.3 Overlaid DIY and RBR power spectral density curves constructed from field performance data. 28

Figure 3.1 Map of study sites within the different waterbodies in and surrounding Mobile Bay, Alabama, USA. 66

Figure 3.2 Regression models relating shoot basal diameter to log-transformed fiftieth percentile wave height for both *J. roemerianus* and *S. alterniflora*. 67

Figure 3.3 Regression model relating the percentage of live shoots to log-transformed fiftieth percentile wave height in *J. roemerianus* marsh canopies. 68

Figure 3.4 Regression model relating log-transformed total live root biomass to log-transformed H_{50} wave heights in fringing *J. roemerianus* marshes. 69

Figure 4.1 Map showing the location of the study area, experimental project sites and donor marsh. 103

Figure 4.2 Overview of experimental treatment combinations at the exposed and protected sites. 104

Figure 4.3 Cross sectional view of experimental marsh flumes. 105

Figure 4.4 Mean porewater NO_x concentrations collected from a and b wells at the protected site plotted by initial planting density treatment and sediment type. 106

Figure 4.5 Observed percent cover of the study species (*Juncus roemerianus)* and other species by simulation and by initial planting density treatment at the protected site. 107

Figure 4.6 Observed percent cover of the study species (*Juncus roemerianus*) and other species by simulation and by initial planting density treatment at the exposed site. 108

Figure A.1 Wave test 1 regressions and analysis of differences plots. 132

Figure A.2 Wave test 2 regressions and analysis of differences plots.....133

Figure A.3 Wave test 3 regressions and analysis of differences plots.....134

Figure A.4 Wave test 4 regressions and analysis of differences plots.....135

Figure A.5 Wave test 5 (JONSWAP wave spectra with $H_s = 0.2$, $T_p = 2$, $\gamma = 3.3$) regressions (A-C) and analysis of differences (D-F) plots.....136

Figure A.6 Regression of the field performance test raw pressure data.....137

Figure B.1 Monthly average speed (m/s) and direction of winds in Bon Secour Bay, Alabama, USA.....140

Figure B.2 Wave statistic comparisons at southern facing sites in Mobile Bay.....143

Figure B.3 Wave statistic comparisons at northern facing sites in Mobile Bay.....144

Figure C.1 Experimental mesocosm used at protected site.....148

Figure C.2 General set up facilitating simulated ground water (SGW) flow within experimental flumes.....149

CHAPTER I

INTRODUCTION

1.1 Impetus for Dissertation

Coastal wetland loss continues at alarming rates (Weston 2014). As a result, the prevalence of marsh construction as a part of coastal conservation, restoration, and enhancement projects has increased. There are many factors to consider when designing or constructing a coastal restoration project. One of the most important of these factors, and one that has a significant influence on project design, is wave climate.

Wave climate is a major driver of many coastal processes (e.g., shoreline erosion, sediment transport, vegetation persistence etc.) that influence coastal conservation, restoration, and shoreline enhancement projects, such as green infrastructure and living shorelines (Leonardi *et al.* 2017, Roland and Douglass 2005). However, wave climate assessment is limited largely because of the high cost of commercial gauges. Modelling approaches can be effective alternatives to commercial gauges but these approaches rely primarily on natural features such as fetch length and wind velocity and do not include human influences, such as boat wake, that are now common features in many coastal environments (Bilkovic *et al.* 2019, Booji 1999, McConchie and Toleman 2003). While modeling works well in open water environments with little human influence (Fonseca *et al.* 2016), many estuaries are composed of narrower waterways (*i.e.,* fetch-limited) and experience frequent human pressures. Furthermore, more restoration and conservation projects occur in waterways where current wave modeling

approaches are not applicable (*e.g.,* narrow bays, bayous, and sloughs). For example, nearly 65% of The Nature Conservancy and Mobile Bay National Estuary Program-led living shorelines projects in Alabama occur along fetch-limited shorelines (Herder 2016). Additionally, most waterfront properties suitable for shoreline enhancement or protection occur along these shorelines. These sensitive areas are environmentally and economically important: fringing marshes and oyster reefs in narrow waterways support commercial and recreational fisheries that are often staples of coastal economies (Barbier *et al.* 2011, NOAA 2015, Gittman *et al.* 2016) and generate additional benefits, such as nutrient removal (Sparks *et al.* 2015). Though these fetch-limited shorelines are particularly vulnerable to waves, many restoration guides do not account for their effects or use subjective "rules of thumb" (Hardaway *et al.* 2010, NOAA 2015) despite the need for objective design criteria and potential impact of boat wakes (*e.g.,* Glamore 2008). Low-cost wave gauges could substantially improve wave climate assessment and would replace limited modelling approaches and subjective assessment techniques. Further, these gauges could be an important tool for land managers designing coastal restoration, conservation and enhancement projects.

Limited access to wave gauges has also limited our understanding of the ways that plants respond to waves. Historically, research examining plant responses to waves has focused on how plants affect waves. For example, what factors most influence wave attenuation in marshes (Feagin *et al.* 2009, Mullarney and Henderson 2010, Neumeier and Ciavola 2004, Neumeier and Amos 2006)? The way that waves influence plant growth responses, on the other hand, has received less attention, despite evidence of shifting plant responses from various other environmental factors (Kirwan and Megonigal 2013, Nyman *et al.* 2006, Temple *et al.* 2019, Vasquez *et al.* 2006). Instead, researchers have combined the former "engineering" worldview

and the growth strategy theory of ecology to explain plant features observed in differing wave climate environments (Bouma *et al.* 2010, Puijalon *et al.* 2011, Silinski *et al.* 2018). However, this approach does not fully account for the range of plant growth responses possible along a wave climate gradient and may further limit land manager abilities to design and implement effective projects.

Finally, waves may affect one or more of the ecosystem services often targeted in projects. In their seminal study, Roland and Douglass (2005) demonstrated that plant growth is limited by the increasing regularity of greater magnitude waves, suggesting that limiting waves through design is necessary for successful marsh establishment. However, waves likely affect the ecosystem services provided by marshes as well. Nutrient removal during runoff events is an increasingly important and valuable service provided by marshes (Costanza et al. 2014), is potentially affected by waves, and is especially relevant given the prevalence of coastal eutrophication (Dodds 2006, Rabalais *et al.* 2002). Understanding how waves interact with various site and project design factors such as sediment type, initial planting density, platform elevation and slope is important to further improve project effectiveness.

The purpose of this dissertation was to improve the effectiveness of coastal restoration, conservation and enhancement projects through design and validation of a low-cost wave gauge, by exploring wave climate effects on marsh growth responses, and by investigating the main and interactive effects of various site and design-specific factors on the nutrient removal capacity of constructed marshes at sites exposed to and protected from waves. Moreover, this research is designed to provide and/or enhance decision support tools for coastal land managers while also investigating the current growth-strategy paradigm explaining plant responses to waves (e.g.,

Silinski *et al.* 2018). Thus, this research is valuable from both basic and applied science perspectives and is timely considering the prevalence and need for constructed wetland projects.

1.2 Dissertation Goal and Objectives

The goal of my dissertation was three-fold. First, I sought to develop and validate a wave gauge using a low-cost sensor, housing and data logging equipment. Second, using these validated wave gauges, I used a novel, regression-based approach to explore plant growth and morphological responses at different sites within Mobile Bay and surrounding tributaries and sought to test the current growth strategy paradigm explaining plant responses to waves. Third, I explored the influence of waves on the nutrient removal capacity of constructed marshes in which several other site and design-specific factors were also experimentally manipulated including sediment type, initial planting density, platform slope and position. Within this framework, I developed the following three objectives:

Objective #1: Design and validate a low-cost wave gauge for measuring water waves.

Objective #2: Collect wave, plant and environmental data from sites within Mobile Bay, Alabama and surrounding tributaries so that plant growth and morphological responses can be examined along a wave climate gradient.

Objective #3: Use field experiments to examine the main and interactive effects of sediment type, initial planting density, platform elevation and slope on nitrogen removal at sites protected from and exposed to waves.

1.3 Organization of Dissertation

The research topics addressed in this dissertation are presented in three standalone articles that are prefaced with an introductory chapter and concluded with a synthesis chapter. In

Chapter II, titled, “Low Cost Gauges for Measuring Water Waves,” I describe the development and validation testing of a DIY pressure-based wave gauge. In the following chapter (III), entitled “Plant Responses Along a Wave Climate Gradient,” I review the literature concerning plant responses to waves and describe a large-scale field experiment wherein I deployed several DIY wave gauges at sites within and surrounding Mobile Bay, Alabama and collected wave, plant and ancillary environmental data to examine the current paradigm explaining plant responses to waves. In Chapter IV, titled “Nitrogen Removal in Constructed Marshes at Sites Protected from and Exposed to Waves,” I describe a field experiment in which the nutrient removal capacity of several restoration designs were evaluated at wave-protected and -exposed sites. A summary of experimental findings described in Chapters II-IV and synthesis is provided in the final chapter (V).

1.4 Literature Cited

Barbier, E. B., Hacker, S. D., Kennedy, C., Koch, E. W., Stier, A. C., & Silliman, B. R. (2011). The value of estuarine and coastal ecosystem services. *Ecological monographs, 81*(2), 169-193.

Bilkovic, D. M., Mitchell, M. M., Davis, J., Herman, J., Andrews, E., King, A., ... & Dixon, R. L. (2019). Defining boat wake impacts on shoreline stability toward management and policy solutions. *Ocean & Coastal Management, 182*, 104945.

Booij, N., Ris, R. C., & Holthuijsen, L. H. (1999). A third-generation wave model for coastal regions: 1. Model description and validation. *Journal of geophysical research: Oceans, 104*(C4), 7649-7666.

Bouma, T. J., Vries, M. D., & Herman, P. M. (2010). Comparing ecosystem engineering efficiency of two plant species with contrasting growth strategies. *Ecology, 91*(9), 2696-2704.

Dodds, W. K. (2006). Nutrients and the "dead zone": the link between nutrient ratios and dissolved oxygen in the northern Gulf of Mexico. *Frontiers in Ecology and the Environment, 4*(4), 211-217.

Costanza, R., De Groot, R., Sutton, P., Van der Ploeg, S., Anderson, S. J., Kubiszewski, I., ... & Turner, R. K. (2014). Changes in the global value of ecosystem services. *Global environmental change, 26*, 152-158.

Kirwan, M. L., & Megonigal, J. P. (2013). Tidal wetland stability in the face of human impacts and sea-level rise. *Nature, 504*(7478), 53-60.

Feagin, R. A., Lozada-Bernard, S. M., Ravens, T. M., Möller, I., Yeager, K. M., & Baird, A. H. (2009). Does vegetation prevent wave erosion of salt marsh edges? *Proceedings of the National Academy of Sciences, 106*(25), 10109-10113.

Fonseca, R. B., Gonçalves, M., & Guedes Soares, C. (2016). Comparing the performance of spectral wave models for coastal areas. *Journal of Coastal Research, 33*(2), 331-346.

Gittman, R. K., Peterson, C. H., Currin, C. A., Joel Fodrie, F., Piehler, M. F., & Bruno, J. F. (2016). Living shorelines can enhance the nursery role of threatened estuarine habitats. *Ecological Applications, 26*(1), 249-263.

Glamore, W. C. (2008). A decision support tool for assessing the impact of boat wake waves on inland waterways. *On-Course, PIANC*, 5-18.

Hardaway, C.S., Milligan, D.A., & Duhring, K. (2010). Living Shorelines Design Guidelines for Shore Protection in Virginia's Estuarine Environments. *Special Report in Applied Marine Science and Ocean Engineering*, (421).

Herder, T. (2016) Alabama Living Shorelines: An Educational Tour for Decision-Makers. Co-sponsored by Mississippi-Alabama Sea Grant Consortium, Mobile Bay National Estuary Program, The Nature Conservancy, CSI Media Consultants LLC.

Leonardi, N., Ganju, N. K., & Fagherazzi, S. (2016). A linear relationship between wave power and erosion determines salt-marsh resilience to violent storms and hurricanes. *Proceedings of the National Academy of Sciences, 113*(1), 64-68.

McConchie, J. A., & Toleman, I. E. J. (2003). Boat wakes as a cause of riverbank erosion: a case study from the Waikato River, New Zealand. *Journal of Hydrology* (New Zealand), 163-179.

Mullarney, J. C., & Henderson, S. M. (2010). Wave-forced motion of submerged single-stem vegetation. *Journal of Geophysical Research: Oceans, 115*(C12).

Neumeier, U., & Ciavola, P. (2004). Flow resistance and associated sedimentary processes in a *Spartina maritima* salt-marsh. *Journal of Coastal Research*, 435-447.

Neumeier, U., & Amos, C. L. (2006). Turbulence reduction by the canopy of coastal *Spartina* salt-marshes. *Journal of Coastal Research,* 433-439.

NOAA (2015). Guidance for Considering the Use of Living Shorelines. Silver Spring, Maryland: National Oceanic and Atmospheric Administration, 36p.

Nyman, J. A., Walters, R. J., Delaune, R. D., & Patrick Jr, W. H. (2006). Marsh vertical accretion via vegetative growth. *Estuarine, Coastal and Shelf Science, 69*(3-4), 370-380.

Puijalon, S., Bouma, T. J., Douady, C. J., van Groenendael, J., Anten, N. P., Martel, E., & Bornette, G. (2011). Plant resistance to mechanical stress: evidence of an avoidance–tolerance trade-off. *New Phytologist, 191*(4), 1141-1149.

Rabalais, N. N., Turner, R. E., & Wiseman Jr, W. J. (2002). Gulf of Mexico hypoxia, aka "The dead zone". *Annual Review of ecology and Systematics, 33*(1), 235-263.

Roland, R. M., & Douglass, S. L. (2005). Estimating wave tolerance of Spartina alterniflora in coastal Alabama. *Journal of Coastal Research*, 453-463.

Silinski, A., Schoutens, K., Puijalon, S., Schoelynck, J., Luyckx, D., Troch, P., ... & Temmerman, S. (2018). Coping with waves: Plasticity in tidal marsh plants as self-adapting coastal ecosystem engineers. *Limnology and Oceanography, 63*(2), 799-815.

Sparks, E. L., Cebrian, J., Tobias, C. R., & May, C. A. (2015). Groundwater nitrogen processing in Northern Gulf of Mexico restored marshes. *Journal of environmental management, 150*, 206-215.

Temple, N. A., Grace, J. B., & Cherry, J. A. (2019). Patterns of resource allocation in a coastal marsh plant (*Schoenoplectus americanus*) along a sediment-addition gradient. *Estuarine, Coastal and Shelf Science, 228*, 106337.

Vasquez, E. A., Glenn, E. P., Guntenspergen, G. R., Brown, J. J., & Nelson, S. G. (2006). Salt tolerance and osmotic adjustment of *Spartina alterniflora* (*Poaceae*) and the invasive haplotype of *Phragmites australis* (*Poaceae*) along a salinity gradient. *American Journal of Botany, 93*(12), 1784-1790.

Weston, N. B. (2014). Declining sediments and rising seas: an unfortunate convergence for tidal wetlands. *Estuaries and Coasts*, *37*(1), 1-23.

CHAPTER II

LOW-COST PRESSURE GAUGES FOR MEASURING WATER WAVES

2.1 Abstract

Waves have profound effects on coastal geomorphology but the understanding of wave climate effects on coastal ecology is limited due, in part, to the high cost of commercial wave gauges. In addition to broad ecological implications, high cost gauges also limit the scope of coastal wave models and the ability of coastal land managers to design effective restoration, conservation and enhancement projects. To address this need, a low-cost DIY wave gauge was constructed from commercial plumbing parts and using a pressure sensor, an Arduino© microcontroller and adapted accessories. Performance of the DIY gauge was determined by evaluating agreement of raw pressure data recorded by the DIY gauge and a comparable commercial gauge in a laboratory wave channel study featuring five wave tests of varying amplitude and frequency. Agreement of raw pressure data from each gauge in each of the tests was assessed using paired t-tests and by examining differences along the range of pressure values. Raw pressure data from each gauge were also applied to linear models to determine which wave conditions created the greatest variability between pressure readings. Pressure data agreement between the DIY and commercial wave gauges was excellent in all tests with mean differences between pressure readings consistently near zero and with 95% of all differences lying within ± 0.63 millibar (< 1 cm static water depth), on average. Linear models indicated the greatest variability between readings occurred within tests featuring high frequency waves,

mirroring results reported by others. Still, raw DIY wave gauge data explained, on average, 91% of the variance in raw commercial gauge data. Thus, the DIY wave gauge is an excellent alternative to high-cost gauges that could improve the understanding and management of coastal environments. Details on gauge construction, coding and an instructional video tutorial are also provided.

2.2 Introduction

Waves shape coastal environments (Sorenson 2006) and are a major driver of erosion (Leonardi *et al.* 2016). However, the effects of wave climate on the ecology of coastal environments are not fully understood (Fulton *et al.* 2005, Roland and Douglass 2005). Questions concerning the influence of waves on coastal ecology are especially relevant in areas experiencing rapid wave climate modification from boating activity (McConchie and Toleman 2003) and climate change (Reguero et al. 2019). Assessing wave climate is typically achieved using one of two methods: wind-wave models or field measurement using gauges. Wind-wave models are relatively accessible and inexpensive but are not designed to account for boat wakes, which are the dominant contributor to wave energy in some coastal environments (*e.g.,* rivers; McConchie and Toleman 2003) and are a prominent feature in most inshore coastal areas (*e.g.,* Bilkovic *et al.* 2019). Commercial wave gauges can account for both wind-waves and boat wake waves but are inaccessible to many researchers because of their high cost (Table 2.1). Even if researchers have access to commercial gauges, the high costs may still effectively limit inferences from wave climate studies due to cost-driven limits on spatial resolution. Low-cost wave gauges could allow more researchers to perform direct wave climate assessments and increase the spatial resolution of wave climate data, furthering the understanding of coastal ecology and improving coastal conservation, enhancement, and restoration projects.

To address this need, this paper explores the feasibility of constructing a do-it-yourself (DIY) wave gauge using low-cost materials (*e.g.,* Beddows and Mallon 2018, Lockridge *et al.,* 2016, Mickley *et al.* 2018, Miller 2014) and assesses the gauge's performance by evaluating agreement between the DIY gauge and a commercial gauge in laboratory wave channel and field tests. Results from this study demonstrate that the DIY gauge is an excellent alternative to high-cost commercial wave gauges. Additionally, novice-level details on gauge development, coding instructions, and a discussion of gauge applications and wave data processing are provided.

2.3 Methods

2.3.1 DIY Wave Gauge Description

Construction of the DIY wave gauge seeks a balance between accessibility, utility and practicality. Housing materials include those that are readily available at home improvement stores and high performance electrical components that have many user-friendly features including: easy assembly, user-friendly documentation, and open-source libraries (Table A.1). These features are described in more detail below. In addition, an instructional video detailing each step of gauge construction is provided along with a list of gauge housing materials and electronic components with links for purchasing and current (*i.e.,* 2019) costs in the Appendix (Appendix A, Table A.1).

2.3.1.1 Sensing Water Levels

Similar to comparable commercial gauges, the DIY gauge uses a pressure sensor to measure water levels indirectly by relating pressure to water depth (Table 2.1). The pressure sensor used in DIY gauges is the MS5803-14BA (SparkFun Electronics, USA) and features a piezo-resistive sensor and an integrated 24-bit analog-to-digital converter that is programmable

to various sampling frequencies. Variations of this sensor have been used previously for wave (Herbert *et al.* 2018, Miller 2014), depth (Beddows and Mallon 2014), and tide level measurements (Miller 2014), but literature searches suggest that none have been evaluated for agreement with commercial gauges.

2.3.1.2 Logging Water Levels

The DIY wave gauge is built around the Arduino© hardware and open source software platform, similar to other DIY scientific instruments (*e.g.,* Beddows and Mallon 2018, Lockridge *et al.* 2016). As such, it features several Arduino-based components to control reading and logging of sensor data through time, including an Arduino© Uno microcontroller, a data logging shield (with a built-in, real time clock), a battery, and a power booster (Table A.1). Likewise, the software to control the sensing of water levels and writing of timestamped sensor data to the SD card was developed in the Arduino© integrated development environment (IDE) and uses open source libraries. As currently configured, the DIY gauge runs (sampling at 8 to 10 Hz continuously) for approximately 5.5 days on one 6600 mAh lithium ion battery. This sampling schedule and battery configuration favors event-based gauge deployment (*e.g.,* tropical storms, weekend boat traffic). However, the adaptable nature of the DIY wave gauge housing (discussed below) allows simple battery life extension by increasing the number of batteries or with coding adjustments (*e.g.,* burst sampling). Event-based code for the DIY wave gauge is available for download at the Mississippi State University Coastal Conservation and Restoration Program website (http://coastal.msstate.edu/waves).

2.3.1.3 DIY Wave Gauge Housing and Deployment

Pressure sensor-based gauges are deployed in the water with a waterproof housing necessary for all but the pressure-sensing element of the sensor. In comparison to commercial gauges with specialized machined parts, DIY scientific instruments are typically constructed from non-specialized common materials (Beddows and Mallon 2018, Lockridge *et al.* 2016, Mickley *et al.* 2018, Miller 2014). The DIY wave gauge housing is constructed similarly using common PVC plumbing parts (Figure 2.1A). A standard 7.62 cm (3 inch) diameter pipe cut to 30 cm (~10 inches) length serves as the main body housing the sensitive electrical components (*i.e.,* microcontroller, datalogger, battery and powerbooster). A flat 7.62 cm diameter cap permanently seals one end of the main housing pipe and provides a base for sensor potting (*e.g.*, Beddows and Mallon 2018) within a 3.81 cm (1.5 inch) diameter pipe cut to 3.175 cm (1.25 inch) length and glued approximately in the center of the larger cap using PVC cement (Oatey 31008 Heavy Duty Solvent Cement, Oatey, USA). To pot the sensor (*e.g.,* Beddows and Mallon 2018), a 1.27 cm (0.5 inch) diameter hole is drilled approximately in the center of the smaller pipe and through the flat cap, and thus permitting the sensor wires to be fed to the microcontroller in the main housing pipe. The wired sensor is then set within the smaller pipe on the flat cap using epoxy putty (Rectorseal EP-200, CSW Industrials, USA). Epoxy sealant (Loctite 237116 E-30CL Hysol Epoxy, Henkel AG & Co., Germany) is then poured evenly over the potted sensor so that sensor electronics are sealed while leaving the sensing element of the sensor exposed (Figure 2.1B). After the epoxy is fully cured (approximately 72 hours), the flat cap is glued to the main housing pipe using PVC cement. A removable 7.62 cm cap (Oatey Gripper Mechanical Test Plug, Oatey, USA) provides access to the battery and SD card within the main housing pipe while also providing a watertight seal (Figure 2.1A). Before deployment, desiccant packs and foam

padding are added at either ends of the main housing pipe to buffer the assembled gauge electronics. Constructed DIY wave gauges can be deployed in the field by securing them to anchors, such as boating anchors (Figure 2.1C), cinder blocks, etc., that rest on the sea floor or securing them to pilings. In total, the DIY gauge costs less than $300 USD, including housing and electrical components—an order of magnitude less than the closest comparable commercial gauge (Table 2.1). Details on gauge materials and building instructions, including videos, are available at the Mississippi State University Coastal Conservation and Restoration Program website (http://coastal.msstate.edu/waves, Appendix A.2, Table A.1). Additional building instructions related to sensor testing and gauge coding are provided in the Appendix (Appendix A.3).

2.3.2 Laboratory and Field Testing

DIY wave gauge performance was evaluated in both laboratory and field tests. First, a series of wave tests were conducted in a laboratory wave channel study designed to minimize environmental error and to explore specific conditions known to increase error in pressure gauges (*i.e.,* high-frequency waves; described below). Additionally, overall DIY gauge performance was evaluated in a five-day field deployment test. Details of both tests, as well as special processing procedures for DIY wave gauge data and the statistical methodology used for comparisons are described below.

2.3.2.1 Wave Channel and Wave Test Description

A DIY and commercial wave gauge were programmed to sample at 8 Hz continuously and placed in a wave flume (17.5 m long x 1.5 m wide x 1 m deep; Armfield Limited) at the University of South Alabama (Mobile, Alabama, USA) for testing. The DIY gauge and the

commercial pressure gauge (RBR Solo^3 D depth logger; hereafter "RBR") were attached to a 34-kilogram steel plate resting on the floor of the wave channel at a water depth of 60 centimeters. After the gauges were secure, a series of fifteen 90-second wave tests (five wave tests with three replications each; described below) were conducted using a wave generator (HR Wallingford) within the wave channel, with appropriate breaks in between tests to allow for water level settling.

The different wave tests included regular and irregular wave types and varied in wave characteristics (*i.e.,* frequency and amplitude; Table 2.2). These tests were designed to create conditions that would maximize variability in pressure readings and to emulate real-world waves (*e.g.,* wind-waves and boat wakes). Tests 2 and 3 featured short-period (*i.e.,* high frequency) waves known to increase variability in pressure signals due to pressure sensor limitations (*e.g.,* Lee and Wang 1984) and the physical variability of wave phenomena (*e.g.,* Hoque and Aoki 2006). Waves are rarely regular (*e.g.,* simple sine wave; Figure 2.2A) in the environment and are often irregular in nature (*i.e.,* composite of multiple sine waves of varying frequency and amplitude). Therefore, in addition to tests featuring regular waves (Tests 1-4), Test 5 featured a wave spectra (JONSWAP) consisting of several irregular waves (Figure 2.2B).

2.3.2.2 Field Performance Test

The DIY and RBR gauges were deployed for five days (Thursday, August 30 to Tuesday, September 4, 2018) within Fowl River in Mobile County, Alabama, USA. Wave climate in this mesohaline tributary of Mobile Bay is primarily the result of boating activity (Webb *et al.* 2018). Therefore, the timing (*i.e.,* weekend deployment) and location (30º26'41.77"N, 88º07'40.79"W) were selected to maximize boat wake exposure (Webb *et al.* 2008). This reach of Fowl River is approximately 100 meters wide with maximum depth less than 3 meters and experiences a

diurnal tidal cycle (max tidal range approximately 0.60 m). Black needle rush (*Juncus roemerianus)* marsh flanks both sides of the river channel.

Both gauges were deployed to a depth of 1m at high tide within the subtidal mudflat and approximately 1 m from the marsh edge. The RBR was deployed by attaching the gauge to a PVC pipe driven into earth. The DIY gauge was deployed approximately 1 m from the RBR and parallel to the marsh edge by attaching the gauge to a 6.8 kg (15 lb) anchor (*e.g.,* Figure 2.1C).

In contrast to laboratory wave channel testing, the field setting is characterized by several potentially variable conditions that can increase the variability in gauge pressure readings that ultimately limit individual wave event comparisons. In particular, shoreline bathymetric (*i.e.,* platform slope and elevation) and biological (*e.g.,* presence/absence of biota) features can vary substantially over relatively small distances in the field (Gomes *et al.* 2016), having various effects on wave characteristics (*e.g.,* height and breaking behavior; Sorenson 2006) and subsequent pressure readings. In addition, significant temporal variability in the expression of different wave events is likely due to differences in gauge positioning (*i.e.,* with respect to wave transmission) as boats pass by in different directions. This environmental and temporal variability in the field, coupled with the potential for further variability associated with wave-wave interactions (*e.g.,* wave phase shift) following the simultaneous advancement of two or more boats precludes individual wave event comparisons. However, wave energy density spectra describe the magnitude of wave energy as a function of wave frequency (Sorenson 2016) and are thus unrelated to the timing of events. In addition, spectral analysis methods often incorporate filtering techniques to address environmental noise. These techniques were used to assess field test data agreement and are discussed further below.

2.3.2.3 Gap-filling DIY Pressure Data

Initial processing of DIY pressure data indicated that a small portion (< 1%) of data captures were missing (*i.e.,* no pressure data was recorded; Appendix A.4). Therefore, a gap-filling routine was developed in MATLAB (2017a) using linear interpolation to fill in missing data captures. This routine (available for download at http://coastal.msstate.edu/waves) was used to prepare field and laboratory data for statistical analyses in tests in which missing captures were identified (Table 2.2).

2.3.2.4 Statistical Analyses

Laboratory wave channel and field performance test data were assessed using different statistical procedures according to the objectives associated with each.

Following initial data processing (Appendix A.5), agreement for laboratory test data were determined by comparing paired raw pressure data from each gauge for each wave test. Overall agreement between raw pressure readings was assessed using paired t-tests and by examining differences along the range of pressure readings in each test, following Bland and Altman (1999). In addition, linear regression models were fit to paired raw data. Model coefficients were used to evaluate agreement further, while the coefficient of determination (R^2; hereafter, "model fit") was used to explore the conditions that maximized variability between gauge readings.

Field test data were compared using spectral analysis and linear regression techniques. Processed signals (Appendix A.5) were passed through fast Fourier transform sequences which were then applied to periodograms to construct power spectral density (PSD) curves in MATLAB (2017a). The total energy in the wave field (*i.e.,* area under the PSD curve; m_0) contained in the DIY signal was assessed as a percentage of energy contained in the RBR signal to determine agreement as follows:

$$Percent\ agreement = \frac{m_{0(DIY)}}{m_{0(RBR)}} x\ 100 \quad (2.1)$$

A linear regression model was fit to paired raw pressure data to further evaluate overall field raw data agreement.

All statistical analyses were performed in R (R Core Team 2017). Figures were made using the ggplot2 (Wickham 2009) package.

2.4 Results

Raw DIY pressure data compared very favorably to that of the RBR in each of the wave channel tests (Table 2.2). Paired t-tests indicated no significant differences between gauge pressure readings in any of the tests ($P \geq 0.7$). Indeed, the mean difference between raw DIY and RBR pressure readings was consistently near zero (absolute value of mean difference ≤ 0.004). 95% confidence intervals of mean differences across the range of pressure readings were variable, ranging from ± 45 to ± 166 Pa (Table 2.2, Figures A.1 – A.5), but on average 95% of observed differences fell within ± 63 Pa (< 1 cm static water depth). Linear model coefficients mirrored these results with slopes ranging from 0.81 to 1.08, but having intercepts consistently near zero (Table 2.2). However, model coefficients deviated from within ± 0.1 of predicted values (i.e., slope = 1, intercept = 0) only once, in a test designed to maximize variability (i.e., test 3b; slope = 0.81, Table 2.2). Likewise, model fit was variable as a function of testing design (Figures A.1 – A.5). As expected, model fit was poorest in Tests 2 and 3 ranging in R^2 values from 0.69 to 0.91 (Table 2.2). Model fit was ≥ 0.9 in all other test comparisons and was, on average, 0.91 throughout testing (Table 2.2).

Field performance test data analyses mirrored laboratory wave channel test results. Wave energy density distribution was similar between the gauges (Figure 2.3) and total wave field energy agreement was excellent (92%). Model fit was also excellent ($R^2 = 0.997$) with model coefficients mirroring those found in the majority of wave channel tests (slope = 1, intercept = 0).

2.5 Discussion

To expand on the performance of the DIY wave gauge, DIY and commercial gauge wave channel and field performance test data agreement are discussed in the context of pressure sensor limitations and agreement between other commercial pressure gauges reported elsewhere. This contextual description is followed by a discussion of DIY wave gauge applications, benefits and details concerning data processing for wave climate inferences.

2.5.1 Agreement

This study explored the use of a low-cost DIY wave gauge in comparison with a commercial gauge with similar yet differing pressure sensing technology (*e.g.,* sensor resolution and accuracy; Table 2.1). As such, some variability between DIY and RBR pressure gauge readings was expected, especially in wave channel tests exploring known pressure sensor limitations. Indeed, some wave characteristics resulted in greater variability in gauge pressure readings (Table 2.2). However, variability was low in most tests (≤ 10%) and differences between gauge readings were near zero with relatively little difference between readings across the range of pressure values (±63 Pa). Thus, overall agreement between the DIY and RBR gauges in all wave channel tests was excellent, including results from tests that most mimic real-world waves (Test 5; Figure 2.2B). Field performance testing provides further support as the

DIY gauge tracked the RBR remarkably well (Figure A.6) and captured the range of frequency responses that comprise the total energy in the wave field as recorded by the RBR (Figure 2.3).

Increased variability between pressure readings was expected in wave channel tests 2 and 3 due to the higher frequency waves examined in each of the tests. However, this increase in variability reflects a fundamental limitation of pressure sensors that is exacerbated by profound differences between gauges in electrical configuration (Lee and Wang 1984) and shape (Bishop and Donelan 1987). Discerning differences in the configuration and attributes of electrical components between the RBR and DIY gauges is difficult if not impossible without damaging the RBR. Still, it is reasonable to suspect a number of differences exist between the gauges that contribute to increasing signal noise at higher frequencies including differences in sensor type, power source, and numerical noise from analog to digital conversion (Lee and Wang 1984). The most striking difference between the gauges is shape. Bishop and Donelan (1987) examined the potential effect of gauge shape on pressure signals by adding a sphere to the end of one of pair of identical pressure gauges. They found this slight change in shape increased the error between the gauge signals by five percent. Considering the DIY wave gauge is three times as wide and twice as long as the RBR, these differences in shape are likely another source of error compounded by sensor limitations. Finally, differences in sensor attributes between the two gauges, including sensor resolution and accuracy differences (Table 2.1), are likely amplified during high frequency wave events. While some re-configuring of DIY electronics and/or technological advancement in the quality of components used in DIY gauges may improve agreement in these scenarios (*i.e.,* high frequency waves), several methods have been developed to deal with high frequency signals. As is, DIY pressure data explained, on average, 86% of the variance in RBR pressure data within this frequency (F = 0.99 Hz), which is well within the range of inter-

instrument error reported elsewhere (80%; Bishop and Donelan 1987, Esteva and Harris 1970). This variability decreased with decreasing frequency in wave channel tests (Table 2.2) with similar results reported in the field performance test (Figure 2.3). Thus, the DIY gauge becomes more accurate within the frequency bands that contribute substantially to the energy density spectrum (Sorenson 2006).

In summary, agreement between gauges was within acceptable ranges (Figure 2.2A) to near 100% (Figure 2.2B) in wave channel tests, and excellent overall (92%) in the field performance test. Also, while some wave conditions created more variability between pressure gauges in wave channel tests, mean differences in all tests were essentially zero (Table 2.2). Therefore, the DIY gauge is a viable alternative to commercial wave gauges at a price point well below that of the closest comparable commercial gauges (Table 2.1).

2.5.2 Applications

This study explored a cost-effective tool that would allow researchers to increase the resolution and accuracy of wave climate models and/or pioneer new questions concerning the effects of wave climate on ecosystems. Beyond that, the DIY pressure gauge also has several practical uses including enhanced environmental characterization for restoration and conservation planning by coastal land managers, consultants, contractors, and researchers.

In addition to practical applications, DIY gauges can be easily customized for specific needs. For example, with coding adjustments (*e.g.*, Beddows and Mallon 2018), DIY wave gauges could be configured to sample periodically (i.e., short sampling intervals between longer sleep periods). This sampling adjustment would extend battery life significantly, allowing for longer deployments. In addition, since the gauge housing is also highly customizable, battery life could be extended by simply adding additional batteries. The DIY gauge could also be adapted

for other water level monitoring applications (e.g., river stage assessment, inundation, tide levels).

Finally, an underappreciated asset of low-cost gauges is that they are easily replaceable. Extreme weather events frequently have profound effects on ecosystem structure and function. However, deploying gauges during these events puts expensive equipment at risk. Using DIY gauges can greatly reduce financial risks to equipment associated with these events.

2.5.2.1 Data Processing for Wave Climate Inferences

Additional data processing and analysis is needed to make inferences from wave gauge data. These types of analyses were mostly avoided in this study because they are derivative, and thus do not reflect actual instrument values necessary for agreement assessment (Bland and Altman 1999). Nevertheless, extracting wave characteristics from field pressure data is necessary for wave climate assessment, assessment of the effect of engineered structures on waves and for calculating other wave-induced phenomena (*e.g.,* bed shear stress).

One approach to wave climate assessment takes a statistical approach to wave characteristics. In these statistical analyses, waves are identified from de-trended signals (*e.g.,* mean water levels and/or tides removed) using a zero- crossing method (*e.g.,* zero down-crossing; Foristall 1978) and wave characteristics (*i.e.,* wave height and period) are derived using linear wave theory approximations (Sorenson 2006). Wave characteristics are then sorted in descending order for statistical analyses. Significant wave height ($H_{1/3}$ or sometimes H_s) is the most widely recognized statistic in these types of analyses but it is simply the average of the top third of all wave heights in the record. Other wave statistics describe wave characteristics similarly by averaging within percentile ranges (*e.g.,* $H_{1/10}$ describes the average of the top one tenth of all wave heights in the record), while other statistics describe minimum and maximum

values (*e.g.,* T_{max} describes the maximum wave period of all wave periods in the record). Wave statistics can be examined over the entire record or within discrete time intervals (*e.g.,* windows) throughout the entire record (*e.g.,* Roland and Douglass 2006).

Another approach to wave climate characterization takes an approach similar to that described in the evaluation of field performance test data agreement (*i.e.,* spectral analyses). In general, spectral analyses use a transformation (*e.g.,* fast Fourier transformation) to approximate a de-trended signal, such as a record of water surface elevation data, as a summation of multiple sine waves characterized by differing wave amplitude and frequency. These transformed data are often used to determine the power spectral density contained in time series records as a function of wave frequency. This information can then be used to extract wave height and period parameters, as wave height squared is proportional to the energy contained in waves and wave period is inversely proportional to wave frequency. For example, spectrally significant wave height (H_{m0} or sometimes H_s) is a statistic derived from the total energy in the wave field (*i.e.,* $\sim 4\sqrt{m_0}$).

Deriving these processing routines can be difficult for researchers without signal processing experience. Therefore, to enhance the application of the DIY wave gauge, links for basic processing routines utilizing both methods are available for download at http://coastal.msstate.edu/waves. Directions for using scripts are provided in the Appendix (Appendix A.6).

2.6 Conclusions

The DIY wave gauge presented here is a cost-effective and highly customizable tool for measuring waves. Data accuracy is strong compared to a commercial gauge, and the gauge is easily constructed with little expertise. Several studies have examined the range of effects to

ecosystems and the ecological significance of wave climate (*e.g.,* Heuner *et al.* 2015, Fulton *et al.* 2005, Roland and Douglass 2005, Rupprecht *et al.* 2017). However, this research is limited in contrast to coastal engineering disciplines. DIY gauges can help to bridge this gap and to increase the interdisciplinary discussion necessary to further understand coastal ecology and to address pressing environmental issues like climate change.

Table 2.1 Commercial and DIY pressure gauge features and costs including sensor characteristics.

Gauge	Water level sensor	Sensor resolution	Sensor accuracy	Sampling frequency (output)	Cost (USD)
Nortek Aquadopp	Pressure transducer	Up to 1 Pa	0.5% FS	1 to 2 Hz	$12,000
RBR Solo^3 D	Pressure transducer	Up to 200 Pa	0.05% FS	Up to 32 Hz	$3,000
DIY gauge	Digital pressure	Up to 20 Pa	14.3% FS	Up to 120 Hz	< $300

The DIY gauge features a sensor with capabilities similar to those of commercial gauges but at a lower cost.

Table 2.2 Laboratory wave channel test description and results.

Test Description				**Linear Model**				**Analysis of Differences**			
Test	**Rep**	**F (Hz)**	**A (m)**	**Intercept**	**Slope**	**R^2**	***P***	**Mean difference**	**95% CI Lower (Pa)**	**95% CI Upper (Pa)**	**T-test *P***
1	a	0.5	0.08	0.000	1.08	0.99	0	-0.001	-63.4	63.1	0.93
1	b	0.5	0.08	0.004	1.08	0.98	0	0.003	-80.5	81.2	0.83
1	c	0.5	0.08	0.003	1.09	0.98	0	0.002	-73.2	73.7	0.87
2	a	0.99	0.08	0.000	0.95	0.84	0	0.000	-59.1	59.0	0.97
2	b	0.99	0.08	0.001	0.98	0.91	0	0.001	-44.9	45.2	0.87
2	c	0.99	0.08	0.001	0.93	0.83	0	0.001	-61.6	61.8	0.95
3	a	0.99	0.12	0.000	0.93	0.82	0	0.000	-81.8	81.8	0.99
3	b	0.99	0.12	0.000	0.81	0.69	0	0.000	-108.0	108.0	0.99
3	c	0.99	0.12	0.000	0.93	0.88	0	0.000	-67.1	67.1	0.99
4	a	0.75	0.12	0.003	0.94	0.92	0	0.004	-149.0	149.0	0.9
4	b	0.75	0.12	0.001	0.96	0.98	0	0.001	-70.6	70.7	0.97
4	c	0.75	0.12	-0.001	0.99	0.97	0	-0.001	-74.4	74.2	0.95
5	a	0.5	0.2	0.000	0.98	0.96	0	0.000	-108.0	108.0	0.997
5	b	0.5	0.2	-0.004	1.00	0.99	0	-0.004	-61.8	60.9	0.7
5	c	0.5	0.2	0.000	0.96	0.89	0	0.000	-166.0	166.0	0.99

Wave test description includes information about wave frequency (F) and amplitude (A). Tests 2b, 2c, 3b and 4a results were computed from gap-filled DIY gauge data. Test 5 uses JONSWAP wave spectra with $H_s = 0.2$, $T_p = 2$, $\gamma = 3.3$.

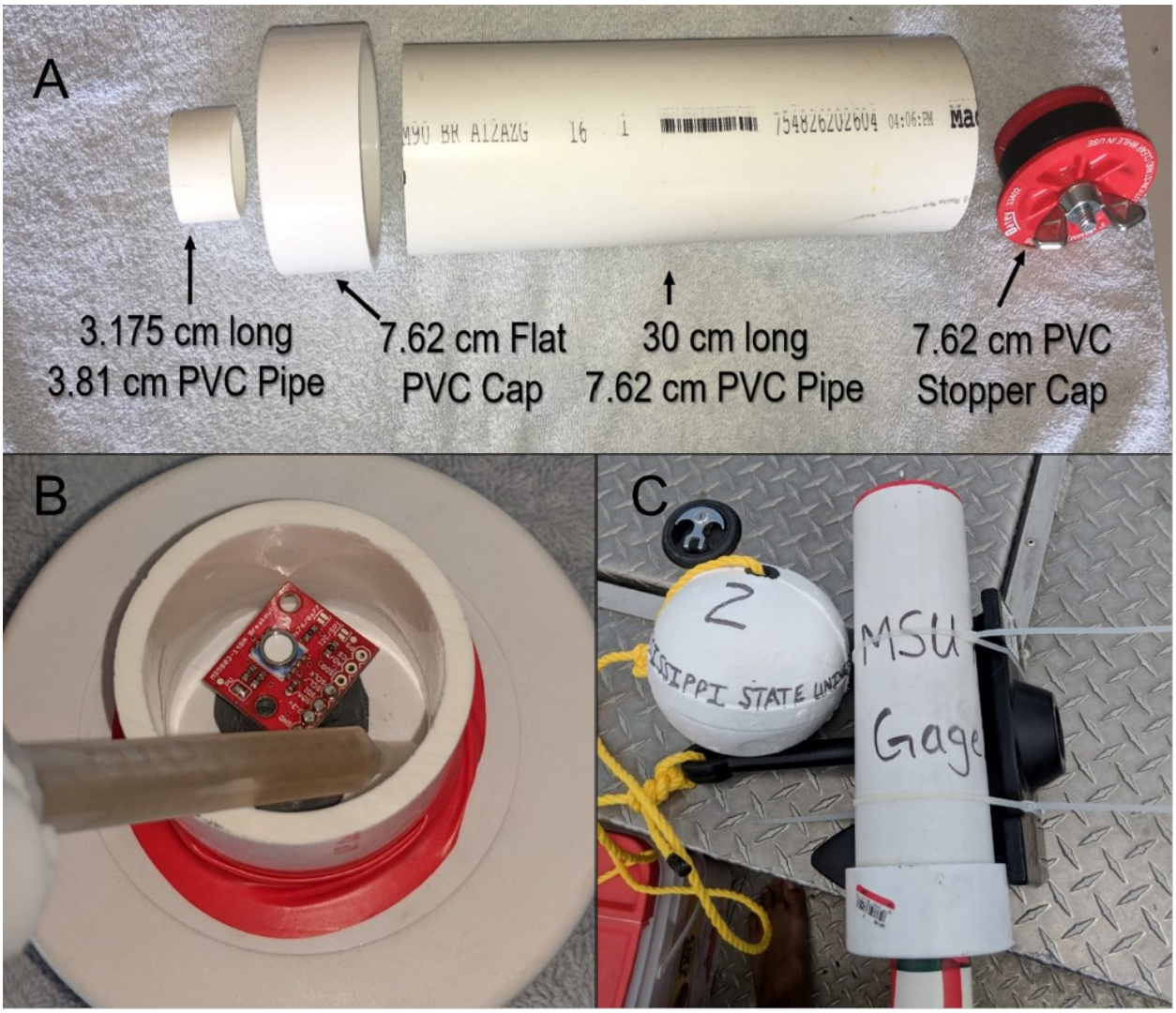

Figure 2.1 DIY wave gauge housing and deployment methods.

(A) The DIY wave gauge is constructed from common PVC plumbing parts. (B) The pressure sensor is mounted within a smaller pipe on top of the flat PVC cap which is waterproofed to the sensing element using epoxy. (C) The assembled gauge can be attached to an anchor fastened to a rope and buoy for easy deployment and retrieval in the field.

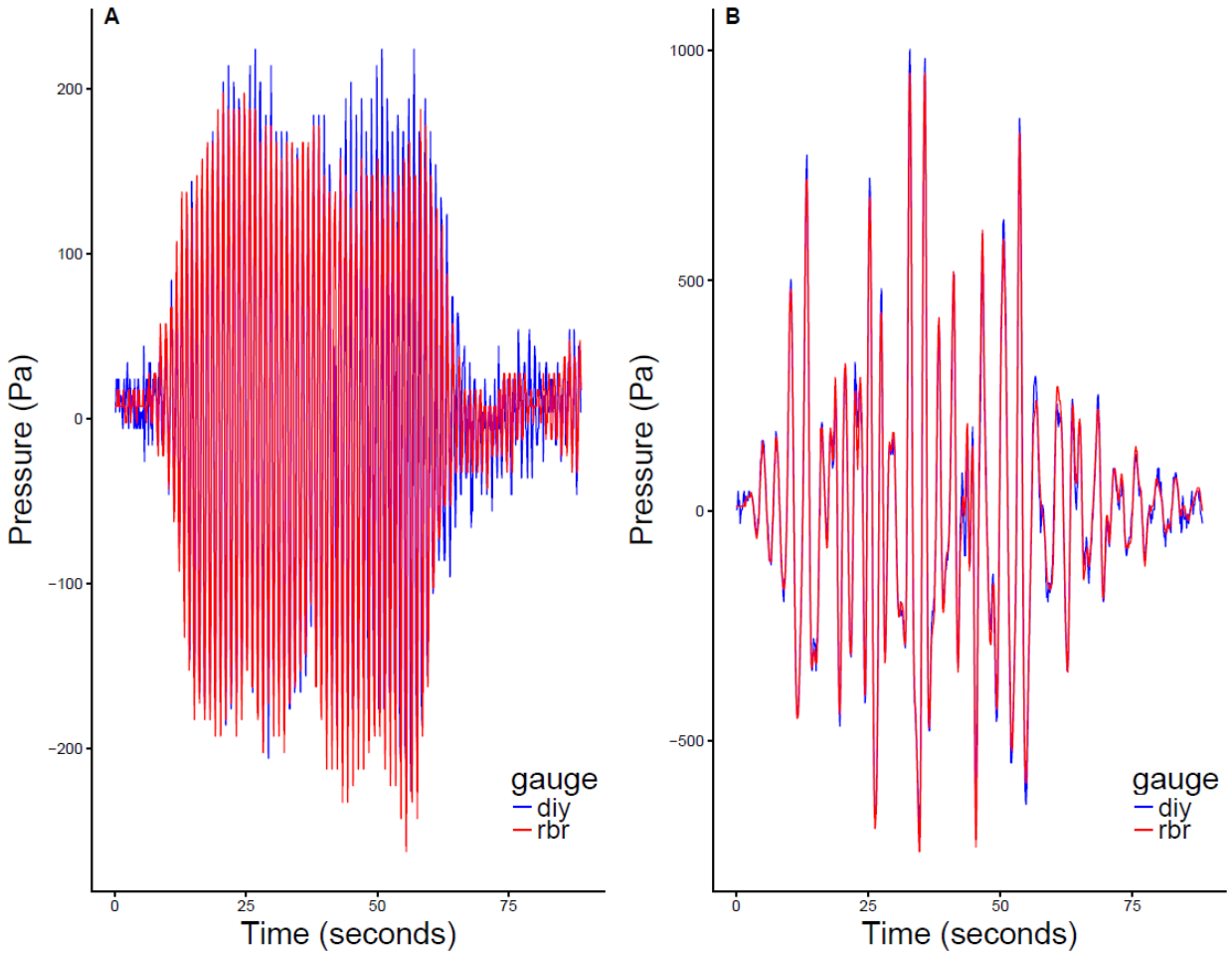

Figure 2.2 Overlaid DIY and RBR pressure signals through time.

Overlaid DIY (blue) and RBR (red) pressure signals (Pa, y axis) through time (seconds, x axis). Panel (A) shows the signals from wave test 3b which features a regular wave (Table 2). Panel (B) shows signals from wave test 5b which features a series of irregular waves (Table 2). The DIY gauge is within acceptable agreement at worst (A) and near 100% agreement at best (B).

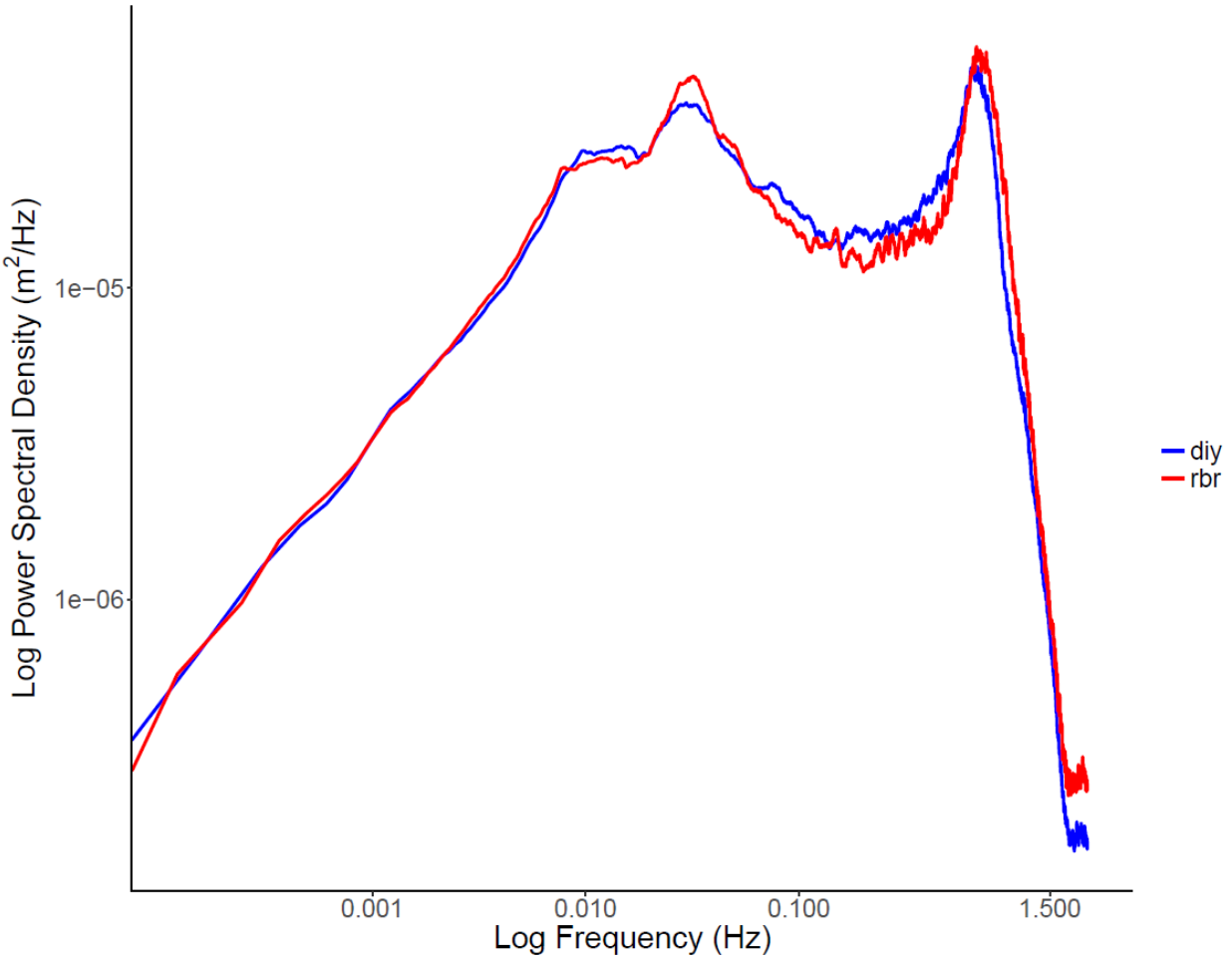

Figure 2.3 Overlaid DIY and RBR power spectral density curves constructed from field performance data.

Overlaid DIY (blue) and RBR (red) power spectral density (PSD) curves constructed from field performance test data. The DIY PSD curve is very similar to that of the RBR across the different frequency bands (x-axis). The total area under each PSD (*i.e.,* m_0) is also similar and overall wave field energy agreement is excellent (92%).

2.7 Literature Cited

Beddows, P. A. & Mallon, E. K. (2018). Cave pearl data logger: A flexible Arduino-based logging platform for long-term monitoring in harsh environments. *Sensors,* 18(2), 530.

Bilkovic, D. M., Mitchell, M. M., Davis, J., Herman, J., Andrews, E., King, A., Mason, P., Tahvildari, N., Davis, J., & Dixon, R. L. (2019). Defining boat wake impacts on shoreline stability toward management and policy solutions. *Ocean & Coastal Management*, https://doi.org/10.1016/j.ocecoaman.2019.104945.

Bland, J. M. & Altman, D. G. (1999). Measuring agreement in method comparison studies. *Statistical methods in medical research, 8*(2), 135-160.

Bishop, C. T. & Donelan, M. A. (1987). Measuring waves with pressure transducers. *Coastal Engineering, 11*(4), 309-328.

Esteva, D. & Harris, D. L. (1970). Comparison of pressure and staff wave gage records. *Proceedings of the Eleventh Coastal Engineering Conference* (Cape Town, South Africa, ASCE), pp. 101-116.

Forristall, G. Z. (1978). On the statistical distribution of wave heights in a storm. *Journal of Geophysical Research: Oceans, 83*(C5), 2353-2358.

Fulton, C. J., Bellwood, D. R. & Wainwright, P. C. (2005). Wave energy and swimming performance shape coral reef fish assemblages. *Proceedings of the Royal Society B: Biological Sciences, 272*(1565), 827-832.

Gomes, E. R., Mulligan, R. P., Brodie, K. L., & McNinch, J. E. (2016). Bathymetric control on the spatial distribution of wave breaking in the surf zone of a natural beach. *Coastal Engineering, 116*, 180-194.

Herbert, D., Astrom, E., Bersoza, A., Batzer, A., McGovern, P., Angelini, C., Wasman, S., Dix, N. & Sheremet, A. (2018). Mitigating erosional effects induced by boat wakes with living shorelines. *Sustainability, 10*(2), 436.

Heuner, M., Silinski, A., Schoelynck, J., Bouma, T. J., Puijalon, S., Troch, P., Fuchs, E., Schroder, B, Meire, P. & Temmerman, S. (2015). Ecosystem engineering by plants on wave-exposed intertidal flats is governed by relationships between effect and response traits. *Plos one, 10*(9), e0138086.

Lee, D. Y. & Wang, H. (1984). Measurement of surface waves from subsurface gage. *Proceedings of the Nineteenth Coastal Engineering Conference* (Cape Town, South Africa, ASCE), pp. 271-286.

Leonardi, N., Ganju, N. K. & Fagherazzi, S. (2016). A linear relationship between wave power and erosion determines salt-marsh resilience to violent storms and hurricanes. *Proceedings of the National Academy of Sciences, 113*(1), 64-68.

Lockridge, G., Dzwonkowski, B., Nelson, R. & Powers, S. (2016). Development of a low-cost arduino-based sonde for coastal applications. *Sensors,* 16(4), 528.

MATLAB 2017a, The MathWorks, Inc., Natick, Massachusetts, United States.

McConchie, J. A. & Toleman, I. E. J. (2003). Boat wakes as a cause of riverbank erosion: a case study from the Waikato River, New Zealand. *Journal of Hydrology (New Zealand),* 163-179.

Mickley, J. G., Moore, T. E., Schlichting, C. D., DeRobertis, A., Pfisterer, E. N. & Bagchi, R. (2018). Measuring microenvironments for global change: DIY environmental microcontroller units (EMUs). *Methods in Ecology and Evolution, 10*(4), 578-584.

Miller, L. (2014). Open wave height logger. https://lukemiller.org/index.php/2014/08/open-wave-height-logger/

R Core Team (2017). *R: A language and environment for statistical computing*. R Foundation for Statistical Computing, Vienna, Austria. http://www.R-project.org/

Reguero, B. G., Losada, I. J. & Méndez, F. J. (2019). A recent increase in global wave power as a consequence of oceanic warming. *Nature communications*, 10.

Roland, R. M. & Douglass, S. L. (2005). Estimating wave tolerance of *Spartina alterniflora* in coastal Alabama. *Journal of Coastal Research*, 453-463.

Rupprecht, F., Möller, I., Paul, M., Kudella, M., Spencer, T., Van Wesenbeeck, B. K., Wolters, G., Jensen, K., Bouma, T.J. & Schimmels, S. (2017). Vegetation-wave interactions in salt marshes under storm surge conditions. *Ecological engineering, 100*, 301-315.

Sorenson, R. M. (2006). Basic Coastal Engineering. New York: Springer Science and Business Media, 324p.

Webb, B. M., Smallegan, S. M., Mazur, E. & Lamonte, L. (2018). Incident boat wake energy and implications for restoration design. Bays & Bayous Symposium, Habitat Management, Nov. 29, 2018. Mobile, AL.

Wickham, H. (2011). ggplot2. *Wiley Interdisciplinary Reviews: Computational Statistics,* 3(2), 180-185.

CHAPTER III

PLANT RESPONSES ALONG A WAVE CLIMATE GRADIENT

3.1 Abstract

Wetlands are increasingly valued for their role in coastal defense. In particular, wetland plants slow the progression of waves by increasing the drag and friction forces they experience, thereby decreasing wave heights, orbital velocities and associated energy. Practical application of these effects has driven substantial research estimating the effects of plants on waves. The effects of waves on plants, however, remains understudied, especially regarding plant responses along a wave climate gradient. To begin to understand these responses, we collected above- and below-ground plant data, wave, and other environmental data from sixty sites across a large estuary and evaluated plant responses along the range of assessed wave climate and environmental conditions. Plant responses observed among the dominant species *Juncus roemerianus* and *Spartina alterniflora* varied among wave and environmental variables. However, in contrast to previous findings, the basal diameter of shoots in both species declined linearly with increasing wave climate conditions. While wave climate had no observable effect on other *S. alterniflora* parameters, the declining diameter of *J. roemerianus* shoots along the same gradient was commensurate with a decline in the percentage of live canopy shoots aboveground and an increase in root and rhizome biomass in the active rooting zone belowground. Other responses, including the height and density of above-ground shoots in both species, were more related to changes in soil bulk density or elevation than wave climate. These

results demonstrate the dynamic interplay between waves, local environmental conditions and plant features that have implications to subsequent wave attenuation and coastal defense.

3.2 Introduction

Coastal wetland plants face many threats including natural stressors such as salinity (Howard and Mendelssohn 1999), erosion from waves and currents (Green and Coco 2014) and interspecific competition for suitable habitat (Pennings *et al.* 2005), and human-induced threats such as development (e.g., "coastal squeeze"; Constantin *et al.* 2019), sediment deprivation (Tweel and Turner 2012), and sea-level rise (Osland *et al.* 2017). While the convergence of these threats can lead to marsh collapse in certain situations (Weston 2014), wetland plants, like other pioneering plant species, have exhibited exceptional adaptive capacity to modify above- and below-ground growth behaviors in response to a dynamic environment. Examples of shifting plant responses in coastal environments include shoot tissue osmotic adjustment in response to increasing salinity (Vasquez *et al*. 2006), enhanced shoot production in response to increasing sediment burial (Temple *et al*. 2019), adventitious rooting in response to increasing inundation (Nyman *et al*. 2006), and biological elevation maintenance (Kirwan and Megonigal 2013). While several studies have identified plant mechanistic responses to common coastal stressors such as salinity, inundation and competition, plant growth responses to waves remain understudied while waves have become an increasingly common feature in most aquatic environments (Bilkovic *et al* 2019, McConchie and Toleman 2003). This information is needed to improve our understanding of the relationship between plants and increasing wave conditions, the potential consequences to coastal ecosystems that may result from shifts in these relationships, and to improve the effectiveness of coastal conservation, restoration and enhancement projects.

When waves interact with plants, they experience increased friction and drag forces that decrease wave orbital velocities, height and associated energy (Neumeier and Amos 2006, Rupprecht *et al*. 2017). The relative effects of these forces, however, are also highly dependent on plant features and hydrodynamic conditions (i.e., wave height and period, and water depth). In general, friction forces increase with an increase in plant surface area exposed to waves. In regard to plant features, this can be accomplished by either increasing the density or biomass of shoots (Bouma *et al*. 2010, Heuner *et al*. 2015). Shoot stiffness/flexibility affects the degree of drag forces experienced by waves through its effects on plant motion in response to waves (Bouma *et al*. 2010, Rupprecht *et al*. 2017). As both friction and drag forces are contingent on plant exposure to wave forces, shoot height may impact the degree to which waves experience both. Water depth has a similar effect on friction and drag forces due to its control over marsh canopy inundation, as waves penetrate a smaller percentage of the marsh canopy with increasing water depth. This is especially relevant during storm events when water levels and wave heights are greatest (Neumeier and Ciavola 2004). While plant-wave interactions are mediated by water depth, the overall impact of plants on waves may also depend on wave characteristics (*e.g*., wave height and period; Bradley and Houser 2009, Maza *et al*. 2015). For example, some research shows thresholds for plant mediated wave energy dissipation, in which plant effects on waves increases to a certain level before declining significantly (Bradley and Houser 2009, Maza *et al*. 2015). Further, both wave conditions and plant growth vary significantly through time. Therefore, drag and friction forces and subsequent wave reductions are expected to be greatest in periods of maximum plant growth, when shoot height and density are greatest (Silinski *et al*. 2017, Vuik *et al*. 2018).

From the plant perspective, the expression of different traits identified in wave attenuation studies is often described as a tradeoff between traits that allow them to avoid wave mechanical stress and those that enhance their ability to slow the progress of waves (*i.e.,* avoidance and tolerance traits; Puijalon *et al*. 2011, Silinksi *et al*. 2018). Avoidance traits are generally described as those that reduce plant exposure to stresses such as increased shoot flexibility (Heuner *et al*. 2015), reduced shoot height (i.e., in relation to water depth; Rupprecht *et al*. 2017), and having a streamlined canopy that reduces the area exposed to wave forces (Puijalon *et al*. 2005). Tolerance traits, on the other hand, are described as those that enhance the ability of plants to endure stresses such as increased shoot density (Peralta *et al*. 2008, Heuner *et al*. 2015), increased shoot biomass (Bouma *et al*. 2010, Heuner *et al*. 2015), increased shoot stiffness (Mullarney and Houser 2005, Rupprecht *et al*. 2017), and increased rooting depth and production (Balke *et al*. 2011, Silinska *et al*. 2017). These traits may also balance tradeoffs between wave defenses and sediment accretion (Puijalon *et al*. 2011). For example, stiffer shoots generally allow for greater reductions in flow velocity and wave energy (Mullarney and Henderson 2005) which, in turn, can increase sedimentation (Kirwan and Megonigal 2013). Alternatively, sedimentation is generally lower among plants characterized by more flexible stems (*e.g.,* seagrasses), but flexible stems are more likely to adapt a protective "shielding posture" (*i.e.*, lying flat) during high energy wave events thereby reducing stem breakage and bed erosion (Rupprecht *et al*. 2017). While these interactions are also mediated by environmental characteristics such as soil properties (*e.g.,* sediment type and bulk density; Feagin 2009, Silinski *et al*. 2018), marsh platform elevation and slope (Morris *et al*. 2002, Silinski *et al*. 2016, Sorenson 2006), they illustrate the potential rippling effects to marsh persistence that may result from changes in either wave conditions or plant traits.

In comparison to other stressors in intertidal coastal wetlands, the ways in which plants alter the expression of traits in response to different or changing wave climate conditions remains understudied. Numerous studies have demonstrated the variability in above- and below-ground plant responses in relation to gradients of salinity (Vasquez *et al*. 2006), sediment addition (Stagg and Mendelssohn 2010, Temple *et al*. 2019), flooding (Morris *et al*. 2002) and nutrient addition (see Morris *et al*. 2013 for a review). While waves also occur along a range of both frequency (*i.e*., how often waves occur) and magnitude, knowledge of their effects on plant responses has often been limited to laboratory wave tank experiments that offer only limited insight to a set of short-term and specific conditions (Balke *et al*. 2011, Bouma *et al*. 2010, Mullarney and Henderson 2010, Rupprecht *et al*. 2017, Silinksi *et al*. 2015). Field studies have also been conducted but these studies have often focused on categorical wave exposure gradients (*i.e.,* exposed or sheltered; Keddy 1985, Coops *et al*. 1994, Silinksi *et al*. 2018) that limit the elucidation of plant relationships to changing wave environments (Cottingham *et al*. 2005). In a comprehensive field study to examine these relationships, Silinski *et al*. (2018) measured several soil characteristics and features of the study plant *Scirpus maritimus* to compare against varying wave height conditions at two nearby sites in a brackish marsh. Compared to specimens at a sheltered site (*i.e.,* an area, on average, experiencing lower magnitude wave heights), Silinski *et al*. (2018) found plants at an exposed site reflected an avoidance strategy to waves with shoots that were shorter in length and featured greater basal diameter and flexibility. These findings, while well in line with previous results from laboratory and field experiments (Bouma *et al.* 2010, Coops and Van der Velde 1996, Silinksi *et al.* 2015), describe responses of a single plant species to wave conditions at only two sites and hence, fail to describe the range of plant responses that could be expected along a gradient of wave conditions. Conversely, Roland and

Douglass (2005) described the presence and absence of *Spartina alterniflora* along a gradient of wave conditions but did not examine any of the features associated with the plants at different sites. Taken together, there is clearly a need to combine elements of both experiments to consider the full range of potential plant responses to varying wave conditions.

Increased knowledge of plant responses to various wave conditions is essential to improve the understanding of basic coastal processes and to ensure the long term persistence of coastal wetlands and the wealth of natural benefits they provide (Barbier *et al.* 2011, Sparks *et al.* 2015, others). Coastal wetland plants are keystone species, and thus, altered plant growth responses in response to changing wave conditions have the potential to create many rippling effects throughout coastal ecosystems. For instance, how do the morphological changes described by Silinski *et al*. (2018) for plants in exposed sites affect the habitat quality of *S. maritimus* marshes? The ways in which these shifting plant responses affect larger coastal ecosystems are also of importance to coastal land managers seeking to maximize many of the natural benefits of marshes. Identifying specific plant responses and potential feedbacks to waves along a wave climate gradient, for example, has the potential to improve modelling capabilities needed for effective design and installation of coastal conservation, restoration and enhancement projects. Therefore, improving our understanding of plant responses to waves is important from both basic and applied science perspectives.

The main objective of this study was to characterize the effects of increasing wave heights, both in magnitude and frequency of occurrence (*e.g.,* Roland and Douglass 2005), on plant growth and morphological responses in a large-scale field study. Previous efforts to measure waves has been limited due, in part, to the high cost of commercial wave gauges (*e.g.,* Silinski *et al.* 2018, Temple *et al.* 2020). However, recent technological advances now permit the

construction of high-quality wave gauges at a fraction of the cost of commercial gauges (Temple *et al*. 2020). In this study, these DIY gauges (Temple *et al*. 2020) were used to collect wave data from sixty sites within a large estuary in Alabama, USA that was processed to reflect the magnitude and frequency of occurrence of wave heights experienced at sites (e.g., Roland and Douglass 2005; hereafter, "wave climate"). We hypothesized that fringing marsh plants would respond to increasing wave climate by increasing shoot density, shoot biomass per shoot, basal stem diameter aboveground and by increasing the rooting depth belowground. To test these hypotheses, we measured above- and below-ground plant responses during the summer months of 2018 (*i.e.,* May – September, when plant productivity in Gulf of Mexico marshes is greatest; Stout 1984) and examined them along the measured wave climate gradient.

3.3 Methods

A comparative regression-based framework was used to explore the potential relationships between site wave climate and plant responses (Cottingham *et al*. 2005, Temple *et al*. 2019). Within this framework, sites were selected using proxies to cover a large gradient in wave conditions (*e.g.,* wave height and frequency of occurrence). Wave and plant response data were then collected from each site for comparison using regression models.

3.3.1 Study Site Description

Sixty sites including twenty within Mobile Bay (West Mobile Bay and Bon Secour Bay; WMB and BSB, respectively) and ten each within Bon Secour (BSR), Fish (FiR), Fowl (FoR), and Magnolia (MaR) Rivers in Baldwin and Mobile Counties, Alabama, USA (Figure 3.1) were examined. As with other estuarine environments, salinity within bay and river sites varies, creating patterns of plant species distribution. Salinity is greatest in the waters along the

southwestern edge of Mobile Bay (*i.e.,* on average 18 PSU; https://arcos.disl.org/) but salinity at all sites within the bay and river sites is generally brackish (0.5 – 18 PSU) and varies as a function of meteorological events (*e.g.,* tides, rainfall), distance from the Gulf of Mexico ("GoM") and, in the case of river sites, distance upstream from the river mouth. Plant communities at the study sites reflect this salinity gradient as the greatest abundance of salt tolerant species such as *Juncus roemerianus* and *Spartina alterniflora* are located in bay sites and at those sites nearest river mouths, while a mix of other species such as *Cladium jamaicense, Phragmites australis, and Typha latifolia* are present or dominant elsewhere where salinity approaches more freshwater conditions. The entire study area experiences a diurnal tidal cycle (max tidal range ~ 0.60 m). Maximum channel depth at river sites and average depth across the bay are similar at ~ 3 m (Noble *et al.* 1996).

The general location of each study site was selected using a combination of Google Earth, boating activity, and wind data (Appendix B.1, Figure B.1) to establish a wave climate gradient so that plant response variables could be examined within a regression statistical framework (*e.g*., Temple *et al*. 2019). Final site selection at all sites was determined in the field. First, relative site locations were found in the field using GPS coordinates generated in Google Earth. Sites were then selected based on the following selection criteria: including a near monotypic stand with patch size measuring at least 3 square meters (3 m x 1 m plot size). As to avoid bias towards sites with vegetation, when no vegetation was found within 100 meters in either direction of the relative site location, the Google Earth-generated GPS coordinates were used as a default final site location.

3.3.2 Wave Data Collection and Processing

A total of 30 pressure sensor-based wave gauges were constructed and deployed in the field during summer 2018 (May – September) following the methods described in *Temple et al*. (2020). As the number of gauges that could be deployed simultaneously was limited, the specific timing of gauge deployments was selected to maximize potential wave events and comparability between sites, and to reduce potential logistical issues (*e.g.,* excessive boat travel to different sites). Therefore, gauges were deployed according to geographic closeness and to coincide with major US holidays in which boating activity is generally high (*e.g.,* Memorial Day, Fourth of July, and Labor Day weekends, Table 3.1). In addition, gauges at all sites were deployed for a total of twenty days in four consecutive five-day long deployments within a roughly one-month period. This deployment schedule helped to minimize any variability associated with meteorological events that could skew wave data at the different sites (*e.g*., rain limited boating activity in river sites). All gauges were programmed to sample continuously at 10 times per second (10 Hz) which is sufficient to measure the short period waves characteristic of the wind- and boat wake-waves in the study area (Temple *et al*. 2020). During the study period, some gauges were lost due to debris impact or theft. In such cases, an additional gauge was built and deployed to ensure equal deployment length at each site.

Pressure data collected during each site deployment was processed individually in MATLAB (2017a). Water level data derived from gauge absolute pressure (gauge pressure + atmospheric pressure) were applied to a moving average routine to identify and remove the slowly varying components associated with the water level signal (*i.e.*, tides and atmospheric pressure). The resulting de-trended signal (*i.e.*, free surface elevation data) was then applied to a wave-by-wave analysis routine that identifies and compiles wave parameters (*i.e.,* height and

period) through time using a zero down-crossing method (*e.g.,* Foristall 1978) and linear wave theory approximations (Temple *et al.* 2020).

Wave frequency of occurrence and magnitude are particularly important for describing biological responses to disturbance events (*e.g.,* Connell 1978, Roland and Douglass 2005). Therefore, wave statistics were derived from within one-hour increments in windowing routines. Windowed wave statistics were then sorted in ascending order and a frequency of occurrence was calculated by dividing the parameter position by the total number of windowed records (*e.g.,* Roland and Douglass 2005). Windowed wave statistics were then compiled according to the frequency of occurrence into discrete percentile rankings along 25 percentage point increments (*i.e.,* 25^{th}, 50^{th}, 75^{th} and 100^{th} percentile rankings; H_{25}, H_{50}, H_{75}, and H_{100}, respectively) for varying magnitude wave events during individual deployments.

All wave statistic data (*i.e.,* record length and windowed wave statistics) at each site were averaged over the four deployment sampling periods (*i.e.,* a total of 20 days).

3.3.3 Plant Response Variables

Following previous research, plant response data were collected at each of the study sites. These data include above- and below-ground responses that are relevant to plant persistence in the presence of waves (*e.g.,* rooting depth, shoot biomass) and those often considered in models predicting wave movement through marshes (*e.g.,* stem height and diameter; Dean 1978).

3.3.3.1 Subplot Establishment and Data Collection

Three 1 m^2 quadrats were established and spaced evenly along the site shoreline within each 3 m x 1 m site plot (*i.e.,* three 1 m^2 boxes within each site plot). Within each quadrat, an open-ended 0.25 m^2 subplot marker constructed using PVC was placed haphazardly to delineate

subplot boundaries. All aboveground biomass within the boundaries of the 0.25 m^2 subplot was then removed at the sediment surface using shears, placed in plastic bags and transported in a cooler to the Weeks Bay National Estuarine Research Reserve (WBNERR) for further processing. Cores (~5 cm diameter) were then collected from within each subplot to assess belowground plant responses. The corer was custom fabricated at the Mississippi State University Coastal Research and Extension Center using steel pipe and featured a metal band-saw blade welded to one side of the corer and a "T" handle at the other. These features were designed to maximize the cutting action of the corer and to minimize compaction of the sediment layers. The corer was driven into the earth using a circular cutting motion until 50 cm depth or refusal was achieved and removed for further sorting on the boat. Using a knife, cores were then cut into four subsections starting from the top of the core (*i.e.,* at the sediment surface) and every 10 cm along the core depth profile to 40 cm or, in the case of shallow refusal, the maximum depth. Core subsections were placed in plastic bags and transferred in a cooler to WBNERR for further processing.

3.3.3.2 Aboveground Plant Data

Plant morphological features vary by species. For example, culms of *Juncus roemerianus* form from underground rhizomes with several upright leaves, often in groups of 1-3, emerging at the sediment surface while culms of *Spartina alterniflora* are characterized by a single upright stem that protrudes from the sediment surface with several alternate leaves protruding laterally along the stem. The functional implications of these morphological differences are not trivial and may have important consequences for the ecological dynamics of the marshes. However, with respect to plant-wave interactions, upright plant parts are functionally similar. Indeed, plant leaf architecture is not often considered in models examining the impact of plants on waves; rather,

aboveground plant parts as ideal cylinders having an average height and diameter (*e.g.,* Augustin et al. 2009, Dean 1978). Therefore, in this study, plant shoots describe all upright plant materials emanating from the sediment surface. As such, upright leaves of *J. roemerianus* and culms of *S. alterniflora* were counted and measured similarly. This context also forms the basis of functional significance with respect to plant-wave interactions useful for other plant features (*e.g.,* live and dead parts).

At WBNERR, shoots collected from each subplot were sorted by species into live (green) and dead (brown) parts. After sorting into live and dead parts, the percentage of live and dead shoots was measured and recorded. The total number of shoots (*i.e.,* stem density) included live and dead parts, as these parts are functionally similar with respect to plant-wave interactions (discussed above). Following sorting, the length (cm) of each stem was measured and sorted according to basal shoot diameter in ascending order. The basal diameter (mm) of three shoots with the largest diameter was measured at 15 cm above the base of the shoot to account for any deformation resulting from field shearing (*e.g*., widening/flattening). Shoots were then placed into paper bags according to species and live and dead parts and transported to the University of Southern Mississippi Gulf Coast Research Laboratory (GCRL) for further processing. At GCRL, shoots were dried at 50^{o}C to constant mass in a commercial drying oven and weighed to the nearest 0.1 gram (g).

3.3.3.3 Belowground Biomass

Core subsections were processed individually as follows. First, cores were rinsed of all sediments and debris using a 2000 micron sieve. All remaining materials were then placed in a ~23 cm x 33 cm x 8 cm glass dish which was then filled with water. Roots were sorted by live and dead parts, and by fine roots (≤ 1 mm diameter) and coarse roots/rhizomes. Live roots were

identified via elutriation (*e.g.*, Temple *et al.* 2019) while dead roots were picked free of debris including other inorganic (*e.g.,* glass) and non-root decaying organic materials (*e.g.,* partially decayed invertebrates). Sorted roots were then placed in paper sandwich bags and transported to GCRL for further processing. Following the methods described for plant shoots, roots were dried at 50ºC to constant mass in a commercial drying oven and weighed to the nearest 0.1 gram (g).

3.3.4 Environmental Characteristics

Several environmental characteristics can have direct and indirect effects on plant responses (Kirwan and Megonigal 2013). Of particular interest in this study, are those characteristics that affect both wave parameters (*e.g.,* wave height and period; Sorenson 2006) and plant responses (*e.g.,* inundation and position within the marsh platform; Morris et al. 2002), as determined by previous research examining similar relationships (Feagin *et al.* 2013, Silinski *et al.* 2015, Silinski *et al.* 2018). Therefore, in addition to wave and plant response data, soil bulk density, marsh platform elevation and slope data were collected from each of the study sites.

3.3.4.1 Soil Bulk Density

A mini-Russian corer (1.65 cm radius x 18 cm length) was used to extract cores from each site plot. The length of cores extracted in the field were recorded and then placed in storage bags for cooler transport to the Dauphin Island Sea Lab (DISL; Dauphin Island, Alabama, USA) for processing. At DISL, cores were gently blotted, placed in pre-weighed aluminum dishes and weighed before drying at 50ºC to constant mass in a commercial drying oven. Bulk Density was calculated as the dried core mass (g) divided by the core volume (cm^3).

3.3.4.2 Marsh Platform Elevation and Slope

A six meter transect running perpendicular from the center of each site shoreline was established. Using a Trimble© Real Time Kinematic (RTK) Global Positioning System (TSC-2 controller and Trimble-R8 Model-3 rover), a total of six elevation measurements and coordinate points were recorded using the NAVD88 datum along the perpendicular transect at 1 m increments so that three elevation points were taken above and below the center of plot shorelines. Marsh platform elevation was calculated as the average of the two points closest to the plot center point. All elevation data were adjusted in reference to local mean sea level (MSL) at the Dauphin Island tide station (https://tidesandcurrents.noaa.gov/stationhome.html?id=8735180; *e.g.,* Constantin *et al.* 2019). Slope was assessed at each site by fitting elevation data to linear models.

3.3.5 Statistical Analyses

Previous work on plant responses to varying frequency and magnitude wave events is limited (though see Roland and Douglass 2005, Keddy 1982); therefore, both linear and non-linear models were considered to accommodate all potential response patterns. Plant responses were first evaluated graphically following Zuur *et al*. (2010). Initial exploration of the relationships between plant response variables and wave climate data indicated similarity between plant responses at and above 50th percentile significant wave heights; therefore, 50th percentile significant wave height (*i.e.,* H_{50}) was used as the main wave predictor variable in all plant response models (see section 3.3.2). Site physical characteristic data were analyzed in two ways, i.e., as covariates in wave models and as main predictor variables for plant responses in simple linear regression. In addition to linear models, Pearson's correlation coefficients were used to summarize relationships (*i.e.,* strength and direction of correlation) between all plant

response variables and wave and environmental data collected. Akaike Information (Burnham and Anderson 2002) for linear and non-linear plant response models was used to guide final model selection. Model fit was evaluated using model coefficients and residual plots of transformed data, where appropriate, to meet model assumptions (Zuur *et al*. 2007). To compare within and across study sites for wave and environmental characteristics ANOVAs or non-parametric analogues (*i.e.,* Kruskwal-Wallis test of medians) were used. R was used for all statistical analyses (R core team 2017).

3.4 Results

3.4.1 Wave climate

Wave period data reflected the predominant drivers of wave action at the different sites (*i.e.*, wind and boat-wake at bay and river sites, respectively; Webb *et al*. 2018). Significant wave period (T_s) was, overall, greatest in bay sites as compared to river sites (2.67 s and 1.63 s median T_s, respectively, Kruskal-Wallis $p < 0.001$). T_s at WMB bay sites (mean = 3.39 s, Table 3.3) declined linearly from ~ 4 to ~2.5 seconds with distance away from the mouth of Mobile Bay ($R^2 = 0.82$, $p < 0.001$). However, T_s within other regions of Mobile Bay (*i.e.,* within BSB sites) averaged 2.5 seconds which, while still greater than average T_s at river sites, was well within the range of wave period conditions observed in those areas (Table 3.3). In addition, within-waterbody T_s variance was minimal in BSB and across each of the river sites (≤ 0.07 second) during the study period as compared to WMB (within site variance = 0.33 second).

Each of the wave height statistics measured, including both record-length (*i.e.,* H_{avg}) and windowed statistics (*e.g.,* H_{50}), showed similar overall trends of varying wave heights at study sites and confirmed the establishment of the wave climate gradient. Record-length average wave height (H_{avg}) conditions were greatest at bay sites as compared to river sites ($p < 0.001$, Table

3.2). However, differences between individual waterbodies did not necessarily fall in line with differences in waterbody types. For example, mean H_{avg} conditions were nearly identical between FoR and WMB sites, which both averaged 13 cm, and were greater than all other bay and river sites examined ($p < 0.001$; Table 3.3). Twenty-fifth percentile windowed wave heights (H_{25}) averaged less than 1 cm (± 0.14 SE) differences and were statistically similar to mean site H_{avg} conditions (t-test $p = 0.9$; Table 3.3). All other windowed wave height statistics (*i.e.*, H_{50}, H_{75}, and H_{100}) revealed similar trends across study sites but at varying magnitude wave heights, as a function of the rareness of wave height events (*i.e.,* greater wave heights are associated with higher percentile windowed wave heights; Table 3.3). Thus, across all sites, the wave climate gradient was established for both common and rare events. While there were exceptions, bay sites along the northern reaches of the bay (*i.e.*, facing southward) were generally characterized by greater H_{50} wave heights, though these differences were not significant ($p > 0.05$). River site H_{50} data was highly variable and reflected various underlying factors that may control the magnitude and frequency of occurrence for wave events such as a site's proximity to major boating channels or no wake zones, the speed of boats passing, the range of boat hull types, and existence of permanent or temporary obstructive structures (*e.g.,* pier or boathouse pilings and floating tree logs, respectively) that can act to attenuate waves (Glamore 2008). Predicting the causes and covarying factors driving these wave events was not a focus of this study. However, increases in H_{50} and H_{avg} were predicted to increase from up- to down-river sites. We found no evidence of this relationship in any of the rivers examined in this study. On the contrary, H_{50} wave heights increased log-linearly with increasing distance up-river in MaR ($R^2 = 0.59$, $p = 0.01$). This trend, however, was not observed elsewhere.

Platform elevation and soil bulk density also varied across study sites and were evaluated against the wave climate gradient in linear models to assess any potential covarying relationships. However, while increases in soil bulk density were related to increasing H_{50} wave heights ($p = 0.003$), this relationship was weak ($R^2 = 0.15$) and driven mostly by wave and bulk density characteristics in WMB. Elevation was not related to changes in H_{50} wave heights ($p = 0.83$). These variables were, however, used to further evaluate plant responses to different environmental conditions.

3.4.2 Site environmental characteristics

Site environmental characteristics, including soil bulk density, elevation, and slope varied across and within waterbodies (*i.e.,* regions along the bay or individual rivers) but were, on average, within range of those reported within the study area (Constantin *et al*. 2019, Gailani *et al*. 2001) and characteristic of coastal marshes in the Northern GoM region (Feagin *et al*. 2009, McKee and Cherry 2009). Soil bulk density was greatest at WMB sites where sandy sediments are common along the shoreline (Gailani *et al.* 2001). Bulk density at WMB averaged 1.15 g cm^3 and ranged from 0.66 to 1.50 g cm^{-3} (Table 3.3), and was nearly an order of magnitude greater than bulk density observed at any of the other study waterbodies ($p \leq 0.05$; Table 3.3). Bulk density at BSB sites averaged 0.21 g cm^{-3} and was more similar to bulk density at FiR, MaR and FoR river sites ($p > 0.05$; Table 3.3), which averaged 0.16, 0.14, and 0.14 g cm^{-3}, respectively, than bulk density found at BSR river sites, which averaged 0.31 g cm^{-3} and was significantly greater than all other river sites ($p \leq 0.02$; Table 3.3). In addition, changes in bulk density were not related to increasing distance up-river at any of the rivers examined, as has been observed elsewhere (*e.g.,* Darke and Megonigal 2003). Shoreline slope was steepest at two up-river sites within FiR and MaR at 1.04 and 0.74, respectively. Elsewhere, slope averaged a gentle 0.13,

ranging from near 0 to 0.32, and was not significantly different within or between river or bay sites ($p = 0.10$; Table 3.3). Marsh platform elevation data ranged from 1.33 m below to 0.37 m above MSL (NAVD88 and were, on average, greatest at BSB sites (mean elevation = 0.08 m above MSL); Table 3.3). Platform elevation at BSR, FiR, FoR, MaR and WMB averaged 0.47, 0.24, 0.24, 0.37, and 0.46 m below MSL but were, on average, not significantly different from one another ($p \geq 0.3$; Table 3.3). Within site variation was greatest in WMB (where elevation data ranged from 1.33 m below to 0.24 m above MSL) but was fairly consistent within sites elsewhere ($p > 0.05$; Table 3.3). Elevation tended to increase with increasing distance up-river (*i.e.,* distance from river mouth; p of linear model = 0.02) in MaR but this trend was likely driven by elevated turf-forming clusters of *C. jamaicense* that were especially prevalent in this reach of MaR. Consequently, this trend was not observed in any of the other rivers examined ($p > 0.05$).

3.4.3 Plant responses

3.4.3.1 Diversity across study sites

This study focused on the fringing vegetation situated at the most shoreward extent of established marsh communities (sometimes called the pioneer zone; Bouma *et al*. 2010, Silinski *et al.* 2018). Within this area, a total of ten plant species were found at 51 of 60 sites including three *Spartina* spp. (*alterniflora, cynosuroides*, and *patens*), *J. roemerianus, P. australis, C. jaimasence, Alternantheera philoxeroides, Sagittaria lancifolia, T. latifolia*, and *Panicum repens*. In all, the majority (80%) of plants found at sites were represented by three species: *S. alterniflora* (38%)*, J. roemerianus* (25%), and *C. jamaisence* (17%); all other species were rare (≤ 8%). While *C. jaimasence* was found at 10 sites, its distribution was limited to upstream FiR and MaR river sites, which subsequently limited the exploration of *C. jamaisence* responses along the wave climate gradient. Conversely, both *S. alterniflora* (hereafter, "*Spartina*") and *J.*

roemerianus (hereafter, "*Juncus*"), common estuarine marsh plants throughout the Southeastern United States (Stout 1984), were found within at least four of the waterbodies examined in the study and together accounted for over half (63%) of the plants found at all study sites. Therefore, plant responses along the wave climate gradient focused on these two species.

3.4.3.2 Aboveground shoot responses

The diameter of shoots for both species declined in response to increasing wave climate without any observable change in shoot biomass, density or height/total length along the same gradient, while the latter morphological features (*i.e.,* density and height/total length) and biomass per shoot were predicted by changes in soil bulk density or elevation. The basal shoot diameter response was strongest amongst *Juncus* shoots which declined by nearly 70% (from ~ 6 mm to ~ 2 mm) with increasing H_{50} wave height ($R^2 = 0.51$, $p = 0.004$; Table 3.4; Figure 3.2A) but was still significant for *Spartina* shoots which declined in shoot diameter by nearly 40% from ~ 8 to ~ 5 mm ($R^2 = 0.34$, $p = 0.004$; Table 3.4; Figure 3.2B). Declining shoot diameter was not related to changes in either shoot density, biomass, or height, which remained constant or declined for both species, though not significantly, along the wave climate gradient ($p > 0.05$; Table 3.4).

Juncus shoot density, which averaged 1293 shoots m^{-2} and ranged from 252 to 2880 shoots m^{-2}, was not related to changes in H_{50} ($p = 0.6$; Table 3.4) nor was *Spartina* shoot density, which averaged 202 shoots m^{-2} and ranged from 52 to 532 shoots m^{-2} ($p = 0.2$; Table 3.4). These shoot density responses, however, were significantly affected by other environmental characteristics that were species-specific (Table 3.5). *Juncus* shoot density was negatively correlated with soil bulk density ($r = -0.69$; Table 3.5) and declined linearly along a gradient of soil bulk density which increased from less than 0.1 to over 0.4 g cm^{-3} ($R^2 = 0.48$, $p = 0.006$),

while *Spartina* shoot density was positively correlated with elevation (Table 3.5) and increased along a similar gradient in elevation from less than 0.6 m below to 0.2 m above MSL ($R^2 = 0.47$, $p < 0.001$). Similar, yet contrasting, trends were observed in shoot height, which were also not related to wave climate ($p > 0.05$; Table 3.4) but by other environmental factors (Table 3.5). On the one hand, *Juncus* shoots, which averaged 0.72 m and ranged 0.50 to 1.04 m in total length, were positively correlated with bulk density (Table 3.5) and increased linearly with increasing bulk density ($R^2 = 0.30$, $p = 0.04$). On the other hand, *Spartina* shoots, which averaged 0.66 m and ranged 0.23 to 1.09 m in total length, were negatively correlated with elevation (Table 3.5) and declined linearly with increasing elevation ($R^2 = 0.64$, $p < 0.001$).

These species-specific trends continued with aboveground biomass and biomass per shoot which were not related to wave climate but rather often related to bulk density and elevation, in the case of *Juncus* and *Spartina*, respectively (Table 3.5). *Juncus* aboveground biomass averaged 760 g m^{-2} and was negatively correlated with bulk density (-0.35). Conversely, biomass per shoot tended to increase with increasing bulk density ($r = 0.42$) which is likely due to the simultaneous decline in the number of shoots along the same gradient ($r = -0.69$; Table 3.5). *Spartina* aboveground biomass, which averaged 301.8 g m^{-2}, was not related to elevation change (Table 3.5), as some have found (*e.g.,* DeLaune et al. 1979). However, *Spartina* biomass per shoot, which averaged 2.01 g m^{-2}, tended to decline with increasing elevation ($r = -0.61$, $p < 0.05$) as the number of shoots increased along the same gradient ($r = 0.68$, $p < 0.05$; Table 3.5).

The percent live and dead shoots in plot canopies was assessed for both species at harvest. There was no observable effect of increasing wave climate, soil bulk density or elevation on the percentage of live *Spartina* shoots in plot canopies ($p > 0.05$, Table 3.4; Table 3.5). However, the percentage of live *Juncus* shoots was negatively correlated with both increasing

elevation and H_{50} wave heights ($r = -0.58$ and $r = -0.56$, respectively; $p < 0.05$, Table 3.5). While increasing elevation data were positively correlated with increasing H_{50} wave heights ($r = 0.36$; Table 3.5), this relationship was weak and inclusion of elevation data did not improve the fit of models exploring the live shoot percentage responses, which were best predicted by H_{50} wave heights alone. Along this H_{50} wave height gradient, the percentage of live shoots in plot canopies declined linearly by 15% from ~95% to ~80% ($R^2 = 0.34$, $p = 0.03$; Table 3.4, Figure 3.3).

3.4.3.3 Belowground root responses

Several belowground responses were measured from cores taken from field plots, including root production within 10 cm increments into the active rooting zone (*i.e.,* ≥ 30 cm; McKee and Cherry 2009), total live and dead roots and rhizomes, and root to shoot ratios comparing potential patterns in above- and below-ground resource allocation. However, no patterns were observed for either *Juncus* or *Spartina* roots with respect to various rooting depths (Figure A3.2) and therefore all live root biomass (i.e., roots and rhizomes) within the first three depth increments (i.e., ≤ 30 cm) were lumped together to reflect the total root biomass in active rooting zone (hereafter, "total live roots"). Regarding resource allocation, analysis of root to shoot ratios for both species revealed belowground production estimates that were substantially less than those observed aboveground. Across all sites, total live roots by *Juncus* and *Spartina* averaged only 8 and 13% of total biomass production, respectively, which is well below total production estimates reported elsewhere in the area (75%; Darby and Turner 2008). Further, root to shoot responses were not related to changes in H_{50} wave heights, elevation, or soil bulk density for either species ($p > 0.05$, Table 3.4). While not observed for *Spartina* belowground responses, *Juncus* total live roots did tend to increase with increasing H_{50} ($r = 0.51$) while also

generally decreasing along a similar gradient in soil bulk density ($r \leq -0.38$; Table 3.5). However, these relationships were not statistically significant ($p > 0.05$; Table 3.5).

3.5 Discussion

Coastal marshes are increasingly valued for the wealth of ecosystem services they provide (*e.g.*, Barbier et al. 2010). Of particular interest to coastal property owners and land managers is their role in coastal defense. This interest has led to numerous studies on the effects of various plant features on wave mitigation (*e.g.,* Knustson *et al*. 1982, Augustin *et al*. 2009), which have been useful for refining our understanding of coastal processes, modelling the long-term persistence of marshes, and approximating the relative impact of coastal restoration designs. However, the response of plants to waves is not fully understood and, thus, is limiting our ability to understand past, present, and future marsh conditions and associated services provided.

We hypothesized that fringing marsh plants would respond to increasing wave climate by increasing shoot density, shoot biomass per shoot, basal stem diameter aboveground and by increasing the rooting depth belowground. Together, these hypotheses would represent a generalized plant response to waves, as suggested by growth strategy theory and the findings of field and laboratory studies conducted previously (*e.g.,* Bouma *et al*. 2010, Puijalon *et al*. 2011, Silinski *et al*. 2017). We found limited evidence to support this generalized response, however, and more often found species-specific plant responses that varied as a function of different environmental characteristics including wave climate, marsh platform elevation, and soil bulk density (Table 3.5). While limited, these preliminary results stand in contrast to previously reported findings and suggest a reexamination of expected plant responses to varying wave climate is warranted, especially with respect to plant growth strategy theory that is often used to

characterize these responses (Bouma *et al*. 2010, Puijalon *et al.* 2011, Silinski *et al*. 2018, and others).

In previous studies, the primary reason for evaluating the association between plant morphological and biomechanical features and wave activity was to evaluate the role of plants in attenuating wave energy. Indeed, Knutson *et al.* (1982) based their novel measurement of plant morphological features, including plant height parameters, stem density (on a number of shoots per area basis), and diameter parameters, to "[*facilitate*] *the use of existing wave dynamic and hydraulic theories in the analysis*," following the idealized conditions used by Dean (1978). Results from several laboratory and field experiments have consistently supported the importance of these modelling parameters in attenuating wave heights (Anderson *et al*. 2013, Anderson and Smith 2014, Augustin *et al*. 2009, Huang *et al*. 2011, Ozeren *et al*. 2014) and decreasing other wave-induced phenomena (*e.g.,* erosion via wave orbital velocity; Neumeier and Amos 2006, Green and Coco 2014). These studies, however, have rarely focused on how within-species features change in response to waves.

In their seminal study, Silinski *et al*. (2017) conducted a field study along a gradient of wave conditions at exposed and sheltered sites to begin the exploration of the changing plant response in relationship to different or changing wave conditions. While this experiment is the most comparable to the present study, it differed from the present study in a few important ways that may help to explain the differences between the shoot diameter relationships observed in this study compared to those reported by Silinski *et al*. (2018). First, the gradient of wave climate conditions established by Silinski *et al*. mostly occurred along within-marsh transects from the edge to interior areas of sheltered and exposed marsh sites. This design would correspond to only two marsh edge sites in the present study and, because the main wave climate gradient was

established within marsh sites, interpretation of observations along this gradient are limited due to the highly correlated responses within local marsh communities, as noted by the authors. Considering shoot diameter responses in only the sheltered and exposed marsh edge sites revealed that while the exposed site tended to feature thicker shoots as compared to sheltered sites, these results were not statistically significant. Other plant features examined at the two marsh edge sites, including total length and biomass per shoot were also not significant (*i.e.,* at the $\alpha = 0.05$ level). Second, while rarer wave conditions (*i.e.,* $H_{1/100}$; average of the highest 1% of all wave heights in the record) differed by ~10 cm at exposed and sheltered sites (20 cm and ~9 cm, respectively), more common conditions (*i.e.*, H_s) differed by ~2 cm. In contrast, differences along the wave climate gradient reported in this study, including all record and windowed wave statistics, ranged from as little as 10 cm to nearly 40 cm (Table 3.3). Third, the Silinski *et al*. field experiment examined one plant species (*Scirpus maritimus*) compared to the two species examined in this study. As has been documented by several researchers (*e.g.,* Bouma *et al*. 2010, Paul *et al*. 2012, Langlois *et al*. 2003, and others), the differences in all plant features could be due to species-specific capabilities that may favor the expression of different plant traits and features in response to changing environmental conditions.

Likewise, inherent differences between laboratory wave channel studies and this field study may explain some of the observed differences in results. Notably, the differences in wave conditions, timeframe of experimental manipulation and/or frequency of wave disturbance (*e.g*, as is often the case in laboratory wave flume experiments), the magnitude of plant materials from which plant responses may evolve (Silinksi *et al.* 2016), and other community features that can affect plant responses (*e.g.,* facilitation; Bertness and Hacker 1994, Silliman *et al*. 2015) may all contribute to differing results. The responses of plants to differing wave conditions reported here

further question the current growth strategy paradigm. This paradigm places more emphasis on the plant features known to ameliorate certain wave conditions than on the way in which plant features change in response to waves. For example, this paradigm suggests that advantageous plant responses to stress and plant stress responses are not mutually exclusive even while, in nature, they sometimes are (*e.g.*, threshold plant responses; Silinski *et al.* 2016, Temple *et al*. 2019). This subtle difference has been relatively ignored in the current literature and has the potential to have profound effects on models examining the long-term value of the coastal defense services provided by plants, *e.g.,* a decline in mean shoot diameter in marshes experiencing waves decreases the marsh's ability to attenuate waves. However, further research is needed to evaluate the effects of these shifting relationships and stress responses.

A differing view, aside from the growth strategy framework, and a potential explanation for the observed decline in shoot diameter is that it is the result of an indirect positive feedback to increasing wave activity. In salt and brackish marshes, oxygen availability is a key resource limiting plant growth. Oxygen controls the availability of growth-enhancing nutrients and, when anoxic conditions persist, can result in increasing phytotoxin concentration (*e.g.,* hydrogen sulfides) which can have direct and indirect negative effects on plant growth (Koch *et al*. 1990). To increase nutrient availability and continue aerobic metabolism in the rhizosphere, many marsh plants, including *Juncus* and *Spartina spp*., have developed complex aerenchyma systems to facilitate gas exchange from shoots to roots (Koop-Jakobsen *et al.* 2016, Maricle and Lee 2002, Visser *et al*. 2000). In fact, Maricle and Lee (2002) observed the greatest aerenchyma development in *Spartina alterniflora* plant tissues following periods of prolonged inundation. What has received less attention, however, is whether aerenchyma development declines with increasing oxygen availability, as could occur with the increasing presence of waves (Bornette

and Puijalon 2011, Rolletschek 2007). For example, rates of oxygen diffusion in water are slow and anoxic conditions may develop within the lower elevations along the marsh platform that are typically occupied by fringing vegetation (Maricle and Lee 2006). However, air entrainment resulting from breaking waves (*e.g.*, Chanson et al. 2006) can enhance oxygen availability in fringing marshes. Therefore, wave-induced increases in oxygen availability could illicit a change in the allocation of plant resources that are for the purposes of increasing oxygen availability in rhizosphere (*e.g.*, aerenchyma development). This understudied question could partially explain why shoots tended to be denser (*i.e.,* smaller basal diameter shoots with similar biomass and height) along the wave climate gradient observed in this study. For example, a decline in the development of aerenchyma systems would translate to fewer or less pronounced empty spaces in plant tissues and thus, denser plant tissues overall. Thus, the shoot diameter response would not reflect a plant stress response as predicted by the growth strategy framework, but rather a response to increased oxygen availability resulting from increased wave activity.

Other plant responses to waves were not common between the study species and more often reflected the influence of other environmental gradients. The only other observable response to waves in either of the study species was a change in the ratio of live and dead aboveground biomass (Figure 3.3) and, while limited, in the total live root biomass found in the active rooting zone belowground associated with *Juncus* plants (Figure 3.4). The increase in the ratio of live to dead biomass observed in *Juncus* shoots may reflect a decline in the overall vitality of this fringing community or, alternatively, an increase in marsh canopy complexity, which has been linked to increasing wave tolerance in plant communities (Blackmar *et al*. 2014, Vuik *et al*. 2018). Likewise, the increasing rooting activity along the wave climate gradient observed in total biomass of *Juncus* live roots, has also been linked to increasing wave tolerance

as it relates to the anchoring capacity necessary for successful establishment (*e.g.,* depth or total belowground production; Balke *et al.* 2011) or in resistance to uprooting (Balke *et al.* 2010, Silinski *et al.* 2018). Neither response was observed in *Spartina* plants, which may reflect the species-specific nature of plant responses to waves reported by others (Vuik *et al.* 2018, Bouma *et al.* 2010, Paul *et al.* 2012, Rupprecht *et al.* 2018).

Observed relationships between plant morphological features and other environmental characteristics, were, in some respects, similar to patterns reported by others and distinct in other respects. For example, several researchers have illustrated the impact of elevation and/or inundation, and soil bulk density on above- and below-ground biomass in both of the study species (*e.g.,* Mendelssohn and Seneca 1980, Snedden *et al.* 2015, Wang *et al.* 2016). No significant relationships were observed between the mean aboveground biomass of either species or any of the environmental factors examined in this study (Table 3.5). However, overall aboveground biomass estimates, like those reported for belowground biomass, were low in comparison to estimates reported by others (Darby and Turner 2008, Morris and Haskin 1990, Stout 1984). Interestingly, these responses are contrary to other studies that showed soil bulk density and elevation were good predictors of several plant features also evaluated in this study. We hypothesize that these responses reflect the unique location from which samples were taken. For example, the sparsely vegetated and seaward edge of marshes is sometimes described as the pioneer zone (Bouma *et al.* 2010, Silinski *et al.* 2015, and others). As such, shoots occupying this zone could be more accurately described as pioneering ramets of larger clonal communities (Proffitt *et al.* 2003) with differences in above- and below-ground characteristics expected between pioneering ramets and the mother clones (Xiao *et al*. 2010). While several researchers have examined many of the same plant features examined in this study, few, even those

examining fringing marsh responses, have sampled along the leading edge of the marsh. Silinksi *et al.* (2018) did however, but their results comparing above- and below-ground biomass in this zone with interior zones were conflicting. For example, aboveground biomass estimates of *Scirpus maritimus* in the pioneer zone amounted to approximately 25% of those reported in the most interior zone. Supposing estimates of aboveground productivity reported by others within the study region (*e.g.,* Darby and Turner 2008, Stout 1984) were representative of the biomass estimates that would be expected in the upland areas of the present study sites, the percentage of biomass observed within the present study sites would compare favorably to the results reported by Silinski *et al.* (2018). Unlike Silinski *et al.*, belowground biomass estimates within the present study sites (*i.e.,* in the pioneer zone) were dwarfed by aboveground estimates and would align closer to the root:shoot ratios reported for more upland zones in their study. These differences, however, may also reflect the species-specific responses discussed previously. Moreover, the varying impact of different environmental factors, including soil bulk density, elevation and wave climate, on different plant features illustrates the complex interplay of these factors, all with important consequences to plant persistence within the pioneer zone with an array of potential rippling effects on the ecology of these environments.

As with all studies, interpretation may be limited by the constraints of the experimental design and environmental conditions during the study. For example, tidal amplitude in the study area is small compared to other areas, which may further influence the expression of different plant features not controlled for in this study. In particular, the estimation of wave climate parameters examined in this study occurred over a relatively short time period (~20 days). In an effort to compare these short-term measurements to long-term conditions, we explored how wave statistics generated from gauge data collected during this period compared to those

generated by hind-casted wind-wave models from 10-year wind records (Appendix B.2). Results indicated that gauge-generated statistics were similar to those predicted by 10-year wind records at southern-facing sites (Figure B.2), likely due the predominance of winds from the south during this period (Figure B.1). Along northern-facing shorelines, gauge-generated statistics tended to underestimate conditions predicted by wind-wave models (Appendix B.2, Figure B.3). While two northern facing sites included the study species *Spartina,* gauge statistics most accurately represent the short-term conditions that characterize the wave climate during the study period, which often affect the immediate plant responses examined in this study (Balke *et al.* 2011, Nyman *et al.* 2006, Vasquez *et al.* 2006, Temple *et al.* 2019). Long-term data regarding boat-wakes is limited and modeling is difficult due, in part, to the myriad co-varying parameters involved (Glamore 2008). Therefore, model comparisons to gauge statistics for river site data were not pursued. Boat wake in this study produced waves that were similar to bay sites in height (Table 3.2) but these data were collected from sites during peak periods of boating activity (i.e., US national holidays) and thus, may not reflect the wave climate representative of other periods with less boating activity (e.g., during winter months).

Even if wave climate parameters collected during these peak boating activity periods were higher, on average, than those collected during slack periods, they would still represent the higher end of the potential wave climate conditions, which often have the greatest impact on plant responses (*e.g.,* stem breakage and biomass; Connell 1978, Rupprecht *et al.* 2018) and would still best reflect immediate plant responses to summer wave conditions when plant growth is maximal in this region (Eleuterius 1984, Stout 1980), as noted previously. The magnitude of plant responses may also be limited by within-species genetic similarities and/or differences of plants in the study area (Biber *et al.* 2019). While within-species genetic differences have also

been linked to plant biophysical properties (*i.e.,* diameter, height, and biomass), these responses are known to exhibit a high degree of plasticity that is often linked to varying environmental conditions (*e.g.,* temperature and latitudinal gradients; Crosby *et al.* 2017). Considering the documented plasticity in responses exhibited by both study species (Crosby *et al.* 2017, Eleuterius 1984) suggests that the decline in shoot diameter observed in this study is not solely dependent on the potential genetic differences in waterbody communities across study sites but rather, a response to the differing environmental conditions characteristic of those sites (Gallagher and Plumley 1979). Still, how genetic diversity affects the capacity of different plant species to respond to changing wave climate conditions is likely an important feature of plant responses to waves. Like the comparison of the ebb and flow in wave conditions between bay and river sites, this aspect of genetic diversity is underexplored and warrants further research.

3.6 Conclusions

Coastal marsh plants are often valued for their role in coastal defense. This ecosystem service has, in part, driven the exploration of which plant traits have the greatest impact on waves for use in models exploring the long-term persistence of marshes as well as the extent of coastal marsh with varying plant features in future storm and sea-level rise simulations. These models, however, rarely account for small-scale changes in plant features that may result from changing wave conditions. While relatively small-scale, these shifting plant responses, through their changing of important morphological and biomechanical features affecting wave parameters, have the potential to alter modelled plant effects on wave attenuation. The present research demonstrates that plants may alter their morphological features in response to increasing frequency of greater magnitude wave heights, similar to the way plants alter the expression of other traits to other varying environmental conditions. However, more research examining these

plant traits along a gradient of wave conditions, within varying soil and elevation conditions, is needed to fully understand the capacity of different plant species to adapt to changing environmental conditions, including waves. Data from these experiments could be used to explore subsequent rippling effects of shifting plant responses and should improve the predictive power of models and overall success of conservation, restoration and enhancement projects.

Table 3.1 Gauge deployment schedule within waterbodies and corresponding US National Holidays.

Waterbody	Approx. Start	Approx. End	Major US Holidays
Fish River	24-May	25-Jun	Memorial Day
Magnolia River	24-May	25-Jun	Memorial Day
Bon Secour River	24-May	25-Jun	Memorial Day
Bon Secour Bay	28-Jun	30-Jul	Fourth of July
Fowl River	2-Aug	3-Sep	Labor Day
West Mobile Bay	2-Aug	3-Sep	Labor Day

Table 3.2 Record-length bay and river site wave statistics.

Waterbody Type	Wave statistic	Unit	Mean	Min	Max
Bay	Significant wave period (T_s)	s	2.94 ± 0.13	2.23	4.2
	Significant wave height (H_s)	m	0.18 ± 0.02	0.1	0.35
	Average wave height (H_{avg})	m	0.1 ± 0.01	0.05	0.2
River	Significant wave period (T_s)	s	1.68 ± 0.5	1.35	3.14
	Significant wave height (H_s)	m	0.13 ± 0.02	0.03	0.44
	Average wave height (H_{avg})	m	0.06 ± 0.01	0.02	0.25

Wave statistics include mean (± SE), minimum and maximum values. In general, mean values for significant wave period (the average of the top third of all record wave periods, T_s) , significant wave height (the average of the top third of all record wave heights, H_s) and average wave height (H_{avg}) were greatest in bay sites as compared to river sites.

Table 3.3 Mean (± SE) record wave statistics, windowed wave statistics and environmental characteristics of data collected at each of the study waterbodies.

			Site					
	Sample	**Unit**	WMB	BSB	FoR	FiR	MaR	BSR
Record Wave Statistics	Significant wave period (T_s)	s	3.39 ± 0.17	2.49 ± 0.04	1.71 ± 0.16	1.70 ± 0.03	1.58 ± 0.03	1.76 ± 0.09
	Significant wave height (H_s)	m	0.22 ± 0.02	0.14 ± 0.02	0.24 ± 0.04	0.06 ± 0.01	0.13 ± 0.02	0.08 ± 0.02
	Average wave height (H_{avg})	m	0.13 ± 0.01	0.08 ± 0.01	0.13 ± 0.02	0.03 ± 0.01	0.06 ± 0.01	0.04 ± 0.003
Windowed Wave Statistic Percentiles	Twenty-fifth (H_{25})	m	0.15 ± 0.01	0.08 ± 0.01	0.12 ± 0.02	0.03 ± 0.01	0.05 ± 0.01	0.03 ± 0.002
	Fiftieth/Median (H_{50})	m	0.19 ± 0.01	0.11 ± 0.01	0.18 ± 0.01	0.04 ± 0.01	0.08 ± 0.01	0.05 ± 0.004
	Seventy-fifth (H_{75})	m	0.25 ± 0.02	0.15 ± 0.02	0.27 ± 0.04	0.07 ± 0.01	0.15 ± 0.02	0.09 ± 0.01
	One-hundredth (H_{100})	m	0.43 ± 0.04	0.31 ± 0.05	0.45 ± 0.05	0.14 ± 0.03	0.29 ± 0.05	0.20 ± 0.02
Environmental Characteristics	Soil Bulk Density	$g\ m^{-3}$	1.03 ± 0.15	0.21 ± 0.05	0.14 ± 0.04	0.16 ± 0.04	0.14 ± 0.03	0.31 ± 0.03
	Marsh Platform Elevation	m	-0.46 ± 0.18	0.08 ± 0.05	-0.24 ± 0.05	-0.24 ± 0.04	-0.37 ± 0.07	-0.44 ± 0.03
	Slope	−	-0.14 ± 0.04	-0.17 ± 0.01	-0.1 ± 0.02	-0.12 ± 0.02	-0.1 ± 0.01	-0.13 ± 0.01

Mean (± SE) record wave statistics, windowed wave statistics and environmental characteristics of data collected at each of the study waterbodies: West Mobile Bay (WMB), Bon Secour Bay (BSB), Fowl River (FoR), Fish River (FiR), Magnolia River (MaR), and Bon Secour River (BSR). Record-length wave statistics include significant wave period (the average of the top third of all record wave periods, T_s), significant wave height (the average of the top third of all record wave heights, H_s) and average wave height (H_{avg}). Windowed wave statistics represent significant wave height statistics calculated within one-hour windows through the individual records. The percentile significant wave indicates how often varying magnitude wave heights occur as twenty-fifth percentile significant wave height (H_{25}) represents more common events while one-hundredth percentile significant wave height (H_{100}) represents rarer events. Environmental characteristics include soil bulk density, marsh platform elevation and slope.

Table 3.4 Regression models relating plant response variables to log-transformed fiftieth percentile wave height for both *J. roemerianus* and *S. alterniflora.*

	Juncus roemerianus			***Spartina alterniflora***		
	function	R^2	*p*	function	R^2	*p*
Shoot Basal Diameter	y = -1.7x + 7.48	0.51	< 0.01	y = -1.08x + 8.81	0.34	<0.01
Shoot Height/Length	y = 5.17x + 61.86	ns	ns	y = -14.55x +96.94	ns	ns
Shoot Density	y = 170.7 + 945	ns	ns	y = 66.84x + 61.71	ns	ns
Plot Shoot Biomass	y = 133.9x + 487.1	ns	ns	y = 50.3x +196.58	ns	ns
Biomass per Shoot	y = 0.13x + 0.39	ns	ns	y = -0.46 + 2.97	ns	ns
Percent Live Shoots	y = -6.25 + 97.49	0.34	0.3	y = 1.73x + 91.37	ns	ns
Root Biomass	y = 19.15x – 13.35	0.26	< 0.1	y = -1.02x + 18.77	ns	ns
Root : Shoot	y = -0.01x + 0.1	ns	ns	y = -0.01x + 0.16	ns	ns

Regression models relating plant response variables (y) to log-transformed fiftieth percentile (H_{50}) wave height (x) for both *J. roemerianus* and *S. alterniflora*. Variables include above- and below-ground data collected from each of the study sites in which each of the study species were found. Model fit (R^2) and significance (at the $\alpha = 0.05$ level) is provided for significant relationships between H_{50} wave heights and plant response data.

Table 3.5 Correlation matrices for plant response variables, log-transformed fiftieth percentile wave heights, and environmental characteristics.

		Waves	BD	elevation	diam	length	density	Ab	Sb	Bb	r:s
Juncus roemerianus	**BD**	-0.08	—	—	—	—	—	—	—	—	—
	elevation	0.36	-0.38	—	—	—	—	—	—	—	—
	diam	-0.72*	0.21	-0.5	—	—	—	—	—	—	—
	length	0.22	0.55*	-0.53*	0.18	—	—	—	—	—	—
	density	0.15	-0.69*	0.35	-0.12	-0.18	—	—	—	—	—
	Ab	0.19	-0.35	0.004	0.08	0.47	0.71*	—	—	—	—
	Sb	0.26	0.42	-0.34	0.11	0.84*	-0.38	0.35	—	—	—
	Bb	0.51	-0.44	0.27	-0.09	0.02	0.12	0.15	0.1	—	—
	r:s	-0.07	0.09	-0.05	-0.05	-0.2	-0.28	-0.47	-0.3	0.53*	—
	PL	-0.58*	0.3	-0.56	0.42	0.15	-0.35	-0.22	-0.05	-0.08	0.27
		waves	BD	elevation	diam	length	density	Ab	Sb	Bb	r:s
Spartina alterniflora	**BD**	-0.08	—	—	—	—	—	—	—	—	—
	elevation	0.31	-0.2	—	—	—	—	—	—	—	—
	diam	-0.58*	0.01	-0.39	—	—	—	—	—	—	—
	length	-0.41*	0.27	-0.8*	0.56*	—	—	—	—	—	—
	density	0.3	-0.11	0.68*	-0.39	-0.75*	—	—	—	—	—
	Ab	0.19	0.16	-0.1	0.23	0.04	0.36	—	—	—	—
	Sb	-0.21	0.43*	-0.6*	0.57*	0.8*	-0.57*	0.4	—	—	—
	Bb	-0.04	0.26	0.38	0.08	-0.36	0.31	0.05	-0.29	—	—
	r:s	-0.07	-0.16	0.17	0.15	-0.22	-0.06	-0.32	-0.32	0.51*	—
	PL	0.16	0.14	0.003	0.11	0.1	-0.02	0.18	0.36	-0.15	-0.21

Correlation matrices for plant response variables, log-transformed fiftieth percentile (H50) wave height (waves), and environmental characteristics for both *J. roemerianus* and *S. alterniflora*. Plant responses include basal shoot diameter (diam), shoot height/length (length), the number of shoots m^{-2} (density), aboveground biomass g m^{-2} (Ab), biomass per shoot g (Sb), total live root biomass g m^{-2} (Bb), root to shoot ratio (r:s), and percent live shoots (PL). Environmental characteristics such as marsh platform elevation (elevation) and soil bulk density (BD) are also included. Variables include above- and below-ground data collected from each of the study sites in which each of the study species were found. Significance at the $\alpha = 0.05$ level is denoted by *.

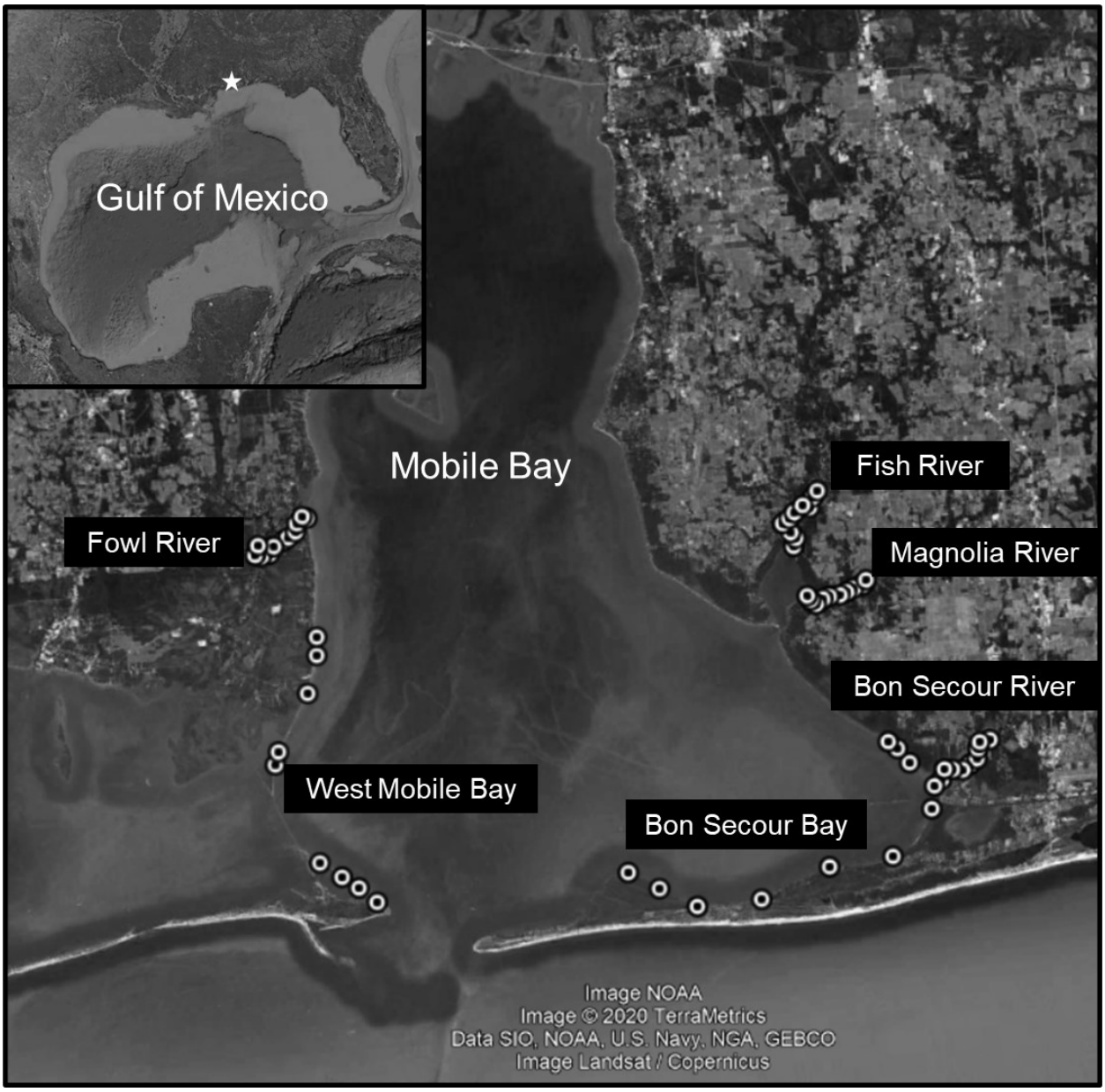

Figure 3.1 Map of study sites within the different waterbodies in and surrounding Mobile Bay, Alabama, USA.

Map of study sites (dotted circles) within the different waterbodies in and surrounding Mobile Bay, Alabama, USA. Mobile Bay is a large estuary located within the Northern Gulf of Mexico (white star in inset photo). 10 sites were established within each of the waterbodies examined: West Mobile Bay (WMB), Bon Secour Bay (BSB), Bon Secour River (BSR), Fish River (FiR), Fowl River (FoR), and Magnolia River (MaR). Both images accessed via Google Earth Pro.

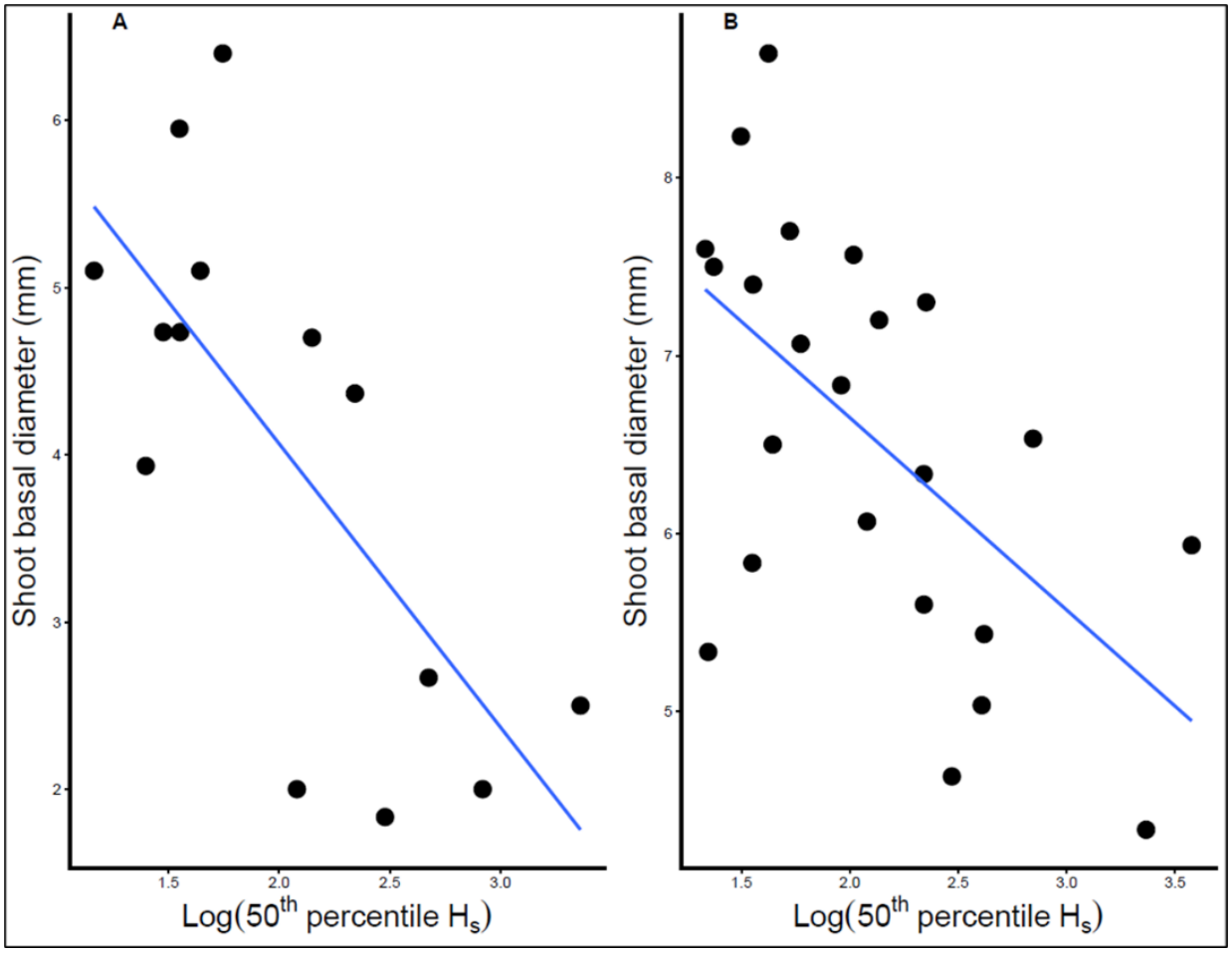

Figure 3.2 Regression models relating shoot basal diameter to log-transformed fiftieth percentile wave height for both *J. roemerianus* and *S. alterniflora*.

Regression models relating shoot basal diameter (y) to log-transformed fiftieth percentile (H_{50}) wave height (x) for both *J. roemerianus* (y = -1.7x + 7.48; A) and *S. alterniflora* (y = -1.08x + 8.81; B). Basal diameter declined in response to increasing H_{50} wave heights in shoots of both species.

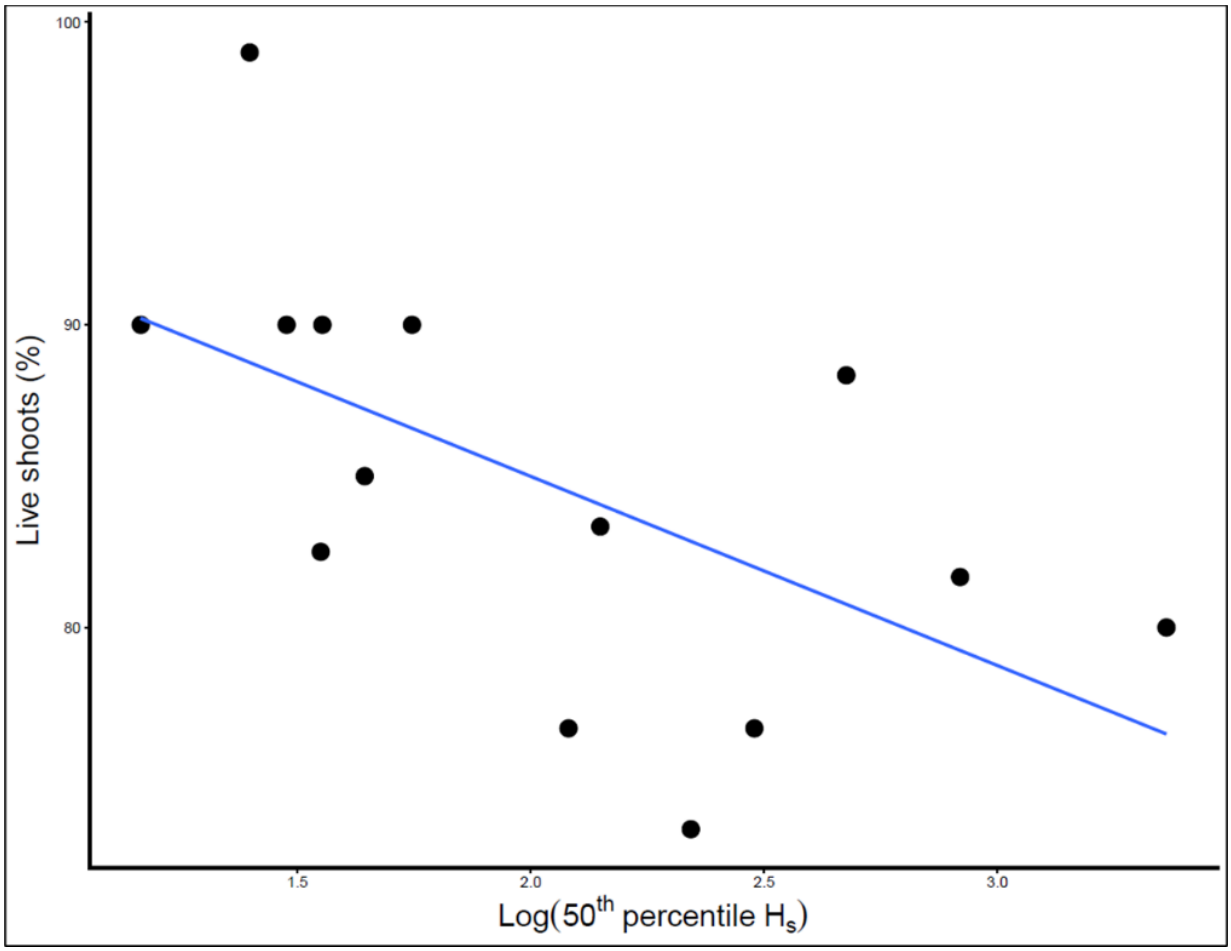

Figure 3.3 Regression model relating the percentage of live shoots to log-transformed fiftieth percentile wave height in *J. roemerianus* marsh canopies.

Regression model relating the percentage of live shoots (y) to log-transformed fiftieth percentile (H_{50}) wave height (x) in *J. roemerianus* marsh canopies (y = -6.25x + 97.49). The percentage of live shoots declined in response to increasing H_{50} wave heights.

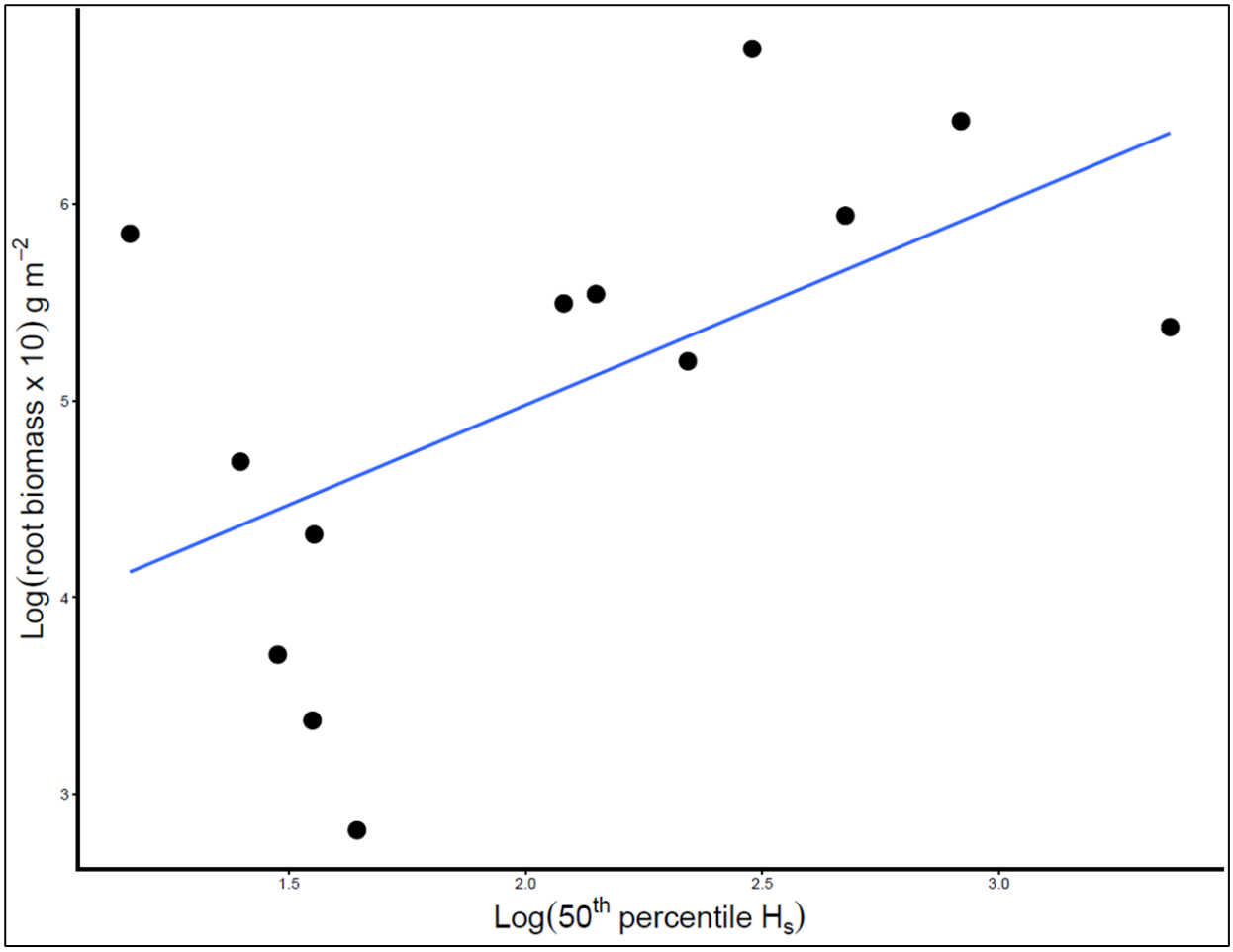

Figure 3.4 Regression model relating log-transformed total live root biomass to log-transformed H_{50} wave heights in fringing *J. roemerianus* marshes.

Regression model relating log-transformed total live root biomass (y) to log-transformed H_{50} wave heights in fringing *J. roemerianus* marshes. Total live root biomass of *J. roemerianus* increased in response to increasing H_{50} wave height (y = 19.15x – 13.35).

3.7 Literature Cited

Anderson, D. R., & Burnham, K. P. (2002). Avoiding pitfalls when using information-theoretic methods. *The Journal of Wildlife Management*, 912-918.

Anderson, M., Smith, J., Bryant, D., & McComas, R. (2013). Laboratory studies of wave attenuation through artificial and real vegetation (No. ERDC TR-13-11). US Army Engineer Research and Development Center.

Anderson, M., Smith, J. (2014). Wave attenuation by flexible, idealized salt marsh vegetation. *Coastal Engineering, 83*, 82–92.

Augustin, L., Irish, J. & Lynett, P. (2009). Laboratory and numerical studies of wave damping by emergent and near-emergent wetland vegetation. *Coastal Engineering, 56*, 332–340.

Balke, T., Bouma, T. J., Horstman, E. M., Webb, E. L., Erftemeijer, P. L., & Herman, P. M. (2011). Windows of opportunity: thresholds to mangrove seedling establishment on tidal flats. *Marine Ecology Progress Series, 440*, 1-9.

Barbier, E. B., Hacker, S. D., Kennedy, C., Koch, E. W., Stier, A. C., & Silliman, B. R. (2011). The value of estuarine and coastal ecosystem services. *Ecological monographs, 81*(2), 169-193.

Bertness, M. D., & Hacker, S. D. (1994). Physical stress and positive associations among marsh plants. *The American Naturalist, 144*(3), 363-372.

Biber, P., Welch, M. & Baldwin, B. (2019). Regional Genetic Diversity in Spartina and Juncus with Implications for Future Salt Marsh Restoration. Conference for the Coastal and Estuarine Research Federation, Mobile, AL.

Bilkovic, D. M., Mitchell, M. M., Davis, J., Herman, J., Andrews, E., King, A., ... & Dixon, R. L. (2019). Defining boat wake impacts on shoreline stability toward management and policy solutions. *Ocean & Coastal Management, 182*, 104945.

Blackmar, P., Cox, D., & Wu, W.C. (2014). Laboratory observations and numerical simulations of wave height attenuation in heterogeneous vegetation. *Journal of Waterway, Port, Coastal, Ocean Engineering, 140*, 56–65.

Bornette, G., & Puijalon, S. (2011). Response of aquatic plants to abiotic factors: a review. *Aquatic Sciences, 73*(1), 1-14.

Bouma, T. J., Vries, M. D., & Herman, P. M. (2010). Comparing ecosystem engineering efficiency of two plant species with contrasting growth strategies. *Ecology, 91*(9), 2696-2704.

Bradley, K., & Houser, C. (2009). Relative velocity of seagrass blades: Implications for wave attenuation in low-energy environments. *Journal of Geophysical Research, 114*.

Chanson, H., Aoki, S., & Hoque, A. (2006). Bubble entrainment and dispersion in plunging jet flows: Freshwater vs. seawater. *Journal of Coastal Research*, 664-677.

Connell, J. H. (1978). Diversity in tropical rain forests and coral reefs. *Science, 199*(4335), 1302-1310.

Constantin, A. J., Broussard, W. P., & Cherry, J. A. (2019). Environmental Gradients and Overlapping Ranges of Dominant Coastal Wetland Plants in Weeks Bay, AL. *Southeastern Naturalist, 18*(2), 224-239.

Coops, H., Geilen, N., & van der Velde, G. (1994). Distribution and growth of the helophyte species Phragmites australis and *Scirpus lacustris* in water depth gradients in relation to wave exposure. *Aquatic Botany, 48*(3-4), 273-284.

Coops, H., & Van der Velde, G. (1996). Effects of waves on helophyte stands: mechanical characteristics of stems of *Phragmites australis* and *Scirpus lacustris*. *Aquatic botany, 53*(3-4), 175-185.

Crosby, S. C., Ivens-Duran, M., Bertness, M. D., Davey, E., Deegan, L. A., & Leslie, H. M. (2015). Flowering and biomass allocation in US Atlantic coast *Spartina alterniflora*. *American Journal of Botany, 102*(5), 669-676.

Darby, F. A., & Turner, R. E. (2008). Below-and aboveground *Spartina alterniflora* production in a Louisiana salt marsh. *Estuaries and Coasts, 31*(1), 223-231.

Darke, A. K., & Megonigal, J. P. (2003). Control of sediment deposition rates in two mid-Atlantic Coast tidal freshwater wetlands. *Estuarine, Coastal and Shelf Science, 57*(1-2), 255-268.

DeLaune, R. D., Buresh, R. J., & Patrick Jr, W. H. (1979). Relationship of soil properties to standing crop biomass of *Spartina alterniflora* in a Louisiana marsh. *Estuarine and Coastal Marine Science, 8*(5), 477-487.

Eleuterius, L. N. (1984). Autecology of the black needlerush *Juncus roemerianus*. *Gulf and Caribbean Research, 7*(4), 339-350.

Feagin, R. A., Lozada-Bernard, S. M., Ravens, T. M., Möller, I., Yeager, K. M., & Baird, A. H. (2009). Does vegetation prevent wave erosion of salt marsh edges? *Proceedings of the National Academy of Sciences, 106*(25), 10109-10113.

Gailani, J. Z., Kiehl, A., McNeil, J., Jin, L., & Lick, W. (2001). Erosion rates and bulk properties of dredged sediments from Mobile, Alabama (No. ERDC-TN-DOER-N10). ARMY ENGINEER WATERWAYS EXPERIMENT STATION VICKSBURG MS ENGINEER RESEARCH AND DEVELOPMENT CENTER.

Gallagher, J. L., & Plumley, F. G. (1979). Underground biomass profiles and productivity in Atlantic coastal marshes. *American Journal of Botany, 66*(2), 156-161.

Glamore, W. C. (2008). A decision support tool for assessing the impact of boat wake waves on inland waterways. On-Course, PIANC, 5-18.

Green, M. O., & Coco, G. (2014). Review of wave-driven sediment resuspension and transport in estuaries. *Reviews of Geophysics, 52*(1), 77-117.

Heuner, M., Silinski, A., Schoelynck, J., Bouma, T. J., Puijalon, S., Troch, P., ... & Temmerman, S. (2015). Ecosystem engineering by plants on wave-exposed intertidal flats is governed by relationships between effect and response traits. *Plos one, 10*(9), e0138086.

Howard, R. J., & Mendelssohn, I. A. (1999). Salinity as a constraint on growth of oligohaline marsh macrophytes. I. Species variation in stress tolerance. *American Journal of Botany, 86*(6), 785-794.

Huang, Z., Yao, Y., Sim, S., Yao, Y., 2011. Interaction of solitary waves with emergent, rigid vegetation. *Ocean Engineering, 38*, 1080–1088.

Keddy, P. A. (1982). Quantifying within-lake gradients of wave energy: interrelationships of wave energy, substrate particle size and shoreline plants in Axe Lake, Ontario. *Aquatic Botany, 14*, 41-58.

Keddy, P. A. (1985). Wave disturbance on lakeshores and the within-lake distribution of Ontario's Atlantic coastal plain flora. *Canadian Journal of Botany, 63*(3), 656-660.

Kirwan, M. L., & Megonigal, J. P. (2013). Tidal wetland stability in the face of human impacts and sea-level rise. *Nature, 504*(7478), 53-60.

Koch, M. S., Mendelssohn, I. A., & McKee, K. L. (1990). Mechanism for the hydrogen sulfide-induced growth limitation in wetland macrophytes. *Limnology and oceanography, 35*(2), 399-408.

Koop-Jakobsen, K., Fischer, J., & Wenzhöfer, F. (2017). Survey of sediment oxygenation in rhizospheres of the saltmarsh grass-*Spartina anglica*. *Science of the Total Environment*, 589, 191-199.

Leonardi, N., Ganju, N. K., & Fagherazzi, S. (2016). A linear relationship between wave power and erosion determines salt-marsh resilience to violent storms and hurricanes. *Proceedings of the National Academy of Sciences, 113*(1), 64-68.

Maricle, B. R., & Lee, R. W. (2002). Aerenchyma development and oxygen transport in the estuarine cordgrasses *Spartina alterniflora* and *S. anglica*. *Aquatic Botany, 74*(2), 109-120.

Maricle, B. R., & Lee, R. W. (2007). Root respiration and oxygen flux in salt marsh grasses from different elevational zones. *Marine Biology, 151*(2), 413-423.

Maza, M., Lara, J. L., Losada, I. J., Ondiviela, B., Trinogga, J., & Bouma, T. J. (2015). Large-scale 3-D experiments of wave and current interaction with real vegetation. Part 2: experimental analysis. *Coastal Engineering, 106*, 73-86.

McConchie, J. A., & Toleman, I. E. J. (2003). Boat wakes as a cause of riverbank erosion: a case study from the Waikato River, New Zealand. *Journal of Hydrology* (New Zealand), 163-179.

McKee, K. L., & Cherry, J. A. (2009). Hurricane Katrina sediment slowed elevation loss in subsiding brackish marshes of the Mississippi River delta. *Wetlands, 29*(1), 2-15.

Mendelssohn, I. A., & Seneca, E. D. (1980). The influence of soil drainage on the growth of salt marsh cordgrass *Spartina alterniflora* in North Carolina. *Estuarine and Coastal Marine Science, 11*(1), 27-40.

Morris, J. T., Sundareshwar, P. V., Nietch, C. T., Kjerfve, B., & Cahoon, D. R. (2002). Responses of coastal wetlands to rising sea level. *Ecology, 83*(10), 2869-2877.

Morris, J. T., Shaffer, G. P., & Nyman, J. A. (2013). Brinson review: perspectives on the influence of nutrients on the sustainability of coastal wetlands. *Wetlands, 33*(6), 975-988.

Mullarney, J. C., & Henderson, S. M. (2010). Wave-forced motion of submerged single-stem vegetation. *Journal of Geophysical Research: Oceans, 115*(C12).

Neumeier, U., & Ciavola, P. (2004). Flow resistance and associated sedimentary processes in a *Spartina maritima* salt-marsh. *Journal of Coastal Research*, 435-447.

Neumeier, U., & Amos, C. L. (2006). Turbulence reduction by the canopy of coastal *Spartina* salt-marshes. *Journal of Coastal Research*, 433-439.

Noble, M. A., Schroeder, W. W., Wiseman Jr, W. J., Ryan, H. F., & Gelfenbaum, G. (1996). Subtidal circulation patterns in a shallow, highly stratified estuary: Mobile Bay, Alabama. *Journal of Geophysical Research: Oceans, 101*(C11), 25689-25703.

Nyman, J. A., Walters, R. J., Delaune, R. D., & Patrick Jr, W. H. (2006). Marsh vertical accretion via vegetative growth. *Estuarine, Coastal and Shelf Science, 69*(3-4), 370-380.

Osland, M. J., Griffith, K. T., Larriviere, J. C., Feher, L. C., Cahoon, D. R., Enwright, N. M., ... & Baustian, J. J. (2017). Assessing coastal wetland vulnerability to sea-level rise along the northern Gulf of Mexico coast: Gaps and opportunities for developing a coordinated regional sampling network. *PloS one, 12*(9).

Ozeren, Y., Wren, D., & Wu, W. (2014). Experimental investigation of wave attenuation through model and live vegetation. *Journal of Waterway, Port, Coastal, Ocean Engineering,* 140.

Pennings, S. C., Grant, M. B., & Bertness, M. D. (2005). Plant zonation in low-latitude salt marshes: disentangling the roles of flooding, salinity and competition. *Journal of ecology, 93*(1), 159-167.

Peralta, G., Van Duren, L. A., Morris, E. P., & Bouma, T. J. (2008). Consequences of shoot density and stiffness for ecosystem engineering by benthic macrophytes in flow dominated areas: a hydrodynamic flume study. *Marine Ecology Progress Series, 368*, 103-115.

Proffitt, C. E., Travis, S. E., & Edwards, K. R. (2003). Genotype and elevation influence *Spartina alterniflora* colonization and growth in a created salt marsh. *Ecological Applications, 13*(1), 180-192.

Puijalon, S., Bouma, T. J., Douady, C. J., van Groenendael, J., Anten, N. P., Martel, E., & Bornette, G. (2011). Plant resistance to mechanical stress: evidence of an avoidance–tolerance trade-off. *New Phytologist, 191*(4), 1141-1149.

R Core Team (2017). R: A language and environment for statistical computing. In. R Foundation for Statistical Computing Vienna, Austria: R Foundation for Statistical Computing. Retrieved from http://www.R-Project.org/

Roland, R. M., & Douglass, S. L. (2005). Estimating wave tolerance of Spartina alterniflora in coastal Alabama. *Journal of Coastal Research*, 453-463.

Rolletschek, H. (1997). Gradients of nutrients, dissolved oxygen and sulfide in wave-protected and unsheltered stands of *Phragmites australis*. *Internationale Revue der gesamten Hydrobiologie und Hydrographie, 82*(3), 329-339.

Rupprecht, F., Möller, I., Evans, B., Spencer, T., & Jensen, K. (2015). Biophysical properties of salt marsh canopies—Quantifying plant stem flexibility and above ground biomass. *Coastal Engineering, 100*, 48-57.

Rupprecht, F., Möller, I., Paul, M., Kudella, M., Spencer, T., Van Wesenbeeck, B. K., ... & Schimmels, S. (2017). Vegetation-wave interactions in salt marshes under storm surge conditions. *Ecological engineering, 100*, 301-315.

Silinski, A., Heuner, M., Schoelynck, J., Puijalon, S., Schröder, U., Fuchs, E., ... & Temmerman, S. (2015). Effects of wind waves versus ship waves on tidal marsh plants: a flume study on different life stages of *Scirpus maritimus*. *PLoS One, 10*(3).

Silinski, A., van Belzen, J., Fransen, E., Bouma, T. J., Troch, P., Meire, P., & Temmerman, S. (2016). Quantifying critical conditions for seaward expansion of tidal marshes: a transplantation experiment. *Estuarine, Coastal and Shelf Science, 169*, 227-237.

Silinski, A., Schoutens, K., Puijalon, S., Schoelynck, J., Luyckx, D., Troch, P., ... & Temmerman, S. (2018). Coping with waves: Plasticity in tidal marsh plants as self-adapting coastal ecosystem engineers. *Limnology and Oceanography, 63*(2), 799-815.

Silliman, B. R., Schrack, E., He, Q., Cope, R., Santoni, A., van der Heide, T., ... & van de Koppel, J. (2015). Facilitation shifts paradigms and can amplify coastal restoration efforts. *Proceedings of the National Academy of Sciences, 112*(46), 14295-14300.

Snedden, G. A., Cretini, K., & Patton, B. (2015). Inundation and salinity impacts to above-and belowground productivity in *Spartina patens* and *Spartina alterniflora* in the Mississippi River deltaic plain: Implications for using river diversions as restoration tools. *Ecological Engineering, 81*, 133-139.

Sorensen, R. M. (2005). Basic coastal engineering (Vol. 10). Springer Science & Business Media.

Sparks, E. L., Cebrian, J., Tobias, C. R., & May, C. A. (2015). Groundwater nitrogen processing in Northern Gulf of Mexico restored marshes. *Journal of environmental management, 150*, 206-215.

Stagg, C. L., & Mendelssohn, I. A. (2010). Restoring ecological function to a submerged salt marsh. *Restoration Ecology, 18*, 10-17.

Stout, J. P. (1984). The ecology of irregularly flooded salt marshes of the northeastern Gulf of Mexico: a community profile. National Coastal Ecosystems Team, Division of Biological Services, Research and Development, Fish and Wildlife Service, US Department of the Interior.

Temple, N. A., Grace, J. B., & Cherry, J. A. (2019). Patterns of resource allocation in a coastal marsh plant (*Schoenoplectus americanus*) along a sediment-addition gradient. *Estuarine, Coastal and Shelf Science, 228*, 106337.

Temple, N. A., Webb, B. M., Sparks, E. L., & Linhoss, A. C. (2020). Low-Cost Pressure Gauges for Measuring Water Waves. *Journal of Coastal Research*, DOI: https://doi.org/10.2112/JCOASTRES-D-19-00118.1.

Tweel, A. W., & Turner, R. E. (2012). Watershed land use and river engineering drive wetland formation and loss in the Mississippi River birdfoot delta. *Limnology and Oceanography, 57*(1), 18-28.

Vasquez, E. A., Glenn, E. P., Guntenspergen, G. R., Brown, J. J., & Nelson, S. G. (2006). Salt tolerance and osmotic adjustment of *Spartina alterniflora* (*Poaceae*) and the invasive M haplotype of *Phragmites australis* (*Poaceae*) along a salinity gradient. *American Journal of Botany, 93*(12), 1784-1790.

Visser, E. J. W., Colmer, T. D., Blom, C. W. P. M., & Voesenek, L. A. C. J. (2000). Changes in growth, porosity, and radial oxygen loss from adventitious roots of selected mono-and dicotyledonous wetland species with contrasting types of aerenchyma. *Plant, Cell & Environment, 23*(11), 1237-1245.

Wang, C., Pei, X., Yue, S., & Wen, Y. (2016). The response of *Spartina alterniflora* biomass to soil factors in Yancheng, Jiangsu Province, PR China. *Wetlands, 36*(2), 229-235.

Xiao, Y., Tang, J., Qing, H., Ouyang, Y., Zhao, Y., Zhou, C., & An, S. (2010). Clonal integration enhances flood tolerance of *Spartina alterniflora* daughter ramets. *Aquatic Botany, 92*(1), 9-13.

Zebrowski, J. (1992). Complementary patterns of stiffness in stem and leaf sheaths of *Triticale*. *Planta, 187,* 301-305.

Zuur, A., Ieno, E. N., & Smith, G. M. (2007). Analyzing ecological data. Springer.

Zuur, A. F., Ieno, E. N., & Elphick, C. S. (2010). A protocol for data exploration to avoid common statistical problems. *Methods in Ecology and Evolution, 1*(1), 3-14.

CHAPTER IV

NITROGEN REMOVAL IN CONSTRUCTED MARSHES AT SITES PROTECTED FROM AND EXPOSED TO WAVES

4.1 Abstract

Nutrient removal is among the most valuable ecosystem services provided by marshes and is often a stated goal of coastal restoration projects. However, the removal capacity of constructed marshes is potentially affected by several site-specific and design factors, such as marsh platform elevation, slope, sediment type, initial planting density and wave climate. Here, the main and interactive effects of these factors on the capacity of constructed marshes to remove nitrate from runoff was explored in field experiments at sites protected from and exposed to waves. At both sites, three experimental blocks were established, each with 24 treatment combinations of factors in experimental flumes: two platform elevations (high and low), two slopes (steep and shallow), two sediment types (coarse and fine grain), and three initial planting densities (0%, 50% and 100% cover). Nutrient rich (KNO_3) groundwater solution was fed through the marsh rhizosphere using subsurface diffusers. The relative effects of treatment combinations were then assessed by analyzing porewater NO_x concentrations with ANOVA models. None of the treatment combinations had any observable effect on porewater NO_x concentrations at the exposed site. However, both sediment type and planting density were significant main effects at the protected site with the lowest NO_x concentrations found in flumes with fine sediments and initially planted. These results confirm that design factors can have large

implications on the nutrient removal capacity of constructed marshes in areas protected from waves and that wave energy can substantially reduce the influence of these design factors.

4.2 Introduction

Alarming rates of coastal wetland loss, and the associated loss in natural benefits they provide (*i.e.,* ecosystem services; Mehvar *et al.* 2019), have been driving wetland restoration, conservation, and enhancement efforts. Constructed wetlands, like their natural counterparts, offer many ecosystem services including habitat provisioning for wildlife and fisheries (Gittman *et al.* 2015), storm surge protection (Barbier *et al.* 2015, Gedan *et al.* 2011, Van Slobbe *et al.* 2013), attenuation of waves and subsequent erosion (Bilkovic *et al*. 2019, McConchie and Toleman 2003), nutrient removal (Fisher and Ackerman 2004, Kleinhuizen and Mortazavi 2018, Sparks *et al*. 2015), and cultural benefits (*e.g.,* aesthetic, recreational and educational value; Gupta and Foster 1979, Nassauer 2004). As such, one or several of these benefits are often stated goals of many restoration and conservation projects (Yozzo *et al.* 1996, Zedler 1998). Increased nutrient concentrations and its associated impacts (*e.g.,* harmful algal blooms, hypoxia, *etc.*; Dodds 2006, Rabalais *et al.* 2002) have made runoff nutrient removal one of the top priorities for wetland projects in the Northern Gulf of Mexico.

Current best practices for designing marsh construction projects considers several environmental and material characteristics, including: platform elevation (*i.e.,* position along an elevation gradient as it relates to inundation frequency; Morris *et al.* 2002) and slope (*i.e.,* as it relates to water flow; *e.g.,* Spieles and Mitsch 2000), sediment characteristics (*i.e.,* sediment particle size and organic matter content; Bergamaschi *et al.* 1997, Coops *et al.* 1996, Davis *et al.* 2004, Lucas and Greenway 2008), and wave climate (Roland and Douglass 2005, NOAA 2015). These characteristics are important considerations for marsh establishment, but are also relevant

to the nutrient removal capacity of marshes, especially nitrogen, (Fisher and Acreman 2004) and for associated project costs (NOAA 2015, Sparks *et al.* 2013). Initial planting density may be less important for nitrogen removal as marshes develop (Sparks *et al.* 2015; Kleinhuizen and Mortazavi 2018), but may also present an opportunity for reducing project costs (Sparks *et al.* 2013). While some studies have attempted to quantify the relative influence of one or more of these factors (e.g., Sparks *et al.* 2015, Martin *et al. in review*), none have investigated how combinations of all of these factors affect nitrogen removal. Further, combinations of these factors frequently occur in nature, as a part of site-specific project design, or could be expected in the future with sea level rise. Therefore, better understanding the main and interactive effects of sediment type, platform elevation, slope and initial planting density on the nitrogen removal capacity of constructed marshes in wave exposed and protected sites is needed to maximize the cost-benefit of projects.

Sediment characteristics that could influence nitrogen removal include organic matter content (Davis *et al.* 2004, Howes and Goehringer 1994), surface area and porosity of sediments (Bergamaschi *et al.* 1997). However, these are often not considered during project design. Microbial communities rely heavily on the availability of organic compounds in soils and the exchange of various compounds, including reduced and oxidized forms of nitrogen (*e.g.,* ammonium and nitrate, respectively) during microbial metabolism (Davis *et al.* 2004). Thus, the limited organic matter associated with sandy sediments may not be sufficient to support removal pathways. The greater pore spaces associated with sandy sediments may also facilitate greater flow of solutes through the rhizosphere, including nitrate. Sediment type is also linked to varying microbial community structure (Yamamoto and Lopez 1985), diversity (Jesus *et al.* 2009), and productivity (Sinsabaugh and Findlay 1995), which further influences nitrogen removal in

marshes (Wetzel 2001). While marshes are constructed in varying sediment types, based on location, sediment amendments that may be required with certain site conditions (*e.g.,* severely eroded sites, higher wave energy) rarely use fine grain sediments. Instead, commercially available sandy sediments are most commonly used for backfilling, terracing, sloping or for raising platform elevation as these sediments are heavier and thus, less susceptible to erosion from waves and currents (Woodruffe 2002).

Vegetation presence and density also has direct and indirect effects on nitrogen removal. Plant growth increases with increasing nutrient availability, resulting in greater abundance of above- and below-ground materials (Morris *et al.* 2013) and greater incorporation of nutrients into plant tissues (Morris *et al.* 2013; Silvan *et al.* 2004; Sparks *et al.* 2015). The presence of robust vegetation may also slow groundwater flow through the marsh (Sparks *et al.* 2014), increasing residence time and subsequent removal of nitrogen by marsh vegetation and soil microbes. Plants also indirectly facilitate the removal or transformation of excess nitrogen through their influence on other soil microbial processes (Brix 1997). For example, radial oxygen loss from plant roots (Brix 1997) favors the conversion of reduced nitrogen (*e.g.,* ammonium) to oxidized forms (*e.g.,* nitrate) that are more actively removed by plants or microbes (via denitrification). Decaying plant materials also serve as an important carbon source in microbial metabolism that can further facilitate nutrient removal (Howes and Goehringer 1994). Recently, Sparks *et al.* (2013) demonstrated the project cost savings possible by modifying the initial planting density (*i.e.,* cover) of planted vegetation. Indeed, in subsequent simulated runoff experiments, Sparks *et al.* (2015) found that nitrogen removal was similar in plots planted at 50% and 100% initial planting density.

Elevation and slope are also potentially important considerations for constructed wetland projects because of the role each play in soil conditions. Platform elevation is related to plant growth (Morris *et al.* 2002) via direct and indirect effects on oxygen availability (*e.g.,* varying hydroperiod; Armstrong 1979; Mendelssohn and McKee 1988). Prolonged inundation, as would be expected at lower platform elevations, decreases oxygen availability resulting from plant and microbial metabolism and the slow diffusion of oxygen in water (Armstrong 1979). Hydric soils affect plant nutrient removal in two important ways: by increasing competition for nitrogen with soil microbes (Engelaar *et al.* 2000) and via the accumulation of phyto-toxins (*e.g.,* sulfides) that limit plant growth (Reddy and DeLaune 2008). Thus, nutrient additions to marshes positioned at lower elevations may reverse the negative effects on plant growth associated with hydric soils (Mendelssohn and McKee 1988) and may result in enhanced nutrient utilization. However, at higher platform elevations, the effects of aerobic soil conditions on nutrient removal capacity are mixed. On the one hand, plant growth is maximized at higher elevations (Morris *et al.* 2002) which may favor increased nutrient uptake. Further, aerobic conditions also favor oxidized nutrient species (*e.g.,* nitrate) that may be easily exported from the marsh (Kleinhuizen and Mortazavi 2018). Still, inundation under both scenarios (*i.e.,* low and high platform elevations) is expected to change as sea level rise continues in the future (IPCC 2019). Likewise, though commonly amended or specified in restoration designs, platform slope is rarely investigated within the context of nutrient removal by plants, especially in coastal wetlands. Slope has a strong influence on groundwater flow rate which may affect nutrient removal in wetlands (Spieles and Mitsch 1999). Indeed, Sparks *et al.* (2014) found little nitrate removal in fast flowing sandy soils. Similarly, if gentler slopes reduce water flow, the effect could be an increase in the residence time of nutrients which could allow for further uptake by plants and microbes

(Tobias *et al.* 2001). However, as with platform elevation amendments, it remains unclear if slope amendments improve nutrient removal capacity to levels justifying the increased project costs that would be required.

Finally, the effect of waves (Bilkovic *et al.* 2019, McConchie and Toleman 2003) on the nutrient removal capacity of constructed wetlands is not fully understood. Wave climate has some influence on the establishment of plants (Keddy 1985, Roland and Douglass 2005) and overall plant growth, such that plant growth is generally maximized in areas experiencing smaller wave heights (Roland and Douglass 2005, Silinski *et al.* 2018). As waves increase in frequency or magnitude, their effects on plant growth and persistence could effectively limit the nutrient removal capacity of constructed marshes. However, some aspects of waves may actually improve soil conditions. For example, wave breaking may increase oxygenation of the rhizosphere (e.g., Hosoi *et al.* 1977). Wave action may also encourage plant investment in defenses, including greater production of above- and/or below-ground parts for anchoring or energy attenuation (Feagin *et al.* 2009), which could result in greater nutrient uptake by plants or enhanced oxygenation of the rhizosphere via roots. Alternatively, as wave turbulence increases oxygen availability, it may also facilitate the conversion of nutrients to those more mobile in solution (*e.g.*, NH_4 to NO_3) that are subsequently removed from the system via uptake by plants and microorganisms, leaching or denitrification.

To evaluate the main and interactive effects of the factors mentioned above that could influence the nitrogen removal capacity of constructed marshes, we manipulated sediment type (*i.e.*, coarse and fine), vegetation density (*i.e.,* 0%, 50%, 100%), marsh platform elevation (*i.e.,* position along the marsh platform (Morris *et al.* 2002); high and low) and slope (*i.e.,* steep and gentle) in experimental flumes featuring different treatment combinations at sites with and

without wave exposure. We then simulated upland runoff events by pumping a groundwater nutrient solution through the marsh rhizosphere to evaluate the removal capacity of the treatment combinations (*e.g.,* Sparks *et al.* 2015). Following previous findings investigating some or all of the treatments examined here, we hypothesized that platform elevation and slope would not have a significant effect on nutrient removal and that plots with fine sediments and initially planted at either 50% or 100% density would remove the greatest amount of the groundwater solution as compared to other combinations.

4.3 Methods

4.3.1 Study Site Description

Two sites were selected within Weeks Bay National Estuarine Research Reserve (WBNERR) in Fairhope, Alabama, USA (Figure 4.1) to allow for the comparison of protected and exposed shorelines: one along Fish River (*i.e.,* the exposed site) and another within an adjacent – previously dredged - canal complex (*i.e.,* the protected site; Figure 4.1). Marsh species composition within this mesohaline (salinity ≤ 5) reach of Fish River and within adjacent canals is dominated by the study species, *Juncus roemerianus*, with sub-dominant species *Typha latifolia* and *Cladium jamaisence* also present. Both sites experience a semi-diurnal microtidal regime (tidal range ~ 0.6 m) but differ in their exposure to waves. Boat wake-waves are common at the exposed site whereas boat traffic within the canals at the protected site is limited to only a few slow-moving (*i.e.,* idle speed or trolling) vessels. The exposed and protected sites also differ in shoreline morphology. The shoreline at the exposed site is characterized by intermixed fringing marshes and sandy beaches that slope gently from mean tide level to a depth of 0.25 m over a 3-m distance. In contrast, the shoreline at the protected site features a banked edge

covered by various turf grasses (*Poaceae* spp.) where water depths exceed 1 m in less than 0.3 m.

4.3.2 Experimental Design and Site Construction

The main and interactive effects of varying marsh construction designs on porewater concentrations of oxidized nitrogen species (*i.e.,* NO_x) were evaluated at the protected and exposed sites using ANOVAs. At each study site a total of 24 treatment combinations, including two sediment types (*i.e.*, coarse and fine), two platform slopes (*i.e.,* steep and shallow), two platform positions (*i.e.,* steep and shallow) and three initial planting density (*i.e.,* 0%, 50% and 100% cover), were replicated within three blocks (Figure 4.2).

At the exposed site, the 24 treatment combinations were fully randomized within each of the three experimental blocks (*i.e.,* randomized block design). Treatment combinations were designated in 0.3 m wide x ~1.22 m long experimental flumes running perpendicular along a ~5 m stretch in each block of the exposed site shoreline. Flumes were separated by ~1.27 cm thick x 1.22 m long x 0.6 m tall PVC sheets driven 25 cm (relative to existing grade) into the earth along the ~5 m block transect (Figure 4.2A). Each flume was excavated followed immediately by placement of an impervious clay layer at the base of each flume according the designated slope treatment (0.08 (1:12) for shallow and 0.17 (1:6) for steep). Flumes were then filled to 25 cm above the clay layer with sediments and planted according to planting density and platform position treatments. Sediments were purchased locally and included coarse (sand; grain size 0.25 mm - 2 mm) and fine (topsoil; grain size ≤ 0.25 mm) sediment types. Whole sods (i.e., soil and above- and below-ground vegetation components) measuring 30 cm wide x 30 cm long x 30 cm deep at the base were extracted from a nearby donor marsh (Figure 4.1) for use in experiments following Sparks *et al.* (2014, 2015).

To differentiate platform position and simulate current and future sea-levels, plants and sampling wells were established either at the upper end or lower end of a 60 cm long area in the flumes. Placement of plants for the high platform position treatment (*e.g.,* current sea-level) began 10 cm from the upland edge of flumes, while plants in the lower platform position treatment (*e.g.,* future sea-level) were planted in an area starting 30 cm below the upland edge of flumes (Figure 4.2A). After trimming sods to 25 cm depth, initial planting density treatments were established within the flumes as follows: 2 whole sods back to back for 100% initial planting density and 1 whole sod quartered and arranged in a checkerboard pattern for 50 % initial planting density; 0 % initial planting density plots were left bare (*e.g.,* Sparks *et al.* 2015). Two porewater wells, each constructed from ~3.8 cm diameter x 30 cm tall screened PVC pipe, were then installed in all experimental flumes: within and at the end of the planting area (i.e., wells A and B, respectively; Figure 4.3). An auger was used to install wells which were then filled with sandy sediment, regardless of experimental sediment treatment. Diffuser plates (Sparks *et al.* 2015) were also placed to a depth of 20 cm within a 10 cm buffer area above the planting area to facilitate the even distribution of the nutrient solution during experimental runoff simulations (Figure 4.3; discussed below).

Shoreline morphology at the protected site required alternative methods to establish experimental conditions comparable to those at the exposed site. Notably, the abrupt drop in water depth from the edge of protected site shorelines required platform amendments to achieve elevation (relative to mean high water) similar to that at exposed sites. Therefore, experimental field mesocosms were constructed to house experimental flumes (Figure 4.2B). Mesocosms were framed using dimensional lumber and PVC materials (Figure 4.2B, Appendix C.1) to inside dimensions representing half of the plots within an exposed site block: ~2.5 m wide (parallel to

shoreline) x ~1.22 m long (perpendicular to shoreline) x 25 cm deep (from the base to top of the mesocosm). Three sides of mesocosm frames were constructed using ~5 cm x ~30 cm dimensional lumber, while the seaward side of mesocosm boxes was constructed using ~5 cm x ~5 cm lumber and PVC lattice which was covered in landscaping fabric, so as to facilitate water movement (Appendix C.1). Structural support at the base of mesocosm frames was provided by ~5 cm x ~10 cm lumber running lengthwise from the landward to shoreward edge of mesocosms. Prior to setting within framed mesocosms, eleven ~1.27 cm thick x ~1.27 cm deep grooves were cut lengthwise and spaced evenly (~30 cm width) along the long end of ~2.54 cm thick x ~2.5 m wide x ~1.22 m PVC sheets that would serve as the impermeable base of mesocosms. After base installation, flume walls, constructed from ~1.27 cm thick x ~30.27 cm tall x ~ 1.22 m long PVC sheets, were glued using silicone adhesive and set within grooves to create 12 flumes within mesocosms (Appendix C.1). Mesocosms were set on top of concrete cinder blocks in the water near the edge of protected site shorelines so as to facilitate slope and elevation adjustments comparable to those at exposed sites (described above). However, slope could not be manipulated within the mesocosms. Therefore, within each of the three experimental blocks, two mesocosms were constructed. One mesocosm replicated our steep slope from the exposed site, and the other replicated the low slope. This resulted in a split-plot design (*i.e.,* blocks = whole plots, slope treatments/individual mesocosms = split plots). Combinations of sea-level, planting density, and sediment type were then randomly assigned within the mesocosms (*i.e.,* slope split plots) following the methods described for the exposed sites.

The exposed and protected sites were constructed in May and September 2016, respectively, and allowed to acclimate over winter 2016 before starting experiments.

4.3.3 Experimental Run-off Simulations

Experimental run-off simulations were administered over 10-day periods during May and August 2017 at both the protected and exposed sites to capture any possible changes in nutrient removal that could be attributed to the evolution of growth in *J. roemerianus* marshes typical in the Northern Gulf of Mexico (nGOM; Eleuterius 1976). A 10-day period was chosen to ensure that plots were saturated by the nutrient plume (*i.e.,* steady state) based on calculations from previous experiments in coarse sediments (*e.g.,* Sparks *et al.* 2014) and fine sediments (*i.e.,* Sparks *et al.* 2015). Simulations began on May 11th and August 21st at the protected site and on May 23rd and August 3rd at the exposed site.

To simulate run-off events, a gravity-fed continuous drip system was established to direct a simulated groundwater (SGW) solution from upland reservoirs to experimental flumes via installed subsurface diffusers (Appendix C.2; Figure 4.3; Sparks *et al.* 2014). The SGW was mixed onsite using centrifugal pumps in 208 L mixing containers to produce a concentration of 1000 µM KNO_3 solution. While this is a high concentration, it was necessary due to high dissolved inorganic nitrogen (DIN) concentrations observed in some flume porewater samples collected prior to simulations and from samples collected in similar experiments conducted near the study area (Martin *et al. in review*). After mixing, the SGW was pumped from the mixing containers to individual ~102 L reservoirs (*i.e.,* one reservoir per experimental flume; Appendix 4.2). These reservoirs were connected to subsurface diffusers via 0.95 cm (inside diameter) flexible vinyl tubing and featured an inline valve that allowed drip rate control. The drip rate was set to continuously deliver ~34 L/day over the 10-day simulation period (Sparks *et al.* 2015). During this period, reservoirs were monitored daily and refilled, as necessary.

4.3.4 Porewater Sampling and Processing

Porewater samples were collected from wells before and immediately following simulated run-off events to assess the effect of treatment combinations on NO_x concentrations. Porewater was extracted from wells using sipper tubes (*e.g.,* McKee *et al.* 1988) and stored in plastic scintillation vials which were frozen until subsequent analysis. Nutrient analyses were performed using a Skalar San+ segmented flow autoanalyzer, following standard EPA methods for nutrient analyses, by Technical Support Services at the Dauphin Island Sea Lab, Alabama, U.S.A. (*e.g.,* Sparks *et al.* 2015, Temple *et al.* 2019).

4.3.5 Percent Cover Change

Percent cover of *J. roemerianus* was expected to increase as was found in similar experiments (Sparks *et al.* 2014, Sparks *et al.* 2015). However, *J. roemerianus* is also known to facilitate the growth of other species in similar fringing marshes (Martin *et al. in review*). Therefore, the percent cover of each species in experimental flumes was visually estimated before and after Summer 2017.

4.3.6 Statistical Analyses

The effects of the varying treatment combinations on porewater NO_x concentrations were evaluated using ANOVAs with post hoc tests when appropriate. ANOVA model structure differed between the exposed and protected sites. For the exposed site, slope, sediment type, initial planting density, and platform position were treated as fixed factors while block was treated as a random factor. The model for the protected site featured sediment type, initial planting density, and platform position as fixed factors, and block and slope were treated as random factors. The most offshore porewater wells (B) were lost in one block at the exposed site

due to wave action. Therefore, only data from porewater A wells were considered at the exposed site; whereas, data from both wells were considered at the protected site. Data were transformed as appropriate to meet model assumptions of normal distribution and equal variance. Significance is reported at the $\alpha = 0.005$ level to compensate for the high number (24) of treatment levels. Following full model construction, non-significant factors (i.e., $p > 0.005$; Table 4.1) were removed and the significance (at the $\alpha = 0.05$ level) of main and interactive effects of the remaining factors was evaluated in simpler models. Final model selection was made using Akaike information criteria (AIC; Burnham and Anderson 2002). Percent cover change data at both sites were not normally distributed and could not be corrected using transformations and therefore, these responses were compared individually for each initial planting density treatment at each simulation and between exposed and protected sites using Kruskal-Wallis tests. Statistical analyses were performed in R (R core team 2020), using base packages, "lme4" for model construction (Bates *et al.* 2015) and "emmeans" for multiple comparisons (Lenth 2020).

4.4 Results

4.4.1 Main Treatment Effects

Main treatment effects varied across porewater wells in flumes and across sites (Table 4.1). None of the treatments had any detectable effect on porewater NO_x at the exposed site ($p > 0.005$; Table 4.1). Therefore, no other statistical analyses were run for nutrient concentrations at the exposed site. At the protected site, only sediment type and initial planting density had a significant effect on porewater NO_x ($p < 0.005$; Table 4.1). Neither platform position nor slope had any measurable effects on nutrient concentrations in samples collected after simulations ($p > 0.005$; Table 4.1). The significant effects of sediment type and initial planting density are discussed further below.

4.4.2 Effects of Sediment Type and Initial Planting Density at the Protected Site

Reduced models consistently confirmed the strong main effects of sediment type and initial planting density (Table 4.2). Indeed, these main effects had significant effects on porewater NO_x collected from both wells after each simulation ($p < 0.05$; Figure 4.4, Table 4.2). However, the interactive effects of sediment type and initial planting density on porewater NO_x were significant only in A wells following the second simulation ($p < 0.05$; Table 4.2). Results of pairwise comparisons examining the effects of initial planting density on NO_x in A and B wells collected following simulation 1 and those assessed from B wells collected following simulation 2 varied (Table 4.3). Mean NO_x concentration was significantly lower in planted plots (i.e., 50 and 100% initial planting density) as compared to bare plots in simulation 1-A wells and simulation 2-B wells ($p < 0.05$; Table 4.3). Interestingly, while mean B well NO_x concentration was significantly lower in plots initially planted at 100% density as compared to bare plots following simulation 1 ($p < 0.05$), NO_x concentration in plots initially planted at 50% density was not statistically different from bare plots ($p > 0.05$; Table 4.3). However, mean NO_x concentration was also not statistically different among planted treatments in B wells following simulation 1, as was also observed in A and B wells following simulations 1 and 2, respectively ($p > 0.05$; Table 4.3).

While overall trends in mean NO_x concentrations associated with the different treatment combinations assessed following simulation 2 in A wells were straightforward, pairwise comparisons of these combinations varied (Table 4.4). Overall, NO_x concentrations decreased along a gradient of both sediment type and initial planting density (Table 4.4). The greatest NO_x concentrations were observed in bare plots with coarse sediments while the lowest NO_x concentrations were found in plots initially planted at 100% density in fine sediments (Table

4.4). With the exception of the significantly higher NO_x concentrations observed in bare plots as compared to those initially planted at 100% density in coarse sediments ($p < 0.05$), differences among individual treatment combinations broke mostly along the differing sediment types (Table 4.4). However, even then, NOx concentrations observed in plots initially planted at 100% density in coarse sediments were not statistically different from bare plots and those initially planted at 50 and 100% density in fine sediments ($p > 0.05$; Table 4.4).

4.4.3 Plant Cover at the Exposed and Protected Sites

Whereas observed cover of plant species at protected sites prior to SGW simulations remained mostly consistent with initial planting density treatments (Figure 4.5), observed cover changed within bare plots and plots initially planted at 100% planting density at exposed sites (Figure 4.6). Bare plots in the exposed site saw a 25% increase in cover by simulation 2 ($p < 0.05$), plots planted at 100% planting density declined by nearly 50% ($p < 0.05$), and plots planted at 50% density did not differ significantly from the initial planting ($p > 0.05$; Figure 4.7, Appendix C.3). At protected sites, differences in cover between initial planting density treatments were statistically significant only for 100% plots where covered declined by nearly 20% at simulation 2 ($p < 0.05$; Appendix C.3). Interestingly, observed cover in 50% initial planting density plots did not differ between exposed and protected sites ($p > 0.05$). In contrast, bare plots at exposed sites featured significantly greater plant cover than the those in the protected sites ($p < 0.05$) and 100% initial planting density plots at exposed sites had significantly less cover than their protected counterparts ($p < 0.05$; Appendix C.3). As observed in previous work in the area (Martin *et al. in review*), other plant species besides *J. roemerianus* were found in plots at both sites. Other species found in plots included *Eleocharis robbinsii*, *Typha latifolia*, *Panicum repens, Sagittaria lancifolia*, *Panicum virgatum*, *Spartina patens*,

Alternanthera philoxeroides, *Amaranthus cannabinus*, *Kosteletzkya virginica*, *Distichlis spicata* and *Cladium jamaisence*. However, individual cover of other species did not exceed 2% of the vegetated area in any of the plots. Still, combined cover of these species in plots was, on average, greatest at protected sites (Figures 4.5 and 4.6).

4.5 Discussion

This study builds on the work of others investigating the most cost-effective options for fringing marsh restoration in the nGOM (Martin *et al. in review,* Sparks *et al.* 2013, Sparks *et al.* 2014, Sparks *et al.* 2015). Like others, we found that marshes planted initially at 50% and 100% density were statistically similar in terms of nitrogen removal (Table 4.3, Figure 4.4; Sparks *et al*. 2013; Sparks *et al*. 2015) and that platform position was not a significant factor in nitrogen removal at the protected site (Table 4.1; Martin *et al. in review*). Further, we found a strong effect of sediment type (Table 4.2, Figure 4.4), which agreed with previous experiments conducted individually in fine- and coarse-grained sediments (Sparks *et al.* 2015; Sparks *et al.* 2014). However, we did not anticipate the results observed at the exposed site where none of the factors had any measurable effect on porewater NO_x (Table 4.1).

At the protected site, the effects of sediment type and initial planting density on nitrogen removal were largely expected and may be due, in part, to the effects each has on water flow through the marsh and the abundance of organic materials. Flow is often tied to the rate of nitrogen removal in marshes, with slower flows leading to higher removal rates (Sparks *et al.* 2014, Spieles and Mitsch 1999, Tobias *et al.* 2001). While we did not measure flow through the flumes in this study (constant flow of introduced solution), we manipulated three factors that can influence flow rates in marshes: vegetation density (*i.e.,* initial planting density), slope, and sediment type (Sparks *et al.* 2014, Tobias et al. 2001). Of these factors, only initial planting

density and sediment type had any observable effect on NO_x removal (Table 4.1) and of the two, sediment type appeared to be the most important (Table 4.4). Sparks *et al.* (2014) reported a similar trend among various planting treatments in coarse grain sediments where nutrient removal was similarly low among planting treatments in high flow experimental flumes, even with a modest decline in observed water flow with increasing planting density. These differences stood in stark contrast to previous experiments by the authors showing that planted marshes remove a substantial amount of nutrients in fine and organic soils (Sparks *et al.* 2013, Sparks *et al.* 2015).

Results from protected site experiments help to explain these differing results and lends credence, albeit limited, to the influence of sediment type on the rate of groundwater flow and subsequent biologically mediated nitrogen removal as suggested by Sparks *et al.* (2014). Indeed, sediment type and initial planting density were consistently important factors in NO_x models (Table 4.2). Planted treatments generally removed more NO_x than did bare treatments (Table 4.3) while fine sediments resulted in lower porewater NO_x concentrations (Figure 4.4). The interaction between sediment type and initial planting density was only significant in one of the models examined (Table 4.2) and thus, broad interpretation of these results is limited. However, multiple comparisons analysis did demonstrate the overwhelming influence of sediment type, as treatments with coarse sediments had higher mean NO_x concentrations as compared to treatments with fine sediments. Paired with those of Sparks *et al.* (2013, 2014 and 2015), the results observed at the protected site suggests sediment type is a stronger influencer of flow rate, and likely nutrient removal, than the abundance of plant material.

Fine sediments are also typically rich with particulate organic materials, which may be sufficient to facilitate denitrification, a dominant pathway for nitrogen removal in brackish

marshes (Davis *et al.* 2004, Yamamoto and Lopez 1985), and can be supplemented further via the production of benthic microorganisms even in the absence of plant materials (Hamersley and Howes 2003). We found some evidence to support the dominant influence of this pathway in the multiple comparisons analysis. This analysis showed that non-planted plots with fine sediments were statistically similar to plots initially planted at 100% density in coarse sediments (Table 4.4). Further experiments designed explicitly to examine differing flow rate and soil organic matter content in the context of differing sediment types and planting densities are needed to fully understand the relative effects of each on nutrient removal in marshes.

In contrast to the protected site, sediment type and initial planting density treatments were not statistically significant in exposed site NO_x models, which is likely due to the indirect effects of waves. Conditions at the exposed site differed from those at the protected site and at sites examined in previous experiments (Sparks *et al.* 2013, 2014, 2015) mainly in that it was frequently subjected to waves from passing boats. Here, waves may have mitigated the significant effects of sediment type and initial planting density via two indirect mechanistic pathways: by controlling biomass production and by limiting soil anoxia (*i.e.,* those conditions ideal for denitrification; Davis *et al.* 2004).

Waves are known to influence the structure of coastal plant communities (Roland and Douglass 2005, Woodruffe 2002). For example, Roland and Douglass (2005) found marsh coverage and health diminished with the increasing regularity of large waves (*i.e.*, over 30 cm). Cover at our exposed site suggested a similar limiting effect on plant growth. Indeed, cover within plots initially planted at 100% density declined towards 50% density while cover within 50% density plots remained constant and cover within initially bare plots increased (Figure 4.6). This levelling effect on plant growth may help to explain the observed lack of initial planting

density treatment effects on porewater NO_x concentrations at the exposed site (Table 4.1). In fact, waves are often linked to various morphological features associated with plant growth that could affect nitrogen removal in marshes. These include stem density, height aboveground (Silinski *et al.* 2018), and belowground rooting behavior (Balke *et al.* 2011). Additionally, waves may alter the structure of marsh communities in other important ways that could indirectly affect nitrogen utilization in marshes (*e.g.,* via controls on species distribution or nutrient utilization in plant tissues; Keddy *et al.* 1985). For example, flexibility of plant shoots is thought to increase the wave tolerance of plant tissues (Rupprecht *et al.* 2015, Schulze *et al.* 2019) but is sometimes also linked to the availability and utilization of differing nutrients in plant tissues (*e.g.,* Silinski *et al.* 2018, Sloey and Hester 2018). While plant responses to many stressors is well documented (Kirwan and Megonigal 2013, Nyman *et al.* 2006, Temple *et al.* 2019, Vasquez *et al.* 2006), plant responses to waves are not and need further research.

In addition to its influence on plant growth, wave action may have disrupted denitrification at surface level sediments that would typically go anoxic at the exposed site once the marsh was inundated (*i.e.,* mid to high tide). Nitrogen removal in brackish marshes typically follows two major pathways: uptake by plants and microbenthos during biomass production and microbially-mediated denitrification (Davis *et al.* 2004). Of these two pathways, the latter has often accounted for the greatest pathway of allochthonous nitrogen removal in marshes (VanZomeren *et al.* 2012). For example, several researchers have estimated that over 60% of nitrogen is removed from marshes via this pathway (VanZomeren *et al.* 2012, White and Howes 1994). Various studies have demonstrated the factors controlling denitrification in marshes (Hu *et al.* 2019, Neubauer *et al.* 2019, Zheng *et al.* 2016), but in general, the process requires available nitrate and organic carbon sources, the presence of denitrifying microorganisms and

anaerobic conditions (Davis *et al.* 2004). Both exposed and protected sites were presumably established in a way that would satisfy most of these requirements and for at least part of the day (*e.g.,* as influenced by tidal water movement). For example, while not a focus of this study, it is likely that experimental sods used in planting treatments were similar in terms of soil organic matter and microbial community diversity (*e.g.,* including denitrifying microorganisms) at both the protected and exposed sites since they were harvested from the same donor marsh. Additionally, all flumes were supplied a steady supply of available nitrate. However, soil hydroedaphic conditions within the 25 cm depth of flume sediments and sods likely differed between the two sites due to the potential wave-driven reaeration of these sediment layers (*e.g.,* Hosoi *et al.* 2018) with excessive daytime boating activity. As discussed above, the study area experiences a diurnal microtidal regime. Within this regime, the predominance of daytime high tides shifts semi-annually such that high tides are more frequent during the daytime in summer months and hence, soil anoxia is also most likely during this time. Incidentally, this period (*i.e.,* daytime) also coincides with the greatest frequency of recreational boating traffic (*i.e.,* 8 am to 6 pm; personal observation). As such, wave activity may have reversed the declining hydroedaphic conditions that would be expected with tidal inundation. If so, aerobic soil conditions would persist and thereby limit denitrification (Koch *et al.* 1992). Thus, we speculate that the convergence of these events nullified the strong sediment type effect on NOx at the exposed site, as was observed in protected site flumes receiving fine sediments even in the absence of vegetation (*i.e.*, control plots with fine sediments; Table 4.4). Still, more research is needed to determine the relative influence of waves on various nitrogen removal pathways, including denitrification.

Other factors may also have played a role in the differences in model results observed at exposed and protected sites. While we assumed comparable salinity between sites, the exposed site may have had more contact with higher salinity waters originating from Weeks and Mobile Bays which could also limit denitrification in marshes. For example, Neubauer *et al.* (2019) found that marshes more regularly exposed to higher salinities had a lower abundance of denitrifying microorganisms as compared to reference marshes in tidal freshwater systems. This change in microbial community structure resulted in a nearly 70% decline in denitrification in these marshes. Experimental design differences between the sites may have also played a role. For example, mesocosms effectively eliminated groundwater exposure at the protected site which could have further influenced removal processes at the exposed site. Tidal forcing and exchange of materials between ground- and sea waters within the intertidal zone has been demonstrated to favor certain microbial communities and nitrogen utilization pathways (*e.g.,* Liu *et al.* 2017), for example. A disconnection from groundwater and the lack of potential flushing by waves at the protected site could also lead to higher salinities there that would favor other nitrogen removal pathways as well (Neubauer *et al.* 2019). The mechanisms driving these processes were beyond the scope of this study but warrant further future research.

4.6 Conclusions

Shoreline wetland conservation, restoration, and enhancement can be an effective management tool for reducing the magnitude of upland pollutants introduced to our coastal waters. However, there are several site characteristics that must be considered when designing these projects. Our research suggests that sediment type and vegetation density are among the most important considerations for projects targeting nutrient removal. This research further suggests that while accounting for wave climate is standard practice for the purposes of plant

establishment, it may also be an important consideration for other project goals such as nutrient removal. In fact, wave action may have significant negative consequences to the objectives of coastal restoration, conservation and enhancement projects.

Table 4.1 Results from ANOVA models examining the main effects of experimental treatments at protected and exposed sites for A and B well NOx concentrations.

Site	Main Treatment Effect	Porewater Well	
		A	B
Protected Site	**sediment type**	0.008	0.0001*
	initial planting density	< 0.0001*	< 0.0001*
	platform position	ns	ns
	platform slope	ns	ns
Exposed Site	**sediment type**	ns	NA
	initial planting density	ns	NA
	platform position	ns	NA
	platform slope	ns	NA

None of the treatments were significant at the exposed site. At the protected site, only sediment type and initial planting density were significant main effects. Data pools spring and post summer simulation data collected from protected and exposed sites. Significance at the 0.005 level is denoted by *.

Table 4.2 Reduced ANOVA model results constructed from protected site data collected from a and b wells and following spring and post summer simulations.

Type II ANOVA							
Simulation	**Well**	**Predictor**	**F**	**Df**	**Res Df**	**p**	
1	**A**	**block**	0.21	2	3.54	ns	
		sediment	27.78	1	58.17	< 0.0001	*
		initial planting density	4.93	2	58.07	0.011	*
		interaction	1.34	2	58.07	ns	
	B	**block**	0.33	2	3.12	ns	
		sediment type	143.04	1	56.12	< 0.001	*
		initial planting density	5.46	2	56.10	0.007	*
		interaction	0.11	2	56.11	ns	
2	**A**	**block**	0.38	2	3.80	ns	
		sediment	59.23	1	61	< 0.0001	*
		initial planting density	5.46	2	61	< 0.001	*
		interaction	0.11	2	61	0.02	*
	B	**block**	1.35	2	4.72	ns	
		sediment type	152.80	1	61.00	< 0.0001	*
		initial planting density	7.28	2	61.00	< 0.005	*
		interaction	0.58	2	61.00	ns	

Reduced ANOVA model results constructed from protected site data collected from a and b wells and following spring and post summer simulations (simulations 1 and 2, respectively). The main effects of sediment type and initial planting density on porewater NO_x concentrations were consistently significant in models. However, the interaction of these main effects was only significant in A wells collected following simulation 2. Significance at the 0.05 level is denoted by *.

Table 4.3 Cover contrasts from reduced ANOVA models constructed from protected site data collected from A and B wells and following spring and post summer simulations.

Contrasts				
Simulation	**Well**	**Contrast**	**p**	
1	**A**	**0 – 50**	0.033	*
		0 – 100	0.023	*
		50 – 100	ns	
	B	**0 – 50**	ns	
		0 – 100	0.001	*
		50 – 100	ns	
2	**B**	**0 – 50**	0.001	*
		0 – 100	0.001	*
		50 – 100	ns	

Cover contrasts from reduced ANOVA models constructed from protected site data collected from A and B wells and following spring and post summer simulations (simulations 1 and 2, respectively) without significant interaction terms. Porewater NO_x concentrations collected from vegetated plots were statistically similar and were generally statistically different from control (i.e., non-vegetated) treatments. However, porewater NO_x concentrations collected from control treatments were also not statistically different from half density treatments. Significance at the 0.05 level is denoted by *.

Table 4.4 Pairwise comparisons of sediment type and initial planting density treatments effects on porewater NO_x concentrations collected from A wells following simulation 2.

Contrast			Estimate	SE	Df	t ratio	p	
0,Coarse	-	50,Coarse	0.759	0.227	44	3.348	ns	
0,Coarse	-	100,Coarse	1.258	0.227	44	5.55	< 0.0001	*
0,Coarse	-	0,Fine	1.615	0.227	44	7.128	< 0.0001	*
0,Coarse	-	50,Fine	1.861	0.227	44	8.212	< 0.0001	*
0,Coarse	-	100,Fine	1.832	0.227	44	8.083	< 0.0001	*
50,Coarse	-	100,Coarse	0.499	0.227	44	2.202	ns	
50,Coarse	-	0,Fine	0.857	0.227	44	3.78	0.0059	*
50,Coarse	-	50,Fine	1.102	0.227	44	4.864	0.002	*
50,Coarse	-	100,Fine	1.073	0.227	44	4.736	0.003	*
100,Coarse	-	0,Fine	0.358	0.227	44	1.578	ns	
100,Coarse	-	50,Fine	0.603	0.227	44	2.662	ns	
100,Coarse	-	100,Fine	0.5741	0.227	44	2.533	ns	
0,Fine	-	50,Fine	0.246	0.227	44	1.084	ns	
0,Fine	-	100,Fine	0.217	0.227	44	0.955	ns	
50,Fine	-	100,Fine	-0.0291	0.227	44	-0.128	ns	

With a few exceptions, differences broke mostly along differences in sediment type treatments. Significance at the 0.05 level is denoted by *.

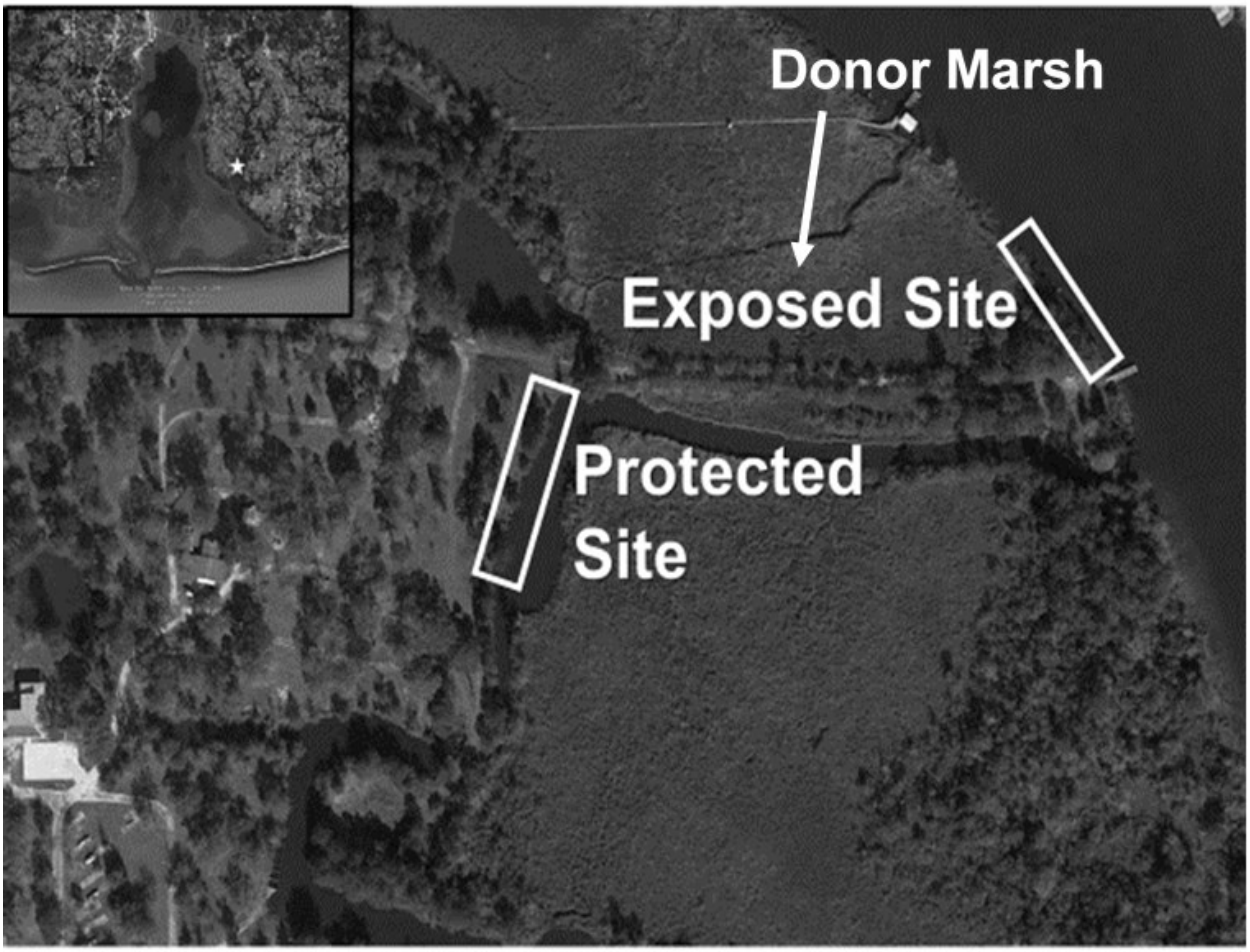

Figure 4.1 Map showing the location of the study area, experimental project sites and donor marsh.

The study was conducted on and near the Fish River near Mobile Bay, Alabama, USA (inset). Sods used in experiments were collected from a nearby donor marsh and transported for use at the site along the Fish River (exposed site) and within a nearby adjacent canal (protected site).

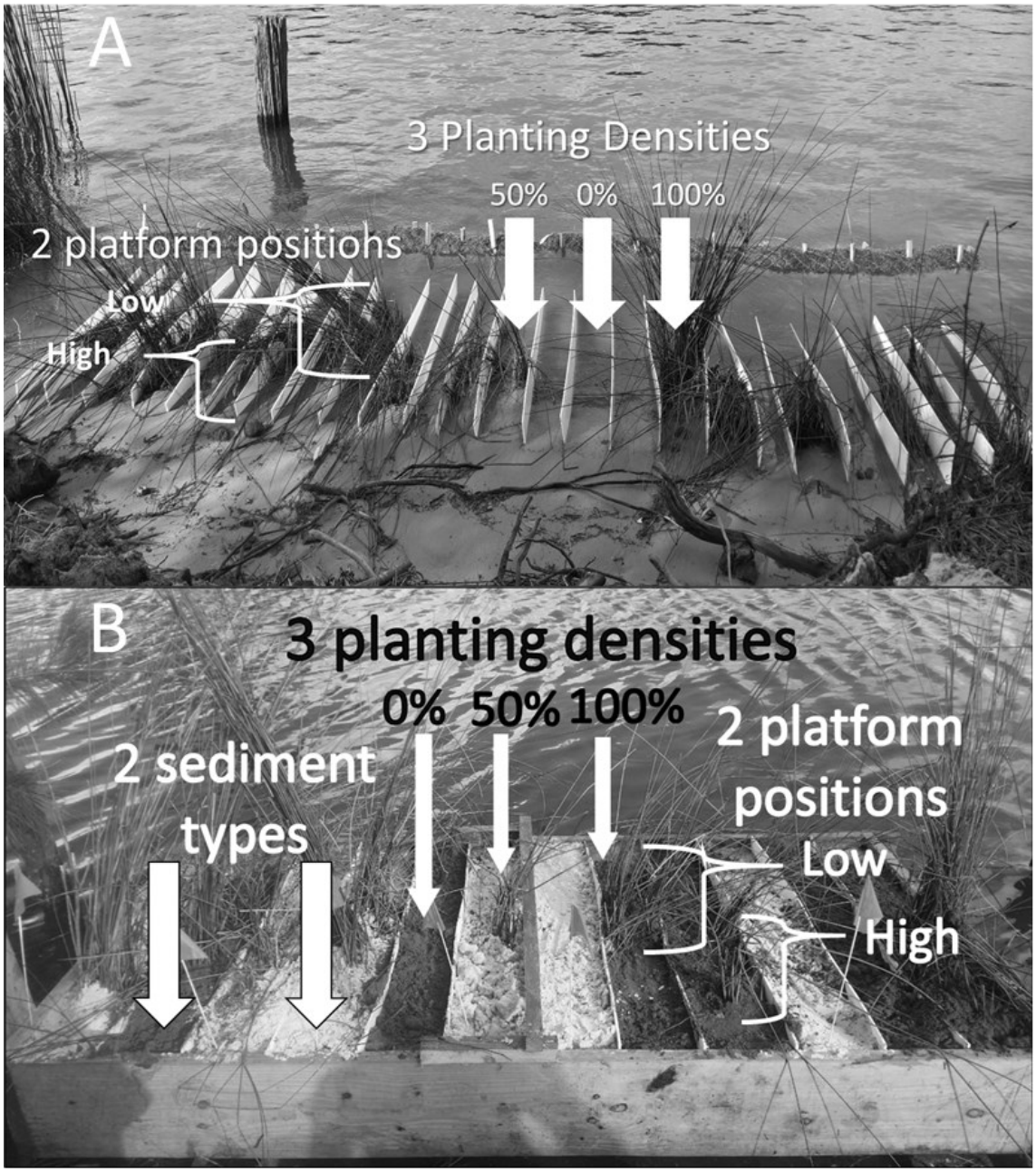

Figure 4.2 Overview of experimental treatment combinations at the exposed and protected sites.

Overview of experimental treatment combinations at the exposed (A) and protected (B) sites. At each site, combinations of two sediment types (coarse and fine), two platform slopes (steep and shallow), two platform positions and initial planting density (0%, 50% and 100% cover), were replicated within three blocks. However, while slope treatments were fully randomized at the exposed site, slope treatments were set within two groups (i.e., steep and shallow) at the protected site (B) due to the fixed nature of experimental mesocosms.

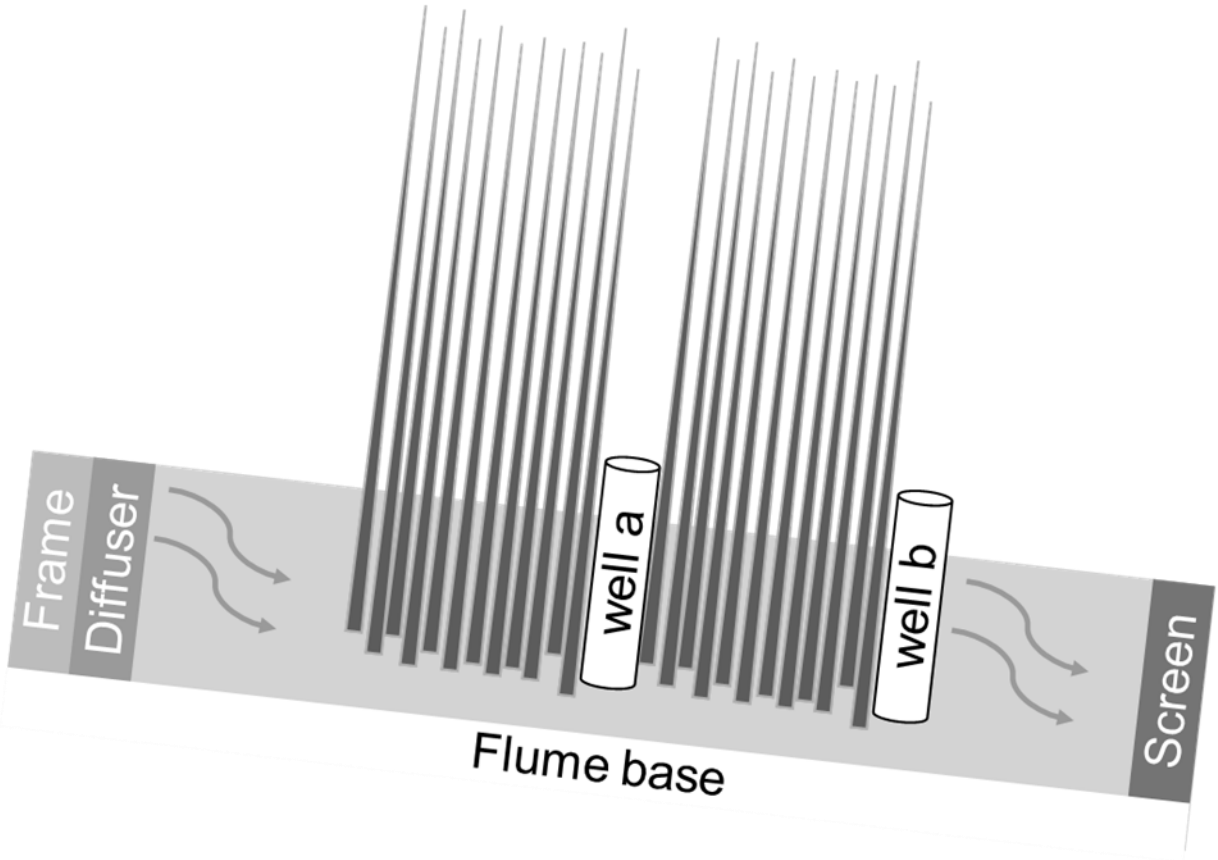

Figure 4.3 Cross sectional view of experimental marsh flumes.

The simulated groundwater solution (SGW) flowed from subterranean diffusers above an impermeable layer (i.e., clay layer at protected site (not shown) or PVC flume base) and through the experimental flumes. After SGW simulations, porewater was collected from wells set within (a) and after (b) the experimental planting area. Diffusers were set to a depth of 20 cm and 10 cm of the upper shoreward boundary of the experimental planting area.

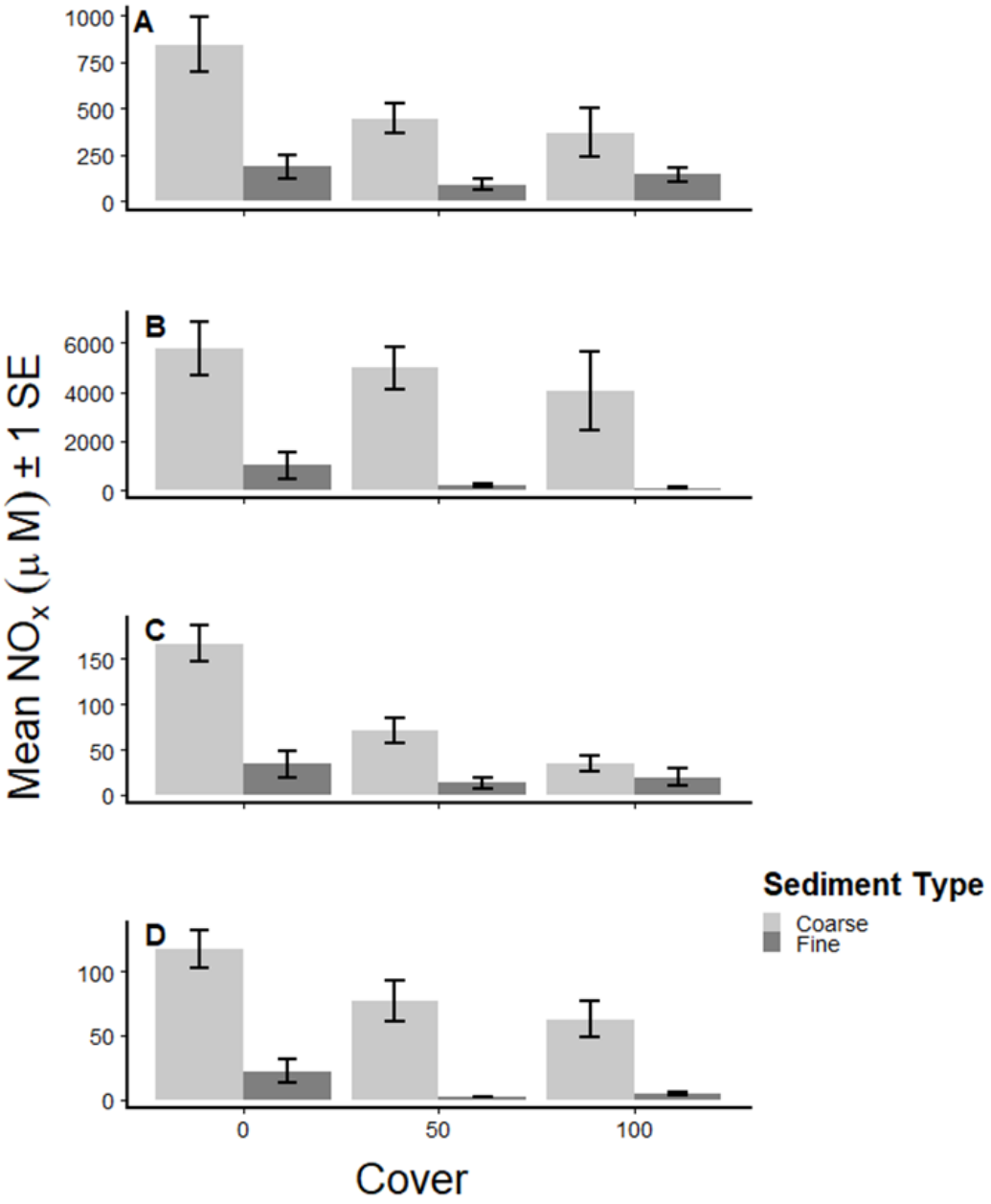

Figure 4.4 Mean porewater NO_x concentrations collected from a and b wells at the protected site plotted by initial planting density treatment and sediment type.

Mean porewater NO_x concentrations (y axis) collected from a and b wells at the protected site plotted by initial planting density treatment (x axis) and sediment type (bar color). Data shows the strong sediment type effect observed in both A wells (A and C panels) and B wells (B and D panels) following simulation 1 (A and B panels) and simulation 2 (C and D panels). Significance of the initial planting density treatments were not as straightforward but, in general, control (i.e., 0 initial planting density) treatments had significantly higher NO_x concentrations as compared to planting treatments. Error bars indicate ± 1 standard error.

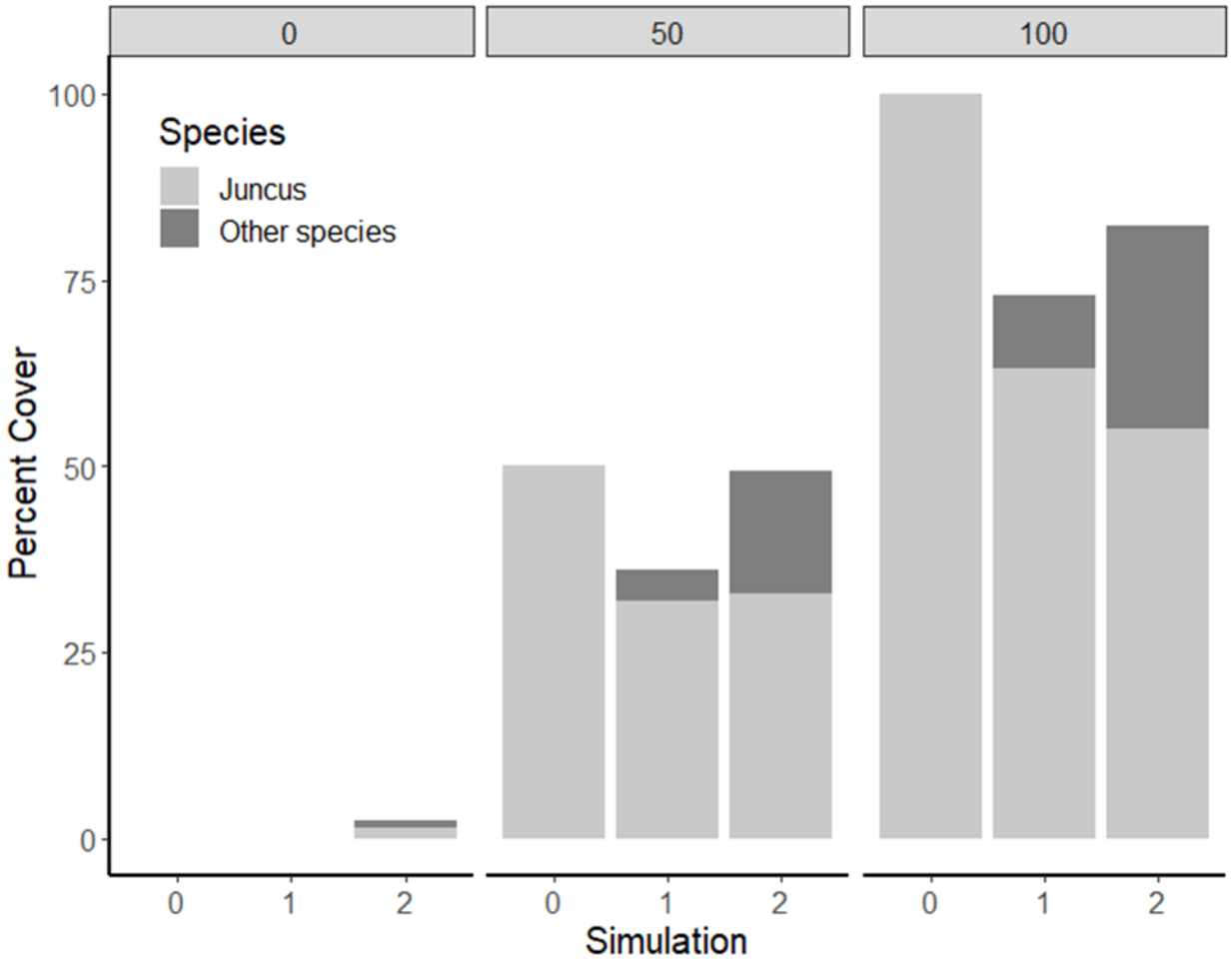

Figure 4.5 Observed percent cover of the study species (*Juncus roemerianus)* and other species by simulation and by initial planting density treatment at the protected site.

Observed percent cover (y axis) of the study species (*Juncus roemerianus*, light gray) and other species (dark gray) by simulation (x axis, bottom) and by initial planting density treatment (x axis, top) at the protected site. Each planting treatment retained similar observed cover from the start and establishment of the experiment (i.e., simulation 0) throughout experimental simulations.

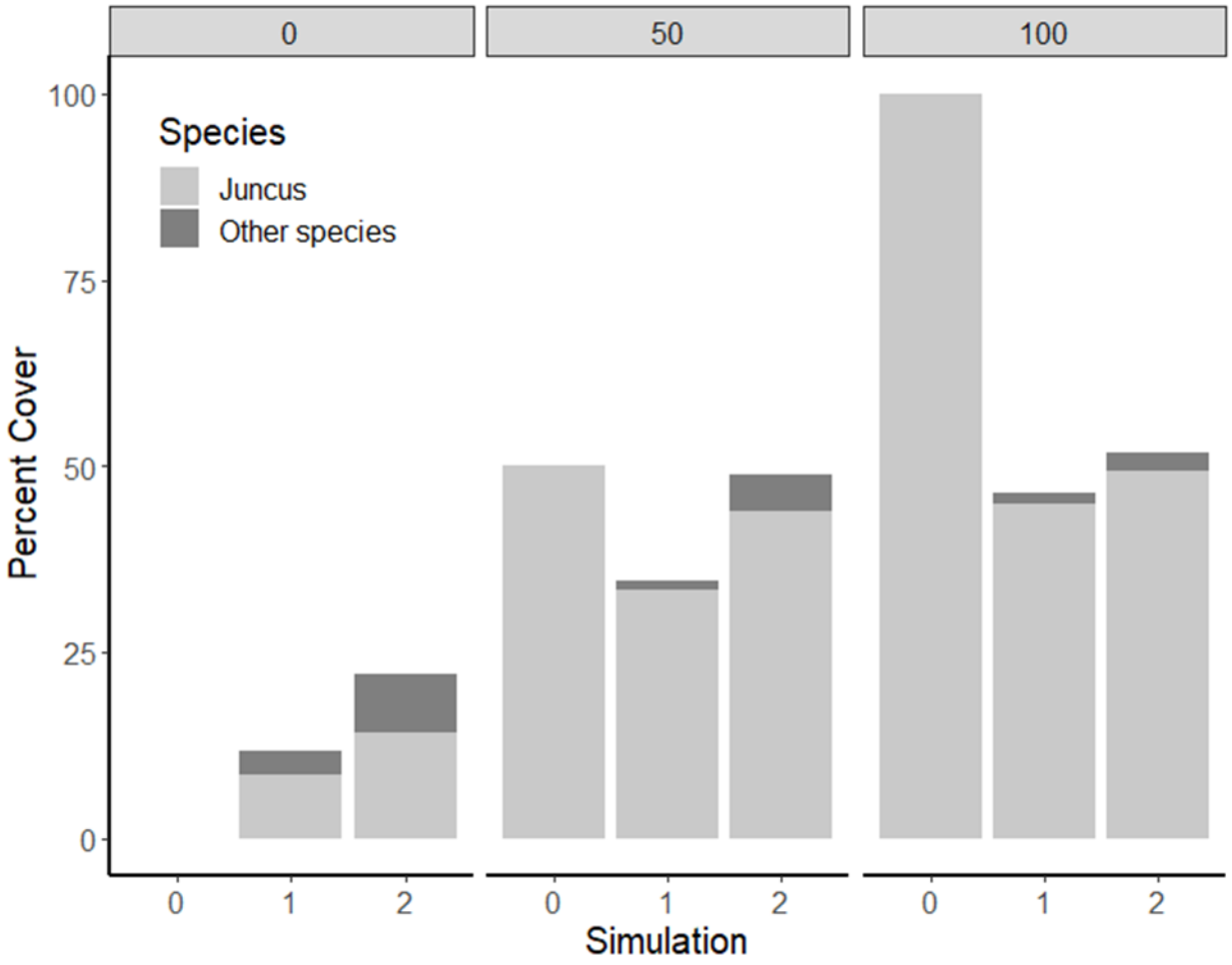

Figure 4.6 Observed percent cover of the study species (*Juncus roemerianus*) and other species by simulation and by initial planting density treatment at the exposed site.

Observed percent cover (y axis) of the study species (*Juncus roemerianus*, light gray) and other species (dark gray) by simulation (x axis, bottom) and by initial planting density treatment (x axis, top) at the exposed site. Only the 50% initial planting density treatment retained similar observed cover from the start and establishment of the experiment (i.e., simulation 0) throughout experimental simulations. The combination of species observed within control and 100% initial planting density treatments increased to 25% cover and declined to 50% cover, respectively.

4.7 Literature Cited

Armstrong, W. (1979). Aeration in higher plants. In Advances in botanical research (Vol. 7, pp. 225-332). Academic Press.

Balke, T., Bouma, T. J., Horstman, E. M., Webb, E. L., Erftemeijer, P. L., & Herman, P. M. (2011). Windows of opportunity: thresholds to mangrove seedling establishment on tidal flats. *Marine Ecology Progress Series, 440*, 1-9.

Barbier, E. B. (2015). Valuing the storm protection service of estuarine and coastal ecosystems. *Ecosystem Services, 11*, 32-38.

Bates, D., Maechler, M., Bolker, B., Walker, S. (2015). Fitting Linear Mixed-Effects Models Using lme4. Journal of Statistical Software, 67(1), 1-48. doi:10.18637/jss.v067.i01.

Bergamaschi, B. A., Tsamakis, E., Keil, R. G., Eglinton, T. I., Montluçon, D. B., & Hedges, J. I. (1997). The effect of grain size and surface area on organic matter, lignin and carbohydrate concentration, and molecular compositions in Peru Margin sediments. *Geochimica et Cosmochimica Acta, 61*(6), 1247-1260.

Bilkovic, D. M., Mitchell, M. M., Davis, J., Herman, J., Andrews, E., King, A., ... & Dixon, R. L. (2019). Defining boat wake impacts on shoreline stability toward management and policy solutions. *Ocean & Coastal Management, 182*, 104945.Brix 1997

Burnham, K., & Anderson, D. (2002). Model Selection and Multi-model Inference: A Practical Information-theoretic Approach. 2nd edition. (Springer: New York.).

Davis, J. L., Nowicki, B., & Wigand, C. (2004). Denitrification in fringing salt marshes of Narragansett Bay, Rhode Island, USA. *Wetlands, 24*(4), 870-878.

Dodds, W. K. (2006). Nutrients and the “dead zone”: the link between nutrient ratios and dissolved oxygen in the northern Gulf of Mexico. *Frontiers in Ecology and the Environment, 4*(4), 211-217.

Coops, H., & Van der Velde, G. (1996). Effects of waves on helophyte stands: mechanical characteristics of stems of Phragmites australis and Scirpus lacustris. *Aquatic Botany, 53*(3-4), 175-185.

Eleuterius, L. N. (1984). Autecology of the black needlerush *Juncus roemerianus*. *Gulf and Caribbean Research, 7*(4), 339-350.

Engelaar, W. M., Matsumaru, T., & Yoneyama, T. (2000). Combined effects of soil waterlogging and compaction on rice (Oryza sativa L.) growth, soil aeration, soil N transformations and 15N discrimination. *Biology and Fertility of Soils, 32*(6), 484-493.

Feagin, R. A., Lozada-Bernard, S. M., Ravens, T. M., Möller, I., Yeager, K. M., & Baird, A. H. (2009). Does vegetation prevent wave erosion of salt marsh edges? *Proceedings of the National Academy of Sciences, 106*(25), 10109-10113.

Fisher, J. & Acreman, M.C. (2004). Wetland Nutrient Removal: A Review of the Evidence. *Hydrology and Earth System Sciences, 8*(4), 673-685.

Gedan, K. B., Kirwan, M. L., Wolanski, E., Barbier, E. B., & Silliman, B. R. (2011). The present and future role of coastal wetland vegetation in protecting shorelines: answering recent challenges to the paradigm. *Climatic Change, 106*(1), 7-29.

Gittman, R. K., Peterson, C. H., Currin, C. A., Joel Fodrie, F., Piehler, M. F., & Bruno, J. F. (2016). Living shorelines can enhance the nursery role of threatened estuarine habitats. *Ecological Applications, 26*(1), 249-263.

Gupta, T. R., & Foster, J. H. (1973). Valuation of Visual-Cultural Benefits from Freshwater Wetlands in Massachusetts. *Journal of the Northeastern Economics Council, 2*(2), 262-273.

Hamersley, M. R., & Howes, B. L. (2003). Contribution of denitrification to nitrogen, carbon, and oxygen cycling in tidal creek sediments of a New England salt marsh. *Marine Ecology Progress Series, 262*, 55-69.

Hosoi, M., Ishida, A., & Imoto, K. (1977). Study on Re-Aeration by Waves. *Coastal Engineering in Japan, 20*(1), 121-127.

Howes, B. L., & Goehringer, D. D. (1994). Porewater drainage and dissolved organic carbon and nutrient losses through the intertidal creekbanks of a New England salt marsh. *Marine ecology progress series, 114*(3), 289-301.

Hu, W., Zhang, W., Zhang, L., Lin, X., Tong, C., Lai, D. Y., ... & Zeng, C. (2019). Short-term changes in simulated inundation frequency differentially affect inorganic nitrogen, nitrification, and denitrification in estuarine marshes. *Ecological Indicators, 107*, 105571.

IPCC, 2019: Climate Change and Land: an IPCC special report on climate change, desertification, land degradation, sustainable land management, food security, and greenhouse gas fluxes in terrestrial ecosystems [P.R. Shukla, J. Skea, E. Calvo Buendia, V. Masson-Delmotte, H.-O. Pörtner, D. C. Roberts, P. Zhai, R. Slade, S. Connors, R. van Diemen, M. Ferrat, E. Haughey, S. Luz, S. Neogi, M. Pathak, J. Petzold, J. Portugal Pereira, P. Vyas, E. Huntley, K. Kissick, M. Belkacemi, J. Malley, (eds.)]. In press.

Jesus, B., Brotas, V., Ribeiro, L., Mendes, C. R., Cartaxana, P., & Paterson, D. M. (2009). Adaptations of microphytobenthos assemblages to sediment type and tidal position. *Continental Shelf Research, 29*(13), 1624-1634.

Keddy, P. A. (1985). Wave disturbance on lakeshores and the within-lake distribution of Ontario's Atlantic coastal plain flora. *Canadian Journal of Botany, 63*(3), 656-660.

Kirwan, M. L., & Megonigal, J. P. (2013). Tidal wetland stability in the face of human impacts and sea-level rise. *Nature, 504*(7478), 53-60.

Kleinhuizen, A. A., & Mortazavi, B. (2018). Denitrification Capacity of a Natural and a Restored Marsh in the Northern Gulf of Mexico. *Environmental Management, 62*(3), 584-594.

Koch, M. S., Maltby, E., Oliver, G. A., & Bakker, S. A. (1992). Factors controlling denitrification rates of tidal mudflats and fringing salt marshes in south-west England. *Estuarine, Coastal and Shelf Science, 34*(5), 471-485.

Lenth, R. (2020). emmeans: Estimated Marginal Means, aka Least-Squares Means. R package version 1.4.6. https://CRAN.R-project.org/package=emmeans

Liu, Y., Jiao, J. J., Liang, W., & Luo, X. (2017). Tidal pumping-induced nutrients dynamics and biogeochemical implications in an intertidal aquifer. *Journal of Geophysical Research: Biogeosciences, 122*(12), 3322-3342.

Lucas, W. C., & Greenway, M. (2008). Nutrient retention in vegetated and nonvegetated bioretention mesocosms. Journal of Irrigation and Drainage Engineering, 134(5), 613-623.

McConchie, J. A., & Toleman, I. E. J. (2003). Boat wakes as a cause of riverbank erosion: a case study from the Waikato River, New Zealand. *Journal of Hydrology (New Zealand)*, 163-179.

Mehvar, S., Filatova, T., Sarker, M. H., Dastgheib, A., & Ranasinghe, R. (2019). Climate change-driven losses in ecosystem services of coastal wetlands: A case study in the West coast of Bangladesh. *Ocean & Coastal Management, 169*, 273-283.

Mendelssohn, I. A., & McKee, K. L. (1988). Spartina alterniflora die-back in Louisiana: time-course investigation of soil waterlogging effects. *The Journal of Ecology*, 509-521.

Morris, J. T., Sundareshwar, P. V., Nietch, C. T., Kjerfve, B., & Cahoon, D. R. (2002). Responses of coastal wetlands to rising sea level. *Ecology, 83*(10), 2869-2877.

Morris, J. T., Shaffer, G. P., & Nyman, J. A. (2013). Brinson review: Perspectives on the influence of nutrients on the sustainability of coastal wetlands. *Wetlands, 33*(6), 975-988.

Nassauer, J. I. (2004). Monitoring the success of metropolitan wetland restorations: cultural sustainability and ecological function. *Wetlands, 24*(4), 756-765.

Neubauer, S. C., Piehler, M. F., Smyth, A. R., & Franklin, R. B. (2019). Saltwater intrusion modifies microbial community structure and decreases denitrification in tidal freshwater marshes. *Ecosystems, 22*(4), 912-928.

NOAA (2015). Guidance for Considering the Use of Living Shorelines. Silver Spring, Maryland: National Oceanic and Atmospheric Administration, 36p.

Nyman, J. A., Walters, R. J., Delaune, R. D., & Patrick Jr, W. H. (2006). Marsh vertical accretion via vegetative growth. *Estuarine, Coastal and Shelf Science, 69*(3-4), 370-380.

R Core Team (2020). R: A language and environment for statistical computing. R Foundation for Statistical Computing, Vienna, Austria. https://www.R-project.org/.

Rabalais, N. N., Turner, R. E., & Wiseman Jr, W. J. (2002). Gulf of Mexico hypoxia, aka "The dead zone". *Annual Review of ecology and Systematics, 33*(1), 235-263.

Reddy, K. R., & DeLaune, R. D. (2008). Biogeochemistry of wetlands: science and applications. CRC press.

Roland, R. M., & Douglass, S. L. (2005). Estimating wave tolerance of Spartina alterniflora in coastal Alabama. *Journal of Coastal Research,* 453-463.

Rupprecht, F., Möller, I., Evans, B., Spencer, T., & Jensen, K. (2015). Biophysical properties of salt marsh canopies—Quantifying plant stem flexibility and above ground biomass. *Coastal Engineering*, *100*, 48-57.

Schulze, D., Rupprecht, F., Nolte, S., & Jensen, K. (2019). Seasonal and spatial within-marsh differences of biophysical plant properties: implications for wave attenuation capacity of salt marshes. *Aquatic Sciences, 81*(4), 65.

Silinski, A., Schoutens, K., Puijalon, S., Schoelynck, J., Luyckx, D., Troch, P., ... & Temmerman, S. (2018). Coping with waves: Plasticity in tidal marsh plants as self-adapting coastal ecosystem engineers. *Limnology and Oceanography, 63*(2), 799-815.

Silvan, N., Vasander, H., & Laine, J. (2004). Vegetation is the main factor in nutrient retention in a constructed wetland buffer. *Plant and Soil, 258*(1), 179-187.

Sinsabaugh, R. L., & Findlay, S. (1995). Microbial production, enzyme activity, and carbon turnover in surface sediments of the Hudson River estuary. *Microbial Ecology, 30*(2), 127-141.

Sloey, T. M., & Hester, M. W. (2018). Impact of nitrogen and importance of silicon on mechanical stem strength in *Schoenoplectus acutus* and *Schoenoplectus californicus*: applications for restoration. *Wetlands Ecology and Management, 26*(3), 459-474.

Sparks, E. L., Cebrian, J., Biber, P. D., Sheehan, K. L., & Tobias, C. R. (2013). Cost-effectiveness of two small-scale salt marsh restoration designs. *Ecological engineering, 53*, 250-256.

Sparks, E. L., Cebrian, J., & Smith, S. M. (2014). Removal of fast flowing nitrogen from marshes restored in sandy soils. *PloS one, 9*(10), e111456.

Sparks, E. L., Cebrian, J., Tobias, C. R., & May, C. A. (2015). Groundwater nitrogen processing in Northern Gulf of Mexico restored marshes. *Journal of environmental management, 150*, 206-215.

Spieles, D. J., & Mitsch, W. J. (1999). The effects of season and hydrologic and chemical loading on nitrate retention in constructed wetlands: a comparison of low-and high-nutrient riverine systems. *Ecological Engineering, 14*(1-2), 77-91.

Temple, N. A., Grace, J. B., & Cherry, J. A. (2019). Patterns of resource allocation in a coastal marsh plant (*Schoenoplectus americanus*) along a sediment-addition gradient. *Estuarine, Coastal and Shelf Science, 228*, 106337.

Tobias, C. R., Anderson, I. C., Canuel, E. A., & Macko, S. A. (2001). Nitrogen cycling through a fringing marsh-aquifer ecotone. *Marine Ecology Progress Series, 210*, 25-39.

VanZomeren, C. M., White, J. R., & DeLaune, R. D. (2012). Fate of nitrate in vegetated brackish coastal marsh. *Soil Science Society of America Journal, 76*(5), 1919-1927.

Van Slobbe, E., de Vriend, H. J., Aarninkhof, S., Lulofs, K., de Vries, M., & Dircke, P. (2013). Building with Nature: in search of resilient storm surge protection strategies. *Natural hazards, 66*(3), 1461-1480.

Vasquez, E. A., Glenn, E. P., Guntenspergen, G. R., Brown, J. J., & Nelson, S. G. (2006). Salt tolerance and osmotic adjustment of *Spartina alterniflora* (*Poaceae*) and the invasive M haplotype of *Phragmites australis* (*Poaceae*) along a salinity gradient. *American Journal of Botany, 93*(12), 1784-1790.

Wetzel, R. G. (2001). Limnology: lake and river ecosystems. Gulf professional publishing.

White, D. S., & Howes, B. L. (1994). Long-term 15N-nitrogen retention in the vegetated sediments of a New England salt marsh. *Limnology and Oceanography, 39*(8), 1878-1892.

Woodroffe, C. D. (2002). Coasts: form, process and evolution. Cambridge University Press.

Yamamoto, N., & Lopez, G. (1985). Bacterial abundance in relation to surface area and organic content of marine sediments. *Journal of Experimental Marine Biology and Ecology, 90*(3), 209-220.

Yozzo, D., Titre, J., Sexton, J., 1996. Planning and evaluating restoration of aquatic habitats from an ecological perspective. Institute for Water Resources, US Army Corps of Engineers, Waterways Experiment Station, Vicksburg, MS, IWR Report 96-EL-4.

Zedler, J. B. (1996). Tidal wetland restoration: a scientific perspective and southern California focus. CALIFORNIA SEA GRANT COLLEGE SYSTEM, UNIV. CALIFORNIA, LA JOLLA, CA(USA). 1996.

Zheng, Y., Hou, L., Liu, M., Liu, Z., Li, X., Lin, X., ... & Jiang, X. (2016). Tidal pumping facilitates dissimilatory nitrate reduction in intertidal marshes. *Scientific reports, 6*, 21338.

CHAPTER V

SYNTHESIS

5.1 Overview

I sought to advance the understanding of plant responses to waves and to create new tools for land managers working on coastal restoration, conservation, and enhancement projects through this dissertation. In Chapter I, I outlined some of the factors currently limiting the effectiveness of projects and outlined the goals and objectives of this dissertation. To accomplish these goals and objectives, I explored the feasibility of a low-cost wave gauge and explored research questions that are important for the effective design and construction of coastal projects. In Chapter II, I described a low-cost pressure sensor-based wave gauge that compared favorably to a commercial gauge in rigorous field and laboratory testing. In Chapter III, I provided a literature review of plant responses to waves and used the low-cost gauges developed in Chapter I to collect wave data and collected above- and below-ground plant data to examine these responses at different sites within Mobile Bay and four surrounding tributaries. In Chapter IV, to begin to explore the effects of waves and other environmental factors on the ecosystem services provided by constructed marshes, I evaluated the main and interactive effects of sediment type, initial planting density, platform elevation and slope on nitrogen removal at sites exposed to and protected from waves. In the final sections of this dissertation, I will provide a high-level summary of each chapter and highlight the major findings of this dissertation research and will

end with a summary of gained insights and suggestions for future research to further improve the effectiveness of coastal restoration, conservation and enhancement projects.

5.2 Development of the Low-cost Wave Gauge

Technological developments have increased researcher access to low-cost electrical and data-logging equipment that has spurred a recent flurry of DIY environmental sensing tools (*e.g.,* Beddows and Mallon 2018, Lockridge *et al.,* 2016, Mickley *et al.* 2018, Miller 2014). Following these examples, I developed a wave gauge using a relatively inexpensive pressure sensor (MS5803-14BA; SparkFun Electronics, USA) and paired it with an Arduino Uno microcontroller and accessories for controlling the sensing and logging of pressure data. These electrical components were then sealed and/or contained within a custom housing configuration using commercial PVC and accessories available at most home stores. The resulting gauge (hereafter, "DIY gauge") cost less than $300 and is an order of magnitude less than the closest comparable gauge (Figure 2.1). It is capable of logging continuously at 8 Hz (*i.e.,* eight times per second) or more for over a week.

The performance of the DIY gauge was evaluated against a comparable commercial wave gauge (i.e., RBR Solo^3 D) in a series of laboratory wave channel tests and in the field. In laboratory wave channel tests, wave amplitude and frequency were manipulated (Table 2.2) using a wave generator (HR Wallingford). In the field, gauges were deployed in tandem within the Fowl River in Mobile, Alabama for approximately one week. Overall agreement between raw pressure readings was assessed using paired t-tests and by examining differences along the range of pressure readings in each test, following Bland and Altman (1999). Paired raw data were also applied to simple linear models and, for field tests, by comparing agreement of power spectral density curves. As expected, the greatest differences in raw pressure readings between

the gauges was observed when wave frequencies approached 1 Hz (Hoque and Aoki 2006, Lee and Wang 1984; Table 2.2). Overall, however, the DIY gauge was similar to the commercial gauge (mean R^2 of linear regressions ≥ 0.90) in both laboratory and field tests and is thus, an accurate and low-cost alternative to high-cost commercial gauges.

5.3 Plant Responses Along a Wave Climate Gradient

In Chapter III, I reviewed the current literature describing plant responses to waves. Past work predominately focused on the ways that plants affect wave characteristics including wave height, period, energy, power and subsequent erosion (*e.g.,* Bradley and Houser 2009, Maza *et al.* 2015). These effects are important for constructed marsh design, but this general approach assumes that plant features are static. While the potential for shifting plant responses to other environmental factors is well known (Kirwan and Megonigal 2013, Nyman *et al.* 2006, Temple *et al.* 2019, Vasquez *et al.* 2006), insights on plant responses to a changing wave environment have been largely ignored or relatively scant due, in part, to the limitations associated with measuring waves in the field (e.g., Silinski et al. 2018). As a result, observed plant features are often assumed as being beneficial in particular wave environments (e.g., Puijalon *et al.* 2011). Therefore, to test this assumption, a large-scale comparative field experiment was conducted to assess above- and below-ground plant responses at different sites at which wave data were collected using the gauges developed in Chapter II.

DIY wave gauges were deployed at a total of 60 sites in Mobile Bay and within four tributary rivers. Wave data were collected at each of these sites for a total of 20 days over the summer, 2018. In addition to wave data, plant data including above- and below-ground biomass, percent live biomass, stem diameter, height and density, and ancillary environmental data including soil bulk density, platform elevation and slope, and salinity data were also collected.

Plant responses were compared along the assessed wave climate gradient using simple linear regression following Temple *et al.* (2019). Correlation coefficients were also used to assess the environmental factors most influencing plant responses following Silinksi *et al.* (2018). Contrary to previous research, plant responses observed along the wave climate gradient were generally not related to traits hypothesized to improve plant persistence at sites exposed to waves (*e.g.,* Silinski *et al.* 2018). For example, wave height and period decrease with increasing stem diameter leading some researchers to interpret greater stem diameter as a defensive growth strategy by plants experiencing greater magnitude wave activity (Silinski *et al.* 2018). On the contrary, Chapter III results demonstrated that varying plant responses in the study plants *J. roemerianus* and *S. alterniflora* were most often related to variations in wave climate, soil bulk density and platform elevation. In particular, stem diameter in both *J. roemerianus* and *S. alterniflora* declined with increasing frequency and magnitude wave conditions.

5.4 Wave and Other Environmental Effects on the Nutrient Removal Capacity of Constructed Marshes

In Chapter IV, I used a field experiment to explore how varying environmental factors, including wave climate, sediment type, planting density, platform elevation and slope effect the ecosystem services provided by constructed marsh projects. These factors were chosen because they vary between project sites and are often specified in project designs (*e.g.,* NOAA 2015). To begin to understand the effects of these factors on marsh ecosystem services, I conducted a field experiment in which combinations of different levels of each of these factors were manipulated in experimental marsh plots. I then collected porewater from experimental plots following two simulated nutrient runoff events and assessed the main and interactive effects of these factor combinations on porewater nitrogen concentrations using ANOVA techniques.

Results from this study suggested that nutrient removal in constructed marshes is most affected by the presence of marsh vegetation, substrate sediment type, and, most importantly, the presence of waves. At the site protected from waves, sediment type and planting density were important factors controlling the removal capacity in experimental plots, with the lowest nitrogen concentrations observed in plots planted with vegetation and within fine sediments ($p < 0.5$; Table 4.3). At the site exposed to waves, none of the treatment combinations were significant.

5.5 Summary of Gained Insights and Recommendations for Future Research

The purpose of this dissertation research was to create the tools and knowledge base needed to measure and better understand the effects of waves on fringing marshes, with the ultimate goal to improve the effectiveness of coastal restoration, conservation and enhancement projects. To that end, I created a low-cost wave gauge that will immediately improve land management and research abilities to measure and collect site-specific wave data. From a basic science perspective, this tool advances our ability to explore the role waves play in shaping coastal environments and the ecosystem services they provide. Indeed, the scope of research pursued in Chapter III would not have been possible without the creation of the low-cost wave gauge and still only scratches the surface with respect to the types of research questions that can be pursued using the gauge. As limited as the scope was, the experimental design used in Chapter III allowed the most robust assessment of plant morphological and growth responses to varying frequency and magnitude wave events than has been done previously. This approach subsequently revealed surprising trends in plant responses to waves that challenge their contemporary interpretation. Likewise, I found that waves can have profound effects on the ecosystem services provided by marshes that are not usually accounted for in marsh construction projects (Chapter IV). Taken together, Chapters III and IV were important first steps in further

understanding the effects of waves on coastal land management but, like much research, spawned even more questions that warrant further research. Some of these questions are discussed further below.

The way that waves impact oxygen availability in the rhizosphere is of particular interest to both Chapters III and IV, and is one recommendation for future research. In Chapter III, shoot diameter declined with increasing wave climate (Figure 3.2) which I speculated was due, in part, to the wave-induced oxygenation of the rhizosphere. Likewise, this process may partly explain the lack of significant factor effects on porewater nitrogen concentration observed in Chapter IV. Interestingly, research exploring this phenomenon is near non-existent, despite other well-known phenomena that may increase oxygen diffusion in water (*i.e.,* air entrainment from wave turbulence; Hoque and Aoki 2006). An important first step to further this research might involve both field and laboratory wave channel experiments: at areas in the field experiencing different wave conditions and, in the laboratory, where wave conditions could be experimentally manipulated. Depending on these results, it may be possible to then begin further exploring the effects of wave-induced rhizospheric oxygenation on plant growth and morphological responses, and the culmination of wave effects on biologically mediated chemical transformations that are important for the effective design of marsh construction projects aimed at reducing upland nutrient pollution.

Another area of that warrants further research is the effects of currents on plant responses and general ecosystem services and how those effects may interact with the wave effects explored in this dissertation. This area of research is also ripe for exploration but, like waves, is limited, in part, by the high cost of commercial equipment (*i.e.,* Acoustic Doppler Current Profiler; "ADCP") needed to measure currents in the field. For example, the cost to purchase a

generic ADCP can easily exceed $20,000 (USD). The main challenge limiting the creation of a low-cost ADCP is two-fold. First, acoustic doppler sensors are available but would require custom coding and hardware libraries to effectively sense and log data. This challenge is distinct from the pressure sensor used in the DIY wave gauge, which came with all of the necessary libraries and test code. Second, these sensors will also require a custom circuit board and possibly special housing materials for effective operation. However, on a positive note, these challenges could be overcome with sufficient research and development, and with proper sensor functioning, could easily be incorporated within the datalogging platform used in the DIY wave gauge.

Finally, as with all pioneering research, the research explored in Chapters III and IV should be replicated but in different ways and for different reasons. The wave climate range observed in Chapter III was sufficient for the exploratory nature of the study but should be further expanded to include a broader wave climate range and a greater number of plant species. By comparison, the number of factors experimentally manipulated in Chapter IV should be decreased to include only initial planting density and sediment type (*i.e.,* the only significant factors; Table 4.1) so as to decrease the noise in porewater data. However, further adjustments would likely also improve insights into the effects of these factors. Importantly, planting density could be pared down to include only planted plots and non-planted plots, while sediment type could be expanded to include a range of sediment grain sizes, which may better reflect the range of substrate conditions possible in the field. Implementing these changes could provide additional opportunities to influence field wave exposure using wave breaks that could be experimentally manipulated.

5.6 Literature Cited

Beddows, P. A. and Mallon, E. K., 2018. Cave pearl data logger: A flexible Arduino-based logging platform for long-term monitoring in harsh environments. *Sensors,* 18(2), 530.

Bland, J. M. and Altman, D. G., 1999. Measuring agreement in method comparison studies. *Statistical methods in medical research,* 8(2), 135-160.

Bradley, K., & Houser, C. (2009). Relative velocity of seagrass blades: Implications for wave attenuation in low-energy environments. *Journal of Geophysical Research, 114*.

Hoque, A., & Aoki, S. I. (2006). Air entrainment by breaking waves: A theoretical study. *Indian Journal of Marine Sciences, 35*(1), 17-23.

Kirwan, M. L., & Megonigal, J. P. (2013). Tidal wetland stability in the face of human impacts and sea-level rise. *Nature, 504*(7478), 53-60.

Lee, D. Y. and Wang, H., 1984. Measurement of surface waves from subsurface gage. *Proceedings of the Nineteenth Coastal Engineering Conference* (Cape Town, South Africa, ASCE), pp. 271-286.

Lockridge, G.; Dzwonkowski, B.; Nelson, R. and Powers, S., 2016. Development of a low-cost arduino-based sonde for coastal applications. *Sensors,* 16(4), 528.

Maza, M., Lara, J. L., Losada, I. J., Ondiviela, B., Trinogga, J., & Bouma, T. J. (2015). Large-scale 3-D experiments of wave and current interaction with real vegetation. Part 2: experimental analysis. *Coastal Engineering, 106*, 73-86.

Mickley, J. G.; Moore, T. E.; Schlichting, C. D.; DeRobertis, A.; Pfisterer, E. N. and Bagchi, R., 2018. Measuring microenvironments for global change: DIY environmental microcontroller units (EMUs). *Methods in Ecology and Evolution,* 10(4), 578-584.

Miller, L., 2014. Open wave height logger. https://lukemiller.org/index.php/2014/08/open-wave-height-logger/

NOAA (2015). Guidance for Considering the Use of Living Shorelines. Silver Spring, Maryland: National Oceanic and Atmospheric Administration, 36p.

Nyman, J. A., Walters, R. J., Delaune, R. D., & Patrick Jr, W. H. (2006). Marsh vertical accretion via vegetative growth. *Estuarine, Coastal and Shelf Science, 69*(3-4), 370-380.

Puijalon, S., Bouma, T. J., Douady, C. J., van Groenendael, J., Anten, N. P., Martel, E., & Bornette, G. (2011). Plant resistance to mechanical stress: evidence of an avoidance–tolerance trade-off. *New Phytologist, 191*(4), 1141-1149.

Silinski, A., Schoutens, K., Puijalon, S., Schoelynck, J., Luyckx, D., Troch, P., ... & Temmerman, S. (2018). Coping with waves: Plasticity in tidal marsh plants as self-adapting coastal ecosystem engineers. Limnology and Oceanography, 63(2), 799-815.

Temple, N. A., Grace, J. B., & Cherry, J. A. (2019). Patterns of resource allocation in a coastal marsh plant (Schoenoplectus americanus) along a sediment-addition gradient. *Estuarine, Coastal and Shelf Science, 228*, 106337.

Vasquez, E. A., Glenn, E. P., Guntenspergen, G. R., Brown, J. J., & Nelson, S. G. (2006). Salt tolerance and osmotic adjustment of *Spartina alterniflora* (*Poaceae*) and the invasive haplotype of *Phragmites australis* (*Poaceae*) along a salinity gradient. *American Journal of Botany, 93*(12), 1784-1790.

APPENDIX A

CHAPTER II APPENDIX

A.1 Mississippi State University Coastal Conservation and Restoration Program (CCR) Waves Website

Building material lists with purchasing links (Table A2.1), a gauge construction video, gauge code and libraries, MATLAB scripts for gap-filling and wave data processing and other resources for building, operating and modifying DIY gauges are available at http://coastal.msstate.edu/waves.

A.2 Video Tutorial

A novice-level instructional video was created to help users build DIY gauges. Access the video on YouTube at the Coastal Conservation and Restoration Program (CCR) channel. A link to that channel can be found at the CCR waves website (http://coastal.msstate.edu/waves).

A.3 Additional Building Instructions

A.3.1 Downloading Arduino© Integrated Development Environment (IDE) and Libraries Required for DIY Gauge Code

After gauge construction is complete, the process of coding the DIY gauge will begin and requires downloading the Arduino© IDE software and uploading the necessary libraries into the Arduino folder on a PC/Mac. Arduino© IDE is available for download as a desktop app and is also available on the web at https://www.arduino.cc/en/main/software. Downloading the IDE software will automatically create an Arduino folder on a PC/Mac. For the DIY gauge to work properly, several open-source libraries will need to be downloaded and stored within the "libraries" folder in the Arduino folder on a PC/Mac. All necessary libraries are available for download at http://coastal.msstate.edu/waves. After downloading the required libraries, download the gauge code folder and save it within the Arduino folder on your PC/mac.

A.3.2 Initial Testing of Sensors and Atmospheric Pressure Adjustments in the Field

No issues with the accuracy or resolution of the MS5803-14BA pressure sensor were experienced during this study. However, it is recommended that sensors are checked to ensure sensor resolution is as advertised in datasheets. Before setting the sensor in epoxy, it is recommended that users run the sensor sketch in the Arduino© IDE to check for potential wiring errors. Instructions for running this sketch are available at https://learn.sparkfun.com/tutorials/ms5803-14ba-pressure-sensor-hookup-guide. After confirming wiring is correct, the sensor can be tested by submerging the sealed sensor (*i.e.,* onboard a fully constructed pressure gauge) in a bucket of water at various depths.

In addition to initial sensor testing, it is important to account for atmospheric pressure in in sensor readings during extended field deployments. The pressure sensor measures absolute pressure which is the combination of atmospheric and water pressures. Therefore, atmospheric pressure must be removed to convert to gauge pressure (*i.e.,* hydrostatic and dynamic pressure components). Atmospheric pressure data are easily accessible online (*e.g.,* https://tidesandcurrents.noaa.gov) for this purpose.

A.3.3 Setting the Real Time Clock (RTC)

Before gauge code is uploaded to the Arduino© Uno, the RTC onboard the data logging shield (Table A2.1) must be set using a separate RTC sketch in the Arduino© IDE. Tutorials outlining this process are available at https://learn.adafruit.com/adafruit-data-logger-shield/using-the-real-time-clock.

Low-cost, commercially available RTC's rarely feature sub-second resolution out of the box. While this is also true of the RTC employed by the DIY gauge, we have found that it can log at 8 to 10 Hz continuously with great accuracy (±1 millisecond) 99% of the time. This value

also includes missing data captures that are not likely a result of RTC error (discussed below). Still, care should be taken to ensure timestamp accuracy between deployments to account for other potential sources of error.

To maintain timestamp accuracy over multiple gauge deployments, we recommend setting the RTC before each deployment to prevent/account for clock drift. Clock drift is a common problem in low-cost electronics and can be caused by electrical irregularities, temperature and equipment age. Though not a focus of this study, several methods have been developed to account for drift (*e.g.,* hardware and software approaches) including several low-cost drift-compensating products, which may be necessary for certain applications (*e.g.,* tide level monitoring over extended/continuous deployment).

A.3.4 Uploading the Gauge Code

Once the RTC is set the gauge code can be uploaded to the microcontroller. First, follow the menu item: File/Open in the Arduino© IDE which will open a new window. In this window, under the "Look in" toggle, select the "Arduino" folder from the drop-down menu, then select the "pressure_gauge" folder and then select the "pressure_gauge.ino" file. The gauge code sketch will then open in a new window and will be ready to upload to the microcontroller. After uploading this sketch to the microcontroller, the gauge is ready for use.

A.3.5 Biofouling

No biofouling of the sensor was observed within the study period. However, biofouling may be a concern in certain field applications. In these applications, biofouling can be minimized by applying a copper mesh to the top of the smaller pipe in which the sensor is located (Figure

1B) or by coating the inside of the smaller pipe surrounding the sensor with a petroleum jelly-cayenne pepper solution.

A.4 DIY Gauge Data Loss

The speed of microcontroller operations (*e.g.,* writing of data to the SD card) can vary. When the time of a particular operation exceeds the designated sampling interval (*e.g.,* 8 Hz = 0.125 seconds = 125 milliseconds) data loss or unequal sampling intervals can occur when sampling at high frequencies continuously, depending on the way operations are timed in the code. We opted to use a timer interrupt (*e.g.,* as used in instruments described by Beddows and Mallon 2018) for operation scheduling in our code. The timer interrupt method executes operations by interrupting all microcontroller processes at a given frequency (*e.g.,* 8 Hz), ensuring that pressure data is always read at the appropriate sampling interval. The tradeoff is that any data not written to the SD card within the sampling interval is lost. In this study, data loss was rare (< 1%). However, data loss is common even among commercial equipment (Kunwar *et al.* 2017) and is easily addressed using gap-filling routines.

To correct for missing data in DIY gauges, we developed a gap-filling routine in MATLAB (2017a) using linear interpolation to fill in missing data captures. This routine is available for download at http://coastal.msstate.edu/waves.

A.5 Data Processing for Statistical Analyses

Some preprocessing of data were required before statistical analyses and proceeded as follows. First, raw RBR data (decibar pressure) and DIY gauge data (millibar pressure) were converted to Pascals. DIY field test data were passed through the gap-filling routine before both the DIY and RBR signals were passed through a band-limiting filter to isolate wave time series

data. These field test data required no further preprocessing before spectral and linear regression analyses. However, for laboratory test data, individual wave test records were then extracted from complete DIY and RBR pressure records (*i.e.,* 15 paired records from the 15 wave tests, Table 2) and passed through de-trending routines (*i.e.,* record mean pressure value removed from individual pressure values). Finally, signals (*i.e.,* pressure data through time) were aligned according to testing start and stop times with gap-filling applied to DIY signals where appropriate (Table 2.2).

A.6 Using MATLAB Scripts

Two fully annotated MATLAB scripts are provided including those for gapfilling DIY wave gauge data and simple wave data analysis. After downloading the "MATLAB code" folder from CCR website (http://coastal.msstate.edu/waves) save the folder to the MATLAB folder on a PC/Mac computer. Then copy the DIY gauge data file into the same folder. Then proceed as follows:

1. Open and run the gapfilling script (Gapfilling.m). Then follow these steps before running:

- Amend the file name (line 9) to match DIY gauge data file name
- Amend sampling frequency (line 31) to match the sampling frequency used in gauge code (*i.e.,* "pressure_gauge.ino"; the default for both MATLAB scripts and the gauge code is 10 Hz)
- After running the code, gap-filled data will appear as "gapfilled_data.csv" in the same MATLAB folder in which the scripts are saved. This gapfilled dataset will include both gapfilled timestamp and pressure data

2. Open the simple wave data analysis script (DIY_wave_analyses_rev0102.m). Then follow these steps before running:

- Amend the fluid density (line 15) according to field conditions
- Amend sampling frequency (line 16) to match the sampling frequency used in gauge code and gapfilling script

Table A.1 A complete list of all materials needed to construct the DIY wave gauge including estimated costs (USD before taxes and based on 2019 prices) and web links for purchasing.

Electrical components		
	Cost (before tax)	**Link**
Arduino Uno	$ 24.95	https://store.arduino.cc/usa/arduino-uno-rev3
Data logging shield	$ 13.95	https://www.adafruit.com/product/1141
CR 1220 coin cell battery	$ 6.99	amazon_coin_cell_battery link
Pressure sensor	$ 59.95	https://www.sparkfun.com/products/12909
6600 mAh Li ion battery	$ 29.50	https://www.adafruit.com/product/353
powerboost 500 c+	$ 14.95	https://www.adafruit.com/product/1944
Deans micro 4b connectors	$ 1.75	deans_microplugs_link
wire (bundle pack 20 awg)	$ 20.45	amazon_wire_link
solder	$ 24.49	amazon_solder_link
Sub total	**$ 196.98**	
Housing materials		
Power cable	$ 5.99	amazon_power_cable_link
Epoxy	$ 16.28	amazon_epoxy_link
epoxy applicator nozzles	$ 15.28	amazon_epoxy_applicators_link
epoxy applicator gun	$ 13.36	amazon_applicator_gun_link
Epoxy putty	$ 3.81	homedepot_epoxy_putty_link
3" PVC cap (flat)	$ 4.38	homedepot_pvcCap_link
3" Oatey Gripper cap	$ 4.76	homedepot_oateyCap_link
10" x 3" PVC pipe	$ 17.41	homedepot_3inch_pipe_link
1" x 1.5" PVC pipe	$ 6.12	homedepot_1.5inch_pipe_link
PVC solvent cement	$ 5.40	homedepot_pvcSolvent_link
Velcro sticky back	$ 7.41	homedepot_velcro_link
Sub total	**$ 100.20**	
Total gauge cost	**$ 297.18**	

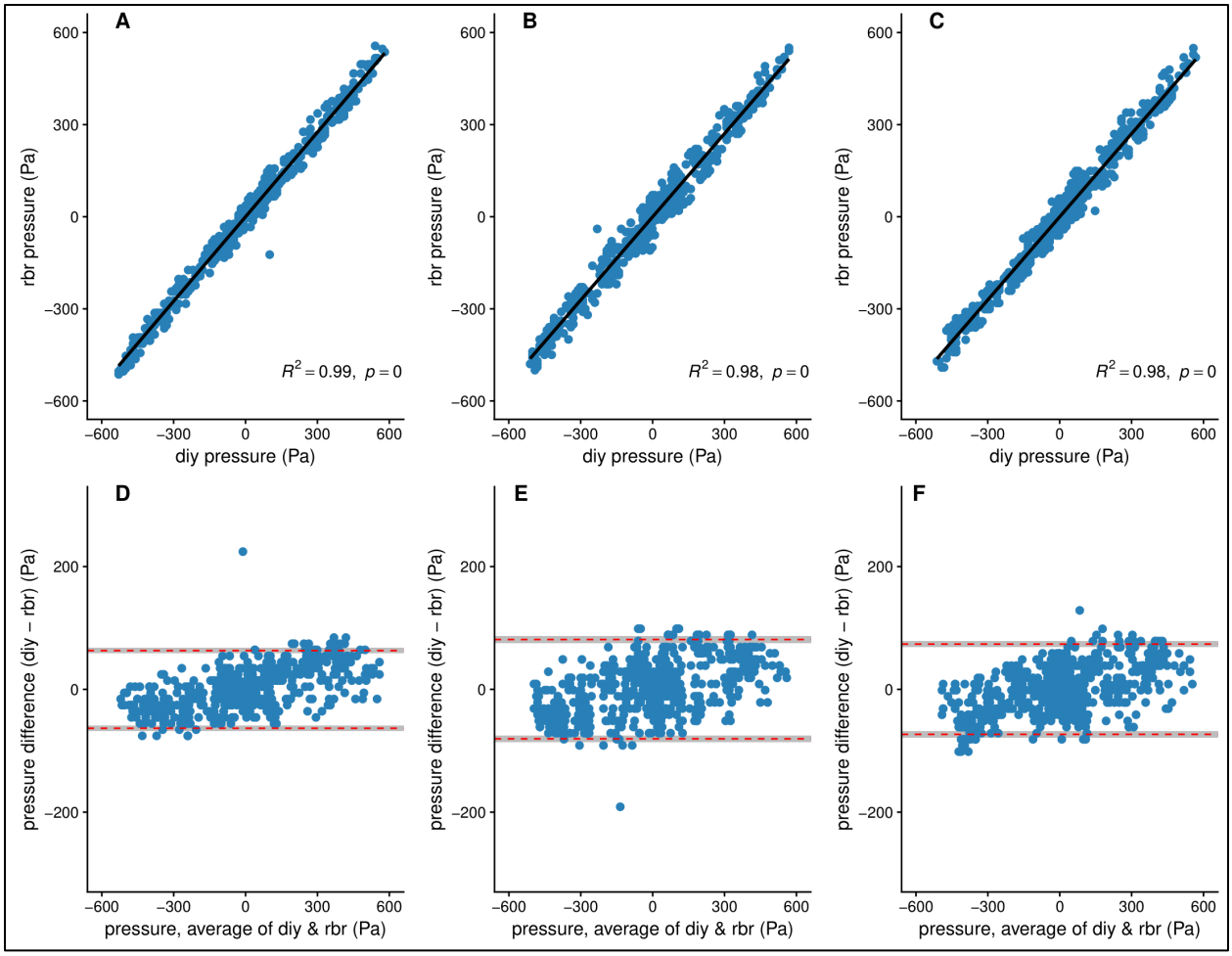

Figure A.1 Wave test 1 regressions and analysis of differences plots.

Wave test 1 (F = 0.5 Hz, A = 0.08 m) regressions (A-C) and analysis of differences (D-F) plots. Panels A, B,and C are regressions constructed from raw DIY pressure data (x axis) and raw RBR pressure data (y axis); panels indicate the different replicates (Table 2). Panels D, E, and F are plots of differences and correspond to the regressions directly above them. In these plots differences in raw pressure readings (y axis) are plotted against the average of the readings (x axis) following Bland and Altman (1999). Dashed red lines indicate bounds of 95% confidence intervals and gray boxes indicate the standard error of the confidence interval lower and upper limits. A slight linear trend is observable in the regression plots (A-C) which is reflective of the greater overall amplitude associated with the DIY pressure signal (*i.e.,* the absolute value of DIY wave peaks and troughs were approximately 20 pascals greater than the absolute value of the RBR). Still, mean differences between the gauges are essentially zero, with 95% confidence intervals ≤ 81 Pascals (< 1 centimeter static water depth). Model fit was also excellent ($R^2 \geq 0.98$).

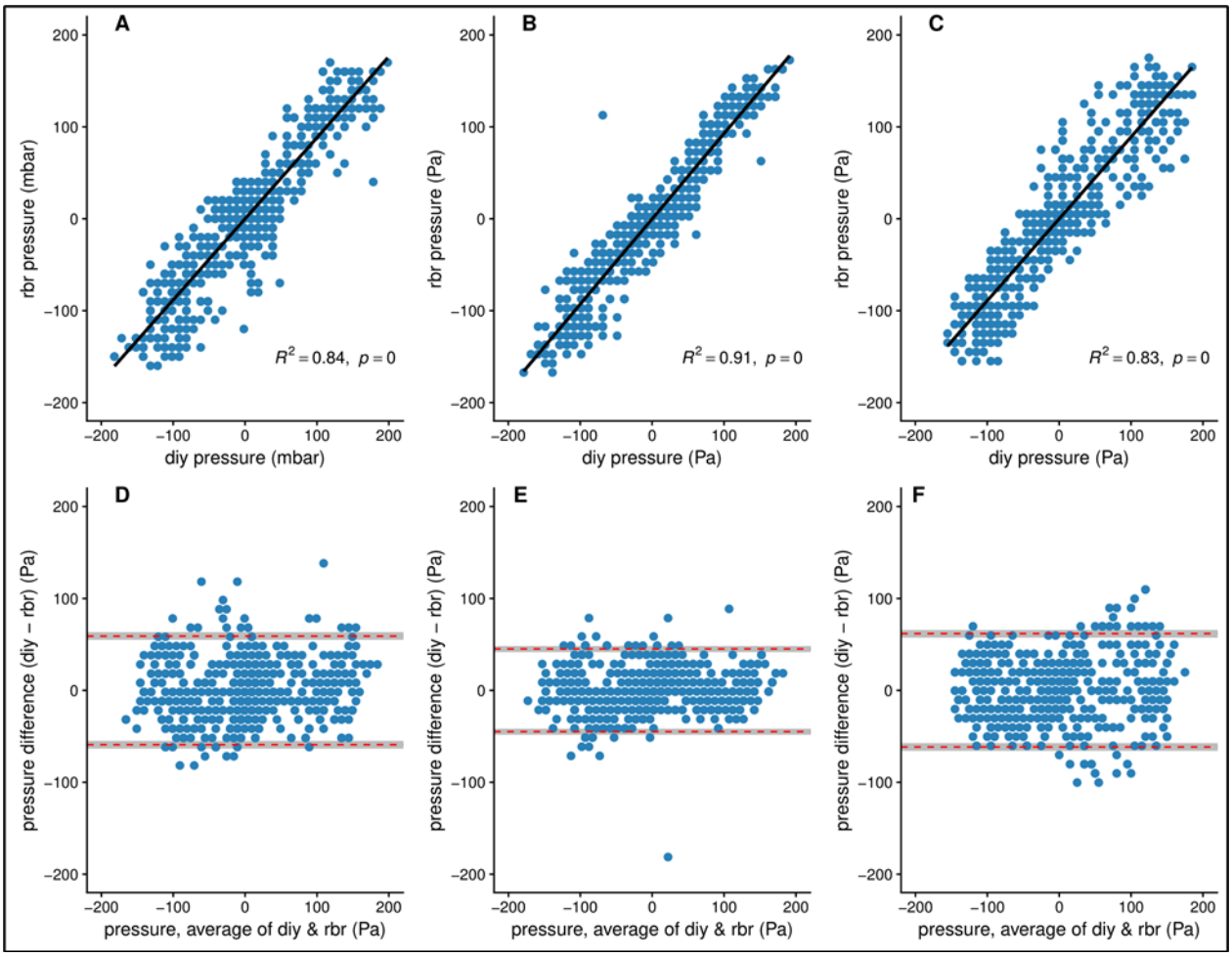

Figure A.2 Wave test 2 regressions and analysis of differences plots.

Wave test 2 (F = 0.99 Hz, A = 0.08 m) regressions (A-C) and analysis of differences (D-F) plots. Panels A, B, and C are regressions constructed from raw DIY pressure data (x axis) and raw RBR pressure data (y axis); panels indicate the different replicates (Table 2). Panels D, E, and F are plots of differences and correspond to the regressions directly above them. In these plots differences in raw pressure readings (y axis) are plotted against the average of the readings (x axis) following Bland and Altman (1999). Dashed red lines indicate bounds of 95% confidence intervals and gray boxes indicate the standard error of the confidence interval lower and upper limits. Mean differences between the gauges are essentially zero, with 95% confidence intervals $\leq \pm 62$ Pascals (< 1 centimeter static water depth). Model fit, as expected given the high frequency wave type, was lower compared to higher frequency wave types but was, on average, within acceptable ranges ($R^2 = 0.86$).

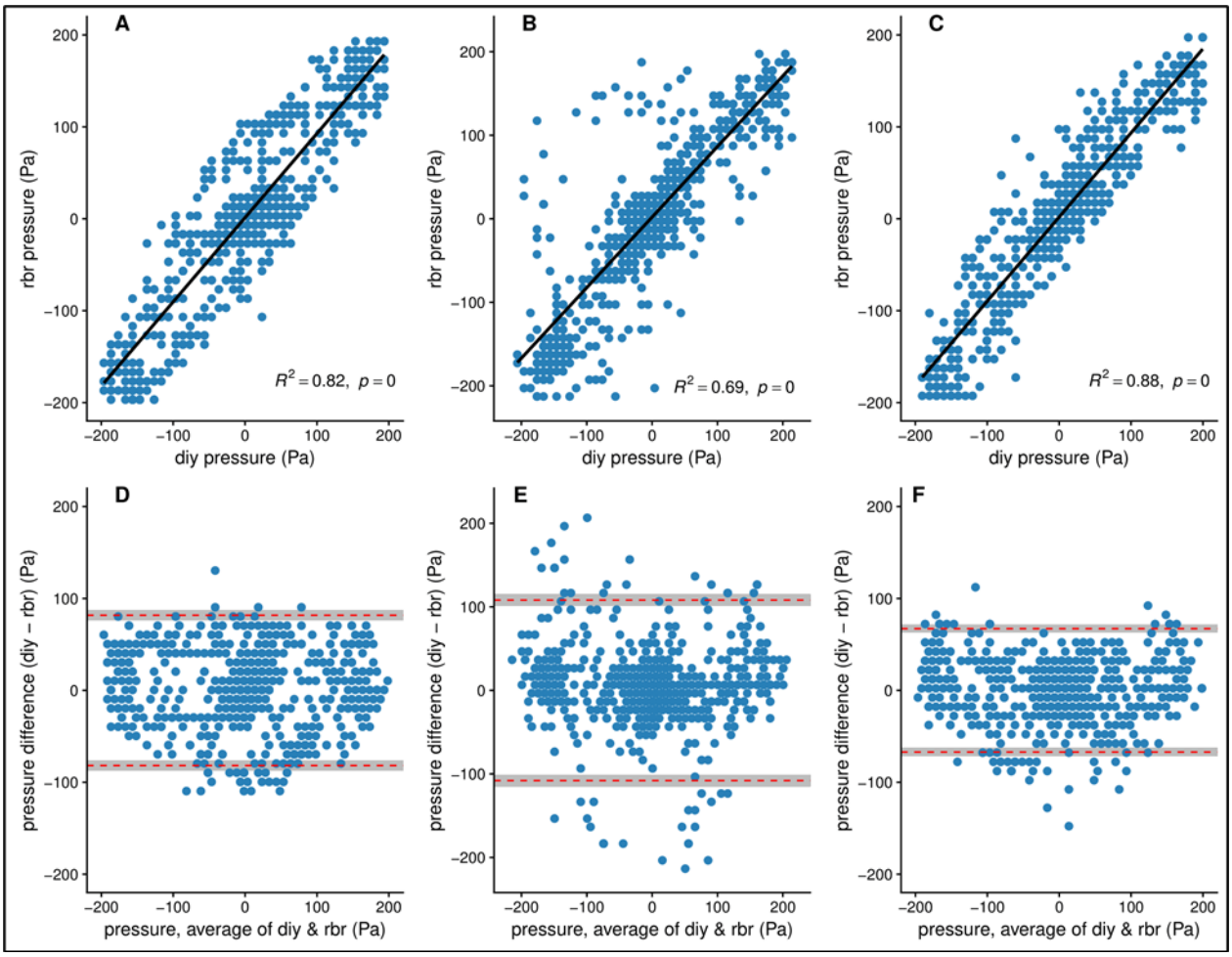

Figure A.3 Wave test 3 regressions and analysis of differences plots.

Wave test 3 (F = 0.99 Hz, A = 0.12 m) regressions (A-C) and analysis of differences (D-F) plots. Panels A, B,and C are regressions constructed from raw DIY pressure data (x axis) and raw RBR pressure data (y axis); panels indicate the different replicates (Table 2). Panels D, E, and F are plots of differences and correspond to the regressions directly above them. In these plots differences in raw pressure readings (y axis) are plotted against the average of the readings (x axis) following Bland and Altman (1999). Dashed red lines indicate bounds of 95% confidence intervals and gray boxes indicate the standard error of the confidence interval lower and upper limits. Mean differences between the gauges are essentially zero, with 95% confidence intervals < ±110 Pascals (< 1.1 centimeter static water depth). Model fit, as expected given the high frequency wave type, was lower compared to higher frequency wave types but was, on average, within acceptable ranges ($R^2 = 0.8$).

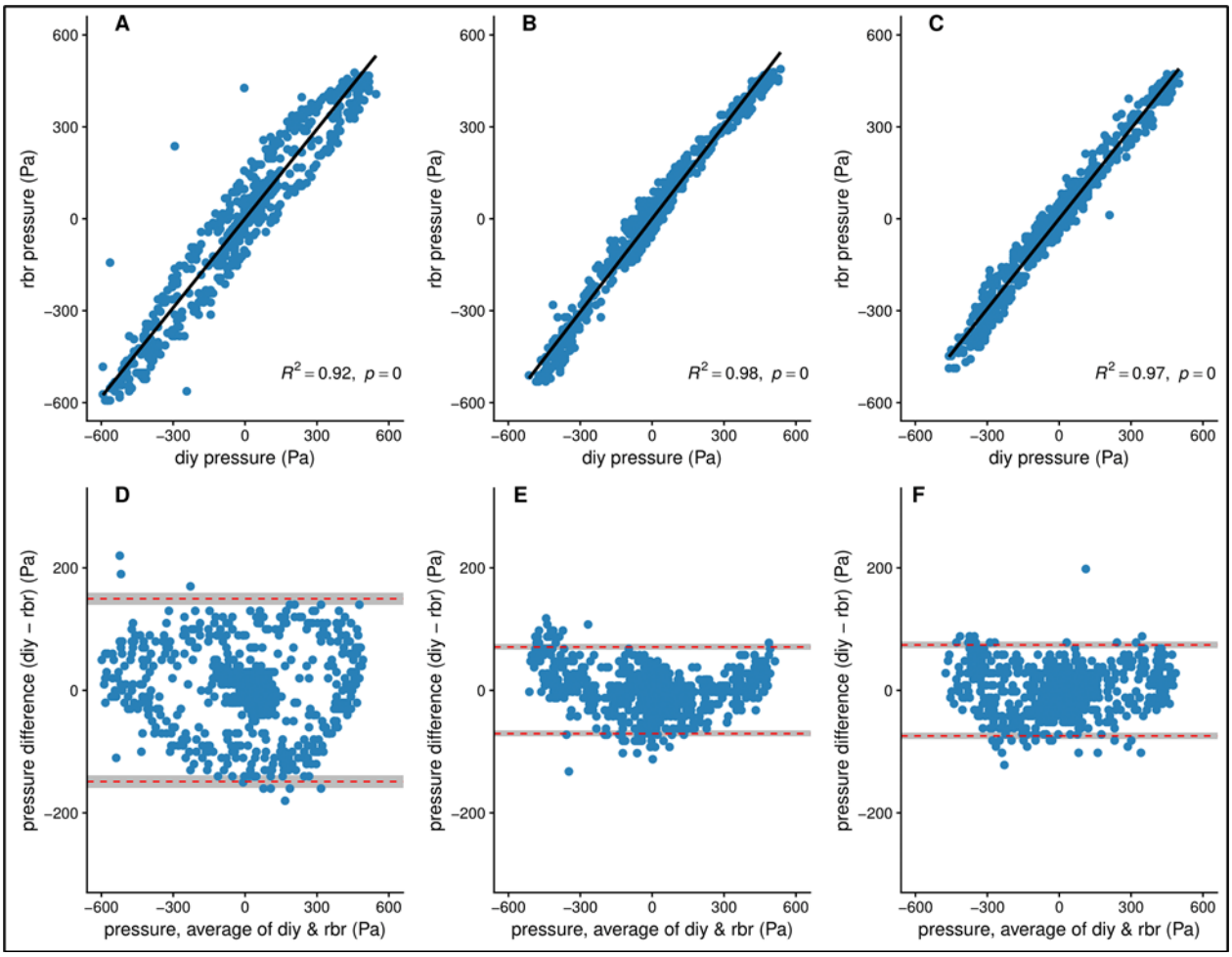

Figure A.4 Wave test 4 regressions and analysis of differences plots.

Wave test 4 (F = 0.75 Hz, A = 0.12 m) regressions (A-C) and analysis of differences (D-F) plots. Panels A, B,and C are regressions constructed from raw DIY pressure data (x axis) and raw RBR pressure data (y axis); panels indicate the different replicates (Table 2). Panels D, E, and F are plots of differences and correspond to the regressions directly above them. In these plots differences in raw pressure readings (y axis) are plotted against the average of the readings (x axis) following Bland and Altman (1999). Dashed red lines indicate bounds of 95% confidence intervals and gray boxes indicate the standard error of the confidence interval lower and upper limits. Mean differences between the gauges are essentially zero, with 95% confidence intervals $< \pm 150$ Pascals (< 1.5 centimeter static water depth). Model fit was also excellent ($R^2 \geq 0.92$).

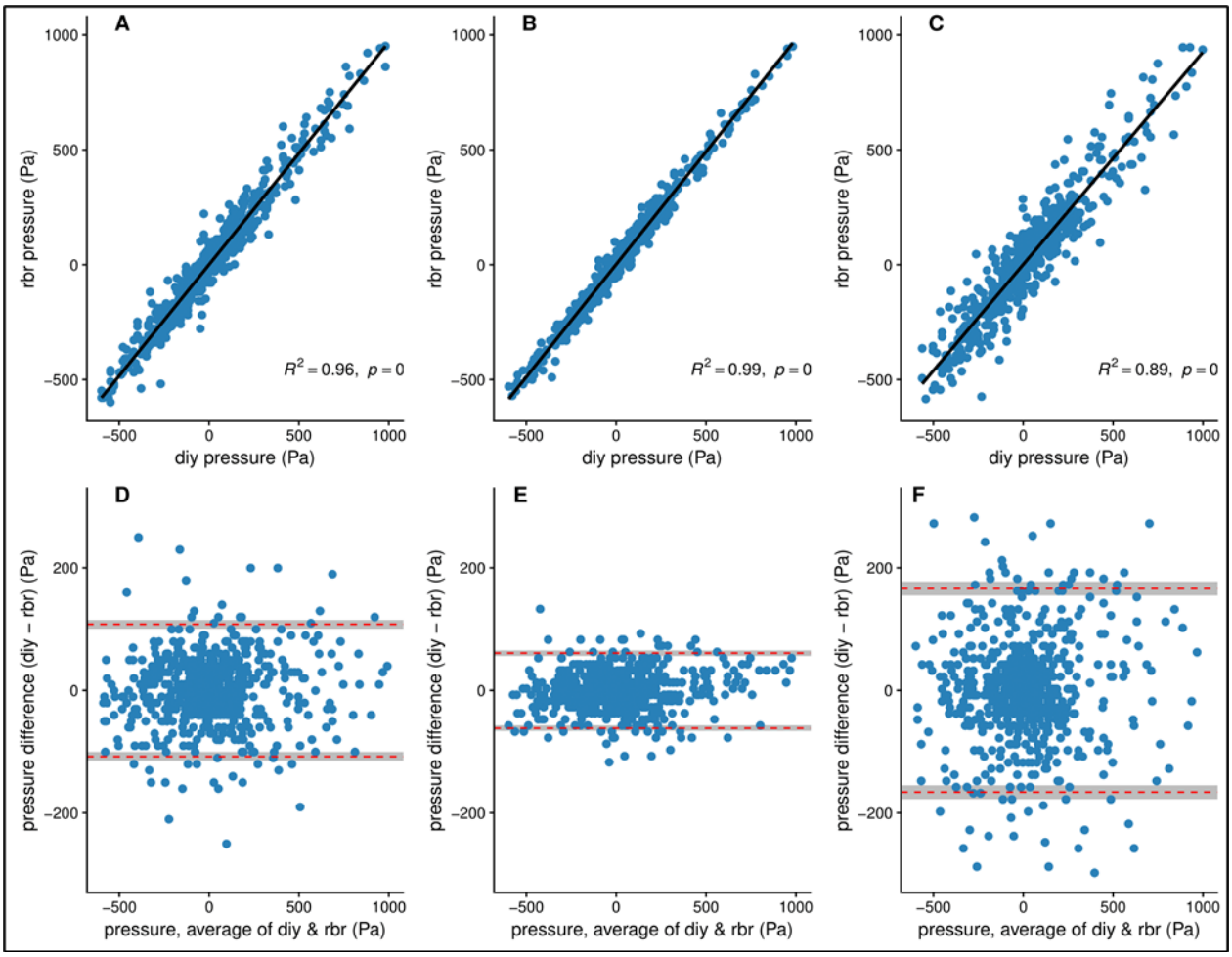

Figure A.5 Wave test 5 (JONSWAP wave spectra with $H_s = 0.2$, $T_p = 2$, $\gamma = 3.3$) regressions (A-C) and analysis of differences (D-F) plots.

Wave test 5 (JONSWAP wave spectra with $H_s = 0.2$, $T_p = 2$, $\gamma = 3.3$) regressions (A-C) and analysis of differences (D-F) plots. Panels A, B, and C are regressions constructed from raw DIY pressure data (x axis) and raw RBR pressure data (y axis); panels indicate the different replicates (Table 2). Panels D, E, and F are plots of differences and correspond to the regressions directly above them. In these plots differences in raw pressure readings (y axis) are plotted against the average of the readings (x axis) following Bland and Altman (1999). Dashed red lines indicate bounds of 95% confidence intervals and gray boxes indicate the standard error of the confidence interval lower and upper limits. Mean differences between the gauges are essentially zero, with 95% confidence intervals < ±170 Pascals (< 1.7 centimeter static water depth). Model fit was also excellent ($R^2 \geq 0.9$).

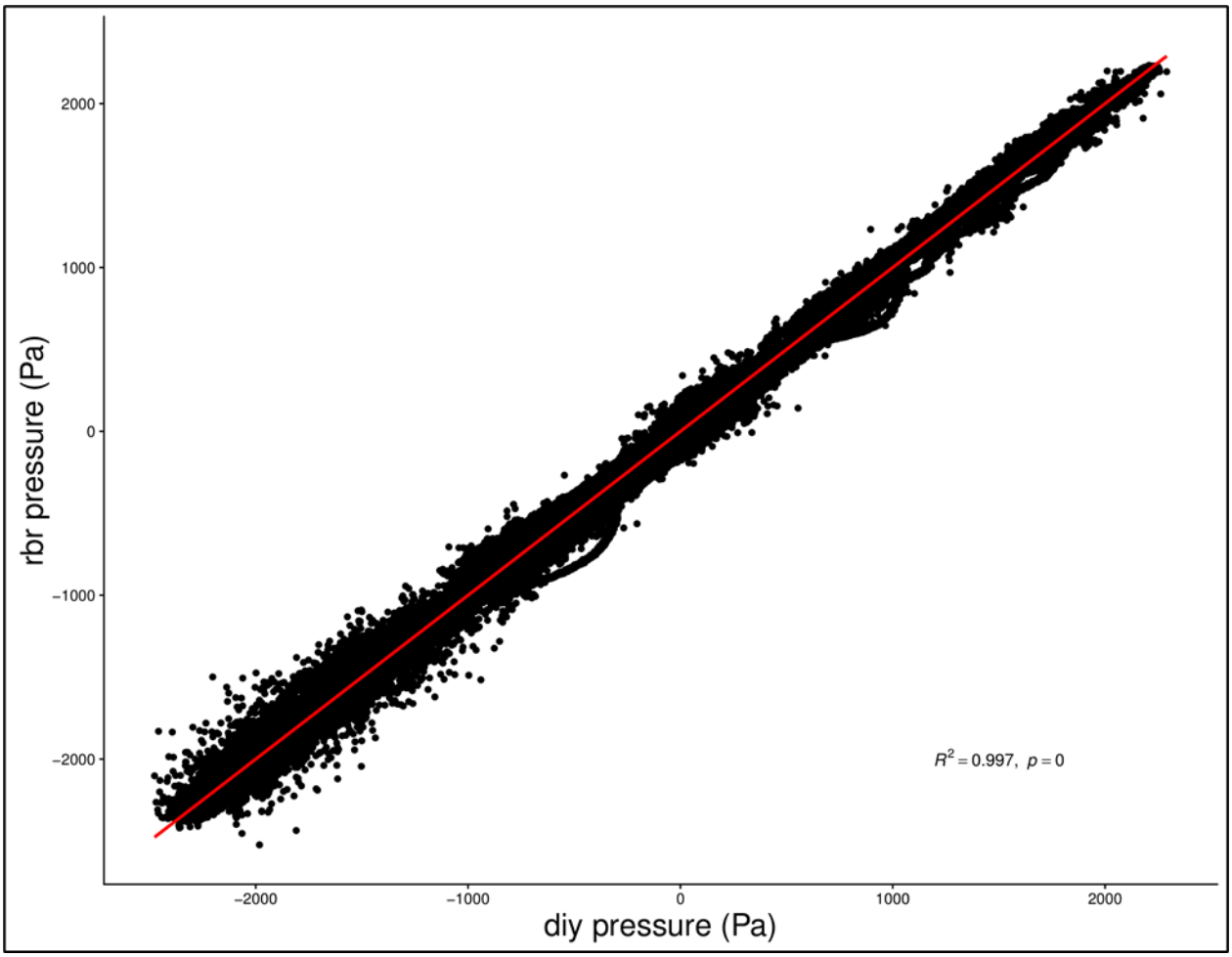

Figure A.6 Regression of the field performance test raw pressure data.

Regression of the field performance test raw pressure data. The linear model (red line; y = 1x) was fit to raw DIY pressure (x axis) and raw RBR pressure data (y axis) recorded by each gauge during a five-day deployment in the Fowl River, Mobile County, Alabama, USA.

A.7 Literature Cited

Beddows, P. A. and Mallon, E. K., 2018. Cave pearl data logger: A flexible Arduino-based logging platform for long-Term monitoring in harsh environments. *Sensors,* 18(2), 530.

Bland, J. M. and Altman, D. G., 1999. Measuring agreement in method comparison studies. *Statistical methods in medical research,* 8(2), 135-160.

Kunwor, S.; Starr, G.; Loescher, H.W. and Staudhammer, C.L., 2017. Preserving the variance of long-term eddy-covariance measurements using parameter prediction in gap filling. *Agricultural and Forest Meteorology,* 232, 635 - 649.

MATLAB 2017a, The MathWorks, Inc., Natick, Massachusetts, United States.

R Core Team, 2017. *R: A language and environment for statistical computing*. R Foundation for Statistical Computing, Vienna, Austria. URL http://www.R-project.org/

Wickham, H., 2011. ggplot2. *Wiley Interdisciplinary Reviews: Computational Statistics,* 3(2), 180-185.

Wilke, C.O., 2016. *cowplot: Streamlined plot theme and plot annotations for 'ggplot2'*. R package version 0.7.0. URL https://CRAN.R-project.org/package=cowplot [accessed 14 May 2018]

APPENDIX B

CHAPTER III APPENDIX

B.1 Wind Rose Data

A wind rose was constructed to guide initial bay site selection. Wind records over a two-year period (i.e., January 2015 – December 2016) were first obtained from the Bon Secour Bay weather station maintained by Dauphin Island Sea Lab (https://arcos.disl.org/stations/disl_stations?stationnew=106). Wind roses were then constructed for each month using the windRose function of the openair package in R (Carslaw and Ropkins 2012). Overall, wind records illustrate a gradient in both direction and speed (Figure B1).

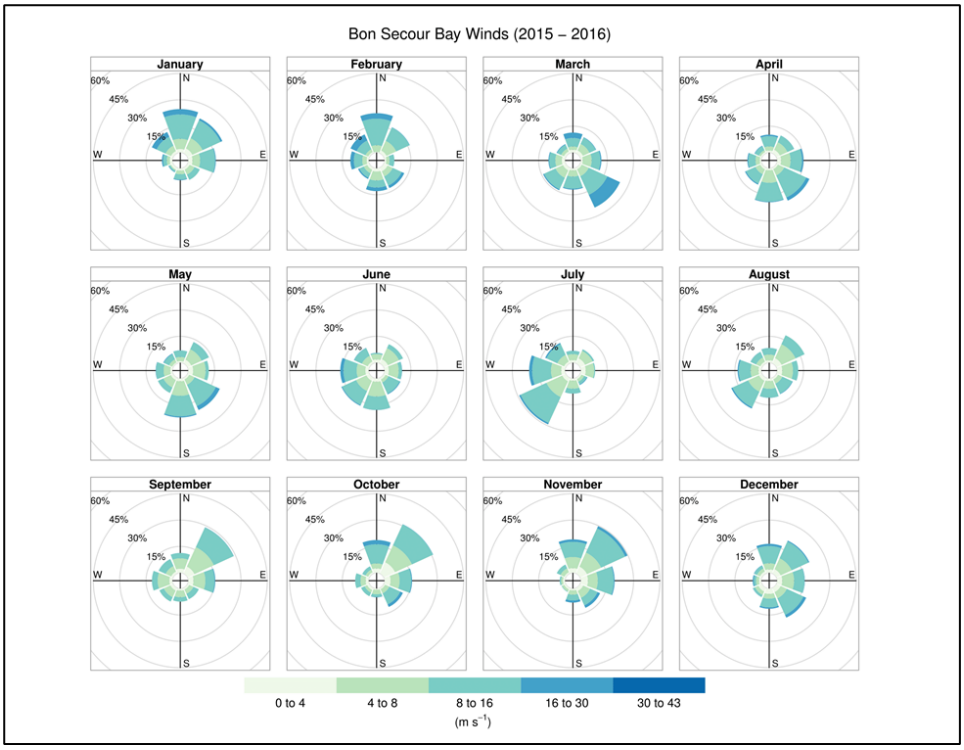

Figure B.1 Monthly average speed (m/s) and direction of winds in Bon Secour Bay, Alabama, USA.

For each month, the spokes protruding from the center indicate how often winds came out of a particular direction (i.e., longer spokes indicate winds blew more frequently from that direction). Different colors indicate how frequently winds blew at a range of wind speeds (0-4, 4-8, 8-16, 16-30, 30-43; bottom legend). As a whole, Bon Secour Bay Winds tend to fluctuate seasonally in both speed and direction.

B.2 Gauge Record Data Comparisons to 10-year Wind-wave Models

Shallowater wave forecasting models were used to hindcast the long-term (i.e., 10-year) wave climate at study sites so that they could be compared to the wave climate estimated from gauge data. These comparisons were not meant to be exhaustive but rather a limited survey of six sites along northern- and southern-facing sites since these sites experience differing wind patterns during the study period (Figure B1).

Shallowater wind-wave models were executed as follows:

1. Ten-year wind records were collected from the Dauphin Island weather station, using data collected hourly (https://tidesandcurrents.noaa.gov/met.html?id=8735180). These data were then organized with 15º bins (e.g., 0º, 15º, 30º …345º) for subsequent analyses.
2. Mobile Bay bathymetric data were acquired from the US National Oceanic and Atmospheric Administration's bathymetric data viewer website (https://maps.ngdc.noaa.gov/viewers/bathymetry/). This bathymetric data layer and site GPS coordinates were then imported into QGIS (QGIS Development Team 2019).
3. In QGIS, line vectors were created from the study sites across Mobile Bay to the closest reciprocal shoreline along each of the 15º directions. Average depth along and total distance (i.e., fetch distance) along these vectors was then extracted using Zonal Statistics in the Raster Analysis toolbox.
4. Wind speed and direction, depth and fetch distance data were then used to generate wave height climate statistics in MATLAB (2017a) routines following spectral methods described in the US Army Corps of Engineer's Shoreline Protection Manual, Volume 1 (1984).

Wind-wave models generated spectrally significant wave height (i.e., H_{m0}) statistics, which while different, are similar to the significant wave height statistics generated for wave gauge record data (Temple et al. 2020). Modelled H_{m0} statistics were then ordered to calculate the frequency of occurrence following the methods described for gauge wave height statistics. Gauge and model-generated wave height statistics were then plotted together for qualitative comparisons of short- and long-term wave climate data. These comparisons illustrate that the similarity between gauge and modelled statistics was greatest at southern sites (Figure B2) as

compared to northern sites (Figure B3), likely due to the predominance of winds out of the south during the study period (Figure B1).

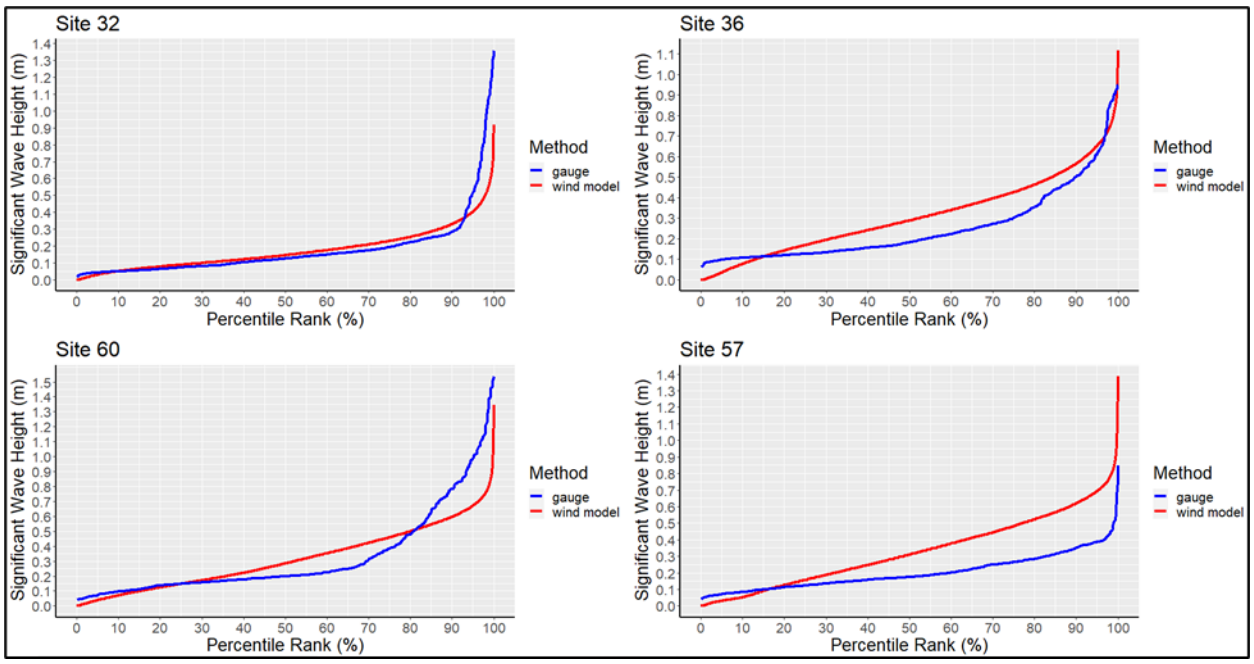

Figure B.2 Wave statistic comparisons at southern facing sites in Mobile Bay.

Significant wave height (y axis; H_s and H_{m0}, for gauge and modelled statistics respectively) is plotted against the percentile rank (x axis; i.e., cumulative frequency of occurrence). There is some deviation between gauge- (blue line) and model- (red line) generated wave statistics at site 57 but overall, gauge statistics were similar to those generated by models considering 10 year conditions.

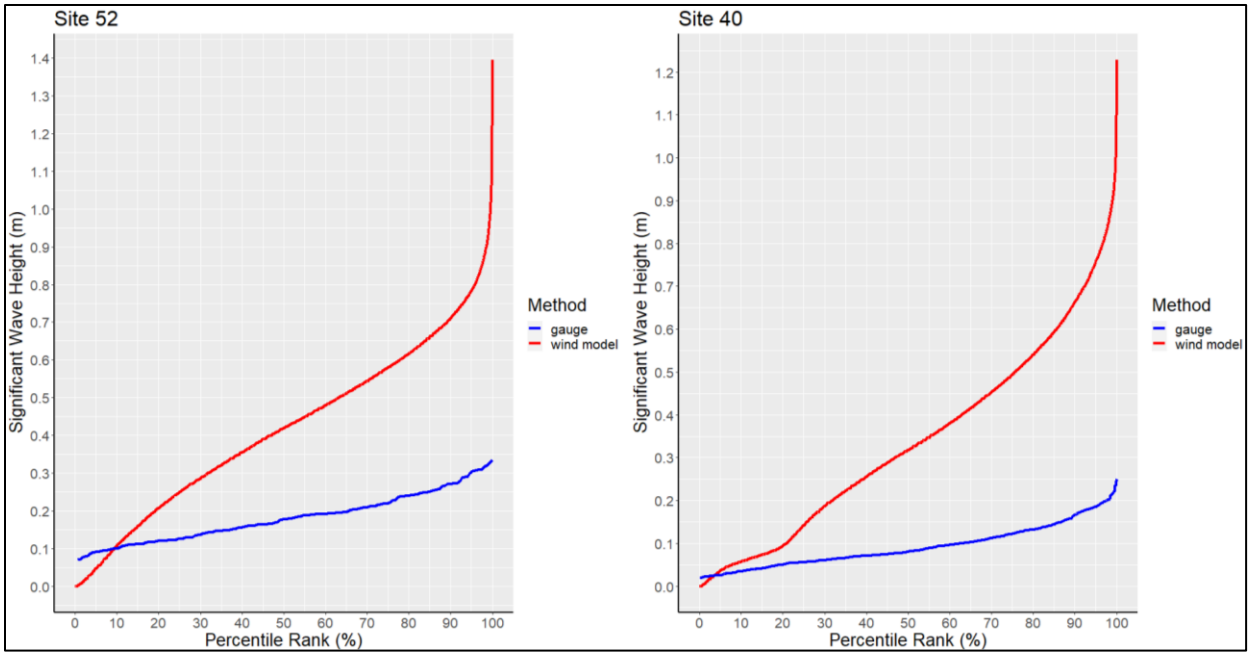

Figure B.3 Wave statistic comparisons at northern facing sites in Mobile Bay.

Significant wave height (y axis; H_s and H_{m0}, for gauge and modelled statistics respectively) is plotted against the percentile rank (x axis; i.e., cumulative frequency of occurrence). At these sites, gauge- (blue line) generated statistics tended to underestimate those generated from long-term models (red line).

B.3 Literature Cited

Carslaw, D.C., Ropkins, K. (2012). "openair — An R package for air quality data analysis." Environmental Modelling & Software, 27–28(0), 52–61. ISSN 1364-8152, doi: 10.1016/j.envsoft.2011.09.008.

QGIS Development Team (2019). QGIS Geographic Information System. Open Source Geospatial Foundation Project. http://qgis.osgeo.org

Temple, N. A., Webb, B. M., Sparks, E. L., & Linhoss, A. C. (2020). Low-Cost Pressure Gauges for Measuring Water Waves. Journal of Coastal *Research*, DOI: https://doi.org/10.2112/JCOASTRES-D-19-00118.1.

United States Army Corps of Engineers (1984). Shore protection manual. US Army Corps of Engineers Research and Development Center, Coastal and Hydraulics Laboratory, Vicksburg.

APPENDIX C

CHAPTER IV APPENDIX

Table C.1 Kruskal-Wallis model results constructed from protected and exposed site observed cover data.

site	initial planting density	p	
Protected	0%	0.680	
	50%	0.887	
	100%	0.001	*
Expected	0%	<0.001	*
	50%	0.890	
	100%	<0.001	*
Between	0%	<0.001	*
	50%	0.888	
	100%	<0.001	*

Observed cover data from both simulations was compared to initial planting density treatment and between sites. Significance at the 0.05 level is denoted by *.

Figure C.1 Experimental mesocosm used at protected site.

Mesocosms were framed using dimensional lumber and PVC materials to inside dimensions: ~2.5 m wide x ~1.22 m long x 25 cm deep (from the base to top of the mesocosm). Three sides of mesocosm frames were constructed using ~5 cm x ~30 cm dimensional lumber, while the shoreward side of mesocosm boxes was constructed using ~5 cm x ~5 cm lumber and PVC lattice which was covered in landscaping fabric, to facilitate water movement. Prior to setting within framed mesocosms, eleven ~1.27 cm thick x ~1.27 cm deep grooves were cut lengthwise and spaced evenly (~30 cm width) along the long end of ~2.54 cm thick x ~2.5 m wide x ~1.22 m PVC sheets that would serve as the impermeable base of mesocosms. After base installation, flume walls, constructed from ~1.27 cm thick x ~30.27 cm tall x ~ 1.22 m long PVC sheets, were glued using silicone adhesive and set within grooves to create 12 flumes within mesocosms.

Figure C.2 General set up facilitating simulated ground water (SGW) flow within experimental flumes.

A gravity-fed continuous drip system was established to direct the simulated groundwater (SGW) solution from upland reservoirs (black bins) to experimental flumes via installed subsurface diffusers. After mixing, the SGW was pumped from the mixing containers to individual ~102 L reservoirs (i.e., one reservoir per experimental flume; black bins). These reservoirs were connected to subsurface diffusers via 0.95 cm (inside diameter) flexible vinyl tubing and featured an inline valve that allowed drip rate control. During this period, reservoirs were monitored daily and refilled, as necessary.